IN MEMORY OF STEFAN CZARNECKI, MAN AND SCIENTIST

The outstanding Polish scientist, in the field of acoustics, Prof. Dr. Stefan CZARNECKI died in Warsaw on 1 September, 1982. Stefan CZARNECKI was born in Warsaw on 20 September, 1925. In 1945 he began his studies at the Gdańsk Technical University, to graduate in 1949 from its Electrical Engineering Department (Radiotechnology Section), achieving the M. Sc. degree with his dissertation *The scaling of dynamic microphones by the reversibility method.* After working a few years at the Central Laboratory of the Polish Radio and at the Warsaw Technical University, in 1953 he began to work at the Institute of Fundamental Technological Research, Polish Academy of Sciences, Warsaw. In 1959 he achieved his D. Sc. degree from the Scientific Council of the Institute of Fundamental Technological Research, Polish Academy of Sciences, Warsaw, for his dissertation *The irregularities of acoustic behaviour in enclosures.* In 1965 he received his habilitation at the Institute of Fundamental Technological Research, for his dissertation *The interaction of Helmholtz resonators with the surrounding medium* and in 1966 he was nominated assistant professor. In 1963-1974, he worked at the Institute of Automation, and subsequently at the Institute of Organization and Management, Polish Academy of Sciences, as head of the Analogy Department. Since 1974 he has worked at the Institute of Fundamental Technological Research, Polish Academy of Sciences, as head of the Aeroacoustics Department. In 1972 he was nominated professor by the State Council and full professor in 1980.

The rich output of Prof. Stefan CZARNECKI's thirty years of scientific research includes more than a hundred publications on subjects related to a variety of fields of acoustics. He has done research in the problems of aerodynamic sound generation, noise control in industrial halls, room acoustics, acoustic screen theory and the identification of sound sources and acoustic energy transmission paths.

His doctoral dissertation already indicated his outstanding researcher's intuition. In this investigation he found and showed the existence of the transient distortions of acoustic behaviour in halls which had not been known before. This discovery became the starting point for further extensive investigations in this field, which have worked towards the development of new criteria for the evaluation of the acoustics of concert halls.

In his habilitation dissertation, on the basis of the fundamental mathematical relations between the laws of reflection and acoustic wave radiation, Stefan CZARNECKI presented analytically the effect of the interaction of the resonator with the surrounding medium. The results obtained he gave in the form of equivalent circuits used in automation. As a result of the relationships derived, he considered theoretically the effect of the surrounding medium on the absorbing properties of Helmholtz resonators in the plane wave field. Subsequently he performed experimental research which fully confirmed his theoretical considerations. The results obtained permitted the explanation of a large number of phenomena occurring in the work of the resonators and can be useful in a variety of fields of acoustics, particularly in noise control.

His other investigations, performed in cooperation with the Institute of Mechanics and Vibroacoustics of the Academy of Mining and Metallurgy, Cracow, have covered a wide range of problems related to the identification of sound sources and vibroacoustic energy propagation paths in various industrial plants. Prof. CZARNECKI has developed a new method for the identification of sound sources which is based on the nearfield methods using the correlation and phase methods, and also the pulse method which has for the first time permitted a practical division of the propagation paths in simple technological systems. He has propagated and developed the methods of energy evaluation of the radiation of surface sound sources, particularly plate systems, seeking significant relationships between the radiated acoustic energy and the vibration of the surface of the source. He has been one of the first in the world to consider the problem of quantitative evaluation of the acoustic field distribution under the conditions of the quasi reverberation field, introducing the method of SPL drops. This method is now used effectively in quantitative evaluation of the acoustic radiation power of sources, eliminating the necessity of reverberation time measurements. Thus the investigations supervised by Prof. CZARNECKI have covered a wide range of the problems of the identification of sound sources and sound transmission paths, both with simple and the complex sources which occur in real industrial conditions.

Prof. CZARNECKI has closely cooperated with a number of research centres in Poland, including the Institute of Mechanics and Vibroacoustics of the Academy of Mining and Metallurgy, Music Academy in Warsaw, the Main Mining Institute in Katowice, Poznań University and Gdańsk Technical University. This cooperation took various forms: common investigations, consultations, seminars and lectures on chosen problems of acoustics.

For a number of years he has had regular lectures on acoustics in Music Academy, Warsaw, and the Engineering School. He has cooperated with Warsaw and Gdańsk Technical Universities. He has tutored a great many M. Sc. degree holders and supervised dozen-odd doctoral dissertations.

One should stress particularly the broad international cooperation in which he has been engaged. He has represented Poland at a large number of

scientific conferences, including the Ist Congress of the Federation of Acoustic Societies of Europe in Paris in 1975, where he delivered the main paper *Acoustic silencers of exhaust noise in industrial installations*. He has also participated in the organization of a number of important international scientific meetings.

His most significant achievements have included the organization of the IInd FASE Congress in Warsaw in 1978 and the International Conference INTER NOISE 79 in 1979. Prof. CZARNECKI has been an active member of the Executive Board of the International Institute of Noise Control Engineering. He has also been a member of the Scientific Council of the International Centre of Building Acoustics of the Council for the Mutual Economic Aid in Bucharest and in 1980 he was nominated *Fellow* of the Acoustical Society of America. The international status of Prof. CZARNECKI is also indicated by his nomination to the session chairman at scientific conferences, e.g. the ICA Congress in Sydney, INTER NOISE conferences in Zurich, San Francisco and Amsterdam.

His activity in noise and vibration control in Poland has been particularly significant and fruitful. In 1970, at the initiative of Prof. S. CZARNECKI and Dr. Cz. PUZYNA, the head of the Committee of Science and Technology set up a team of experts to develop means of noise control in order to diminish the annoyance of industrial noise in Poland. As a result of the work of this team headed by Prof. CZARNECKI, in 1971 the Council of Ministers passed Law 169 on noise control in places of work. The passing of this Law was the turning point in noise abatement in Poland.

Since 1964, first every four years and later on every three years, Prof. CZARNECKI has organized national scientific conferences, with foreign participation, on noise control. These conferences were held in 1962, 1970, 1973, 1976 and 1979 (including the INTER-NOISE 79 Congress). He also co-organized the NOISE CONTROL 82 Conference in Cracow in 1982.

In 1960-1964 Prof. CZARNECKI was the Secretary of the Acoustics Section of the Committee on Electronics and Telecommunication, Polish Academy of Sciences.

From 1964, when the Committee on Acoustics, Polish Academy of Sciences was founded, he was its Scientific Secretary and since 1975 he has been vice-president of the Committee. In 1963 he was one of the member-founders of the Polish Acoustical Society and its vice-president in 1967-1971.

Prof. CZARNECKI was the founder and since 1966 the Editor-in-chief of the quarterly of the Polish Academy of Sciences, *Archiwum Akustyki*; and, since 1976, also its English version *Archives of Acoustics*. He was a member of the State Council for the Protection of the Environment and of the scientific councils of a number of institutions.

As follows from the above short review of the activities of Prof. Stefan CZARNECKI, he has always been at the very centre of what has been happening in Polish acoustics. He has been considered the true "spiritus movens" of the acoustical community and has enjoyed an enormous status. This was the effect

of the extraordinary features of his character. Of himself Prof. CZARNECKI used to say, "It is by no accident that I have devoted myself to acoustics. Acoustics originates from physics and motion is a typical property of physics. And motion is my element!". True, he has been motion itself: extremely active, quick in decision and always moving from place to place. Always full of initiative, he has been ready to take on and carry out all difficult tasks, inspiring with his enthusiasm his collaborators.

The enthusiasm and enterprise have also been typical of his private life. He has been vigorously engaged in sports and tourism. He was a co-author of a skier's guide to the Pieniny Mountains and an encyclopedic handbook on skiing. He has gone on long walks in the mountains. Early in his life he was fond of mountaineering, climbing high in the Alps, Pyrenees and in the Caucas mountains. All his life he has skied regularly. He has always been interested in the political and cultural life in Poland. He has always known about the latest artistic events. How he has managed to have enough time for all this has been his undisclosed secret and the object of his colleagues' envy.

However, it is not only his activity in life and science that has contributed to the very high authority of Stefan CZARNECKI. The main contribution has been the extreme righteousness of his character and his great, truly elemental support for people and matters. He has engaged himself in all actions he considered just and in which he has believed he has been able to assist. He has always tried to help people in need; has always been ready to devote part of his so extremely busy time to the problems of others: to a conversation or an arrangement of matters important for someone.

And there has still been another trait that has made him so outstanding: a tremendous, optimistic, as it were, will power. His friends have known him to say "let the weather beware" when the problem of accomodating trips to the weather arose. And, in effect, despite the unfavourable circumstances, he has rarely failed to carry out his plans.

In 1971, during his stay in the USA, he suffered from a grave disease, where it was necessary to amputate his two kidneys. But those who thought that this would curb his enterprise were much mistaken. Even in the convalescence period and in the long period when in all the weeks he had to spend two days in hospital undergoing dialyses, he resumed his full professional activity, making up for all the lost time.

After a successful kidney transplantation in 1973 he returned to a "normal" way of life, a life of activity above the average. And he has remained such until his very last day, never giving in to the weakening organism, never complaining of anything and never changing his plans.

In his departure Polish acoustics has suffered an irretrievable loss.

Zbigniew Engel
Andrzej Rakowski

Publications of Stefan Czarnecki

1. *The use of the reversibility method for scaling microphones with movable coil* (in Polish), Przegląd Telekomunikacyjny 1, 18-25 (1951).
2. *The significance of analogy in technology, Fundamental problems of modern technology* (in Polish), PWN, Warsaw 1957, pp. 235-271.
3. *Analyse spectrale des ondes acoustiques en regime transitoire dans une chambre close*, Acoustica, 291-295 (1958).
4. *Irregularities of acoustic behaviour in enclosures* (in Polish), doct. diss., Institute of Fundamental Technological Research, Polish Academy of Sciences, Warsaw 1958.
5. *Acoustic vibration. Guide to radio and tele-electrical engineering* (in Polish), PWT, Warsaw 1959, **A**, pp. 204-210.
6. *Electroacoustic elements. Guide to radio and tele-electrical engineering* (in Polish), PWT, Warsaw 1959, **B**, pp. 363-402.
7. *Noise control. Fundamental Problems of Modern Technology* (in Polish), PWN, Warsaw 1960, pp. 273-288.
8. *Acoustic measurements. Mechanical engineering. Technical guide* (in Polish), PWT, Warsaw 1960, **I**, part 3, pp. 724-742.
9. *The effect of an increase in the number of sound sources on acoustic phenomena in enclosures* (in Polish), Poznańskie Towarzystwo Przyjaciół Nauk, Prace Komisji Mat. — Phys., Postępy Akustyki, III, 3/5, 109-118 (1961).
10. *Wave motion and acoustics. Mechanical engineering. Technical guide* (in Polish), PWT, Warsaw 1961, **I**, part 2, pp. 189-249.
11. *Vibration and waves. Guide for construction engineer and technician* (in Polish), Arkady, Warsaw 1964, pp. 681-724.
12. *The coupling of Helmholtz resonators with the surrounding medium*, V Congres International d'Acoustique, Liege 1965, **H**, 48.
13. *The use of analog machinery in chemical industry* (in Polish), Reports of Institute of Automation, Polish Academy of Sciences, 21, 1-24 (1965).
14. *The interaction of Helmholtz resonators with the surrounding medium* (in Polish), habil. diss., Reports of Institute of Automation, Polish Academy of Sciences, 25, 1-72 (1966).
15. *The damping properties of Helmholtz resonators with consideration given to the acoustic conditions of the surrounding medium* (in Polish), Archiwum Akustyki, **1**, 5-24 (1966).
16. *Schallsolierende Wirkungen der Helmholtz-Resonatoren*, Kampf der Lärmm, 6, 1-4 (1966).
17. *The investigation of the acoustic properties of rooms by means of measuring the frequency spectrum of standard music signals*, Archiwum Akustyki, **3**, 2, 189-199 (1968).
18. *Influence of acoustical properties of rooms on the frequency spectrum in transient response*, Proc. IV Acoustical Conference, Budapest 1967, 21 **B2**, 1-4.
19. *Mathematical machinery in automation* (in Polish), Z N, Academy of Mining and Metallurgy, Cracow, Automation, **2**, 219-230 (1967) (with M. Stolarski).
20. *Preobrazovanye akusticheskikh signalov v elektricheskikh ustroystvakh i v slukhovom analizatore*, Proc. III Neurophysiological Conference, Izd. Rostovskogo Universiteta, Rostov 1967, 157-162.
21. *Investigations of the effect of the interior on changes in the frequency spectrum of transient acoustic behaviour* (in Polish), Archiwum Akustyki, **2**, 4, 313-321 (1967) (with M. Vogt).
22. *Spectral analysis of respiratory tract noises of children*, Proc. IV Acoustical Conference, Budapest 1967 (with E. Sławińska, E. Kossowska and Z. Korycki).
23. *Akustische Analyse der Stenosengeräusche bei Erkrankungen der Atmungswege bei Kindern*, Zeitschrift für Laryngologie, Rhinologie, Otologie und ihre Grenzgebiete, 10, 775-781 (1967) (with E. Sławińska, E. Kossowska and Z. Korycki).

24. *Analog machinery as a modelling and teaching tool* (in Polish), Problemy Postępu Technicznego, 1/17 (1968).
25. *Bronchonophonographie*, Les Bronches, **XVIII**, 118-123 (1968) (with E. Sławińska, E. Kossowska and Z. Korycki).
26. *Utilization of non-linear properties of resonators for improving acoustic conditions in rooms*, 6th International Congress on Acoustics, Tokyo, August 1968, 4-5-10.
27. *Reduccion del ruido industrial y de trafico*, Electronica y Fisica Aplicada, XV, 41, 91-96 (1968).
28. *Assessment of potency of the nasophoryny by means of acoustic analysis of the respiratory sound*, Folia Phoniatrica, **23** (1971) (with E. Kossowska, Z. Korycki and E. Sławińska).
29. *Nonlinear absorbing properties of resonance acoustic systems* (in Polish), Archiwum Akustyki, **4**, 1, 37-49 (1969).
30. *Reduction of turbulent noise in industry*, III Conference sur la lutte contre le bruit et les vibrations, Bucarest, May 1969, 17-21.
31. *Investigations of the patency of the nasopharyngeal cavity by acoustical analysis of the respiratory noise* (in Polish), Proc. IV Sci. Conf. on Children's Otolaryngology, Zakopane 28-30 Sept. 1969 (with E. Kossowska, Z. Korycki, A. Kulesza and E. Sławińska).
32. *Analog and hybrid modelling of boundary problems. Scientific problems of mathematical machinery* (in Polish), PWN 1970, pp. 237-243.
33. *Investigation of sound transmission properties of medium resulting from sound wave compensation caused by other sound sources*, Sound and Vibration, **11**, 2, 225-233 (1970).
34. *The use of analog machinery for scientific investigations* (in Polish), Zagadnienia Naukoznawstwa, 22, 27-77 (1970).
35. *Openwork resonance screens working on the principle of acoustic wave compensation* (in Polish), Archiwum Akustyki, **5**, 4, 437-459 (1970) (with M. Vogt).
36. *Model investigations of sound-absorbing barriers* (in Polish), Proc. Noise Control Conference, Warsaw 9-12 September, 1970, 70-75 (with L. Łukaszek and M. Vogt).
37. *Comparative analysis of noise measurement methods* (in Polish), Proc. Noise Control Conference, Warsaw 9-12 September, 1970, 76-81.
38. *Investigations of the reduction of noise from Jelcz-Lux bus* (in Polish), Proc. Noise Control Conference, Warsaw 9-12 September, 1970, 82-86 (with L. Łukaszek, J. Miazga and M. Vogt).
39. *Abatement of turbulent noise occurring at high flow velocities* (in Polish), Proc. Noise Control Conference, Warsaw 9-12 September, 1970, 87-91 (with L. Łukaszek and M. Vogt).
40. *Complex methods of noise control in the Lenin steelworks* (in Polish), Proc. Noise Control Conference, Warsaw 9-12 September, 1970, 92-96 (with E. Garść and W. Szewczyk).
41. *Methodology of carrying out expertises in the field of noise control in the case of some investigations at the Analogy Department of the Institute of Automation*, Polish Academy of Sciences (in Polish), Archiwum Akustyki, **6**, 1, 71-76 (1971).
42. *Sound absorbing and sound-insulating properties of acoustic resonant systems*, Seventh International Congress on Acoustics, Budapest 1971, 21 V. 4 (with M. Vogt and M. Czechowicz).
43. *Acoustical analysis of constriction noise in diseases of the respiratory tract in children* (in Polish), Otolaryngologia Polska, 22, 139-145 (1968) (with E. Kossowska, Z. Korycki and E. Sławińska).
44. *Noise control using Helmholtz resonators*, Noise Control Engineering, Purdue University, Indiana, 1972, pp. 342-345.
45. *Analysis of the conditions of the coupling of acoustic resonators and sound sources* (in Polish), Archiwum Akustyki, **8**, 1, 8-13 (1973).

46. *Investigations of the effect of the absorption and configuration of complex resonance systems on the possibility of extending the frequency band with a high absorption coefficient* (in Polish), Proc. XX Open Seminar on Acoustics, Poznań–Mierzyn 1973, II, 172-173.
47. *Prospects of noise control in industrial plants* (in Polish), Proc. III Noise Control Conference, Warsaw, 5-8 November, 1973, 74-78.
48. *Acoustical and dynamic gas conditions in energy media installations* (in Polish), Proc. III Noise Control Conference, Warsaw, 5-8 November, 1973, 79-83 (with M. Czechowicz).
49. *Sound-insulating properties of acoustic resonators resulting from the principle of acoustic wave compensation* (in Polish), Proc. III Noise Control Conference, Warsaw, 5-8 November, 1973, 84-88 (with M. Vogt).
50. *The use of the cancellation properties of acoustic resonators for the construction of sound-absorbing systems* (in Polish), Proc. III Noise Control Conference, Warsaw, 5-8 November, 1973, 89-94 (with M. Vogt).
51. *Noise abatement in the slabbing mill at the Lenin steelworks* (in Polish), Proc. III Noise Control Conference, Warsaw 5-8 November, 1973, 323-327 (with M. Vogt and L. Łukaszek).
52. *Acoustic model investigations of two versions of a ground-up muffler* (in Polish), Archiwum Akustyki, **8**, 4, 361-382 (1973) (with M. Vogt and M. Czechowicz).
53. *Comparison of the insertion loss of the barrier walls in free and reverberant field*, 2nd Conference on Noise Abatement, Budapest 6-10 May 1974, 3.1 (with E. Glińska and M. Vogt).
54. *Optimal conditions of cancellation of acoustic waves by using acoustic resonators*, Eighth International Congress on Acoustics, London 1974, 47.
55. *Analysis of the acoustic barrier efficiency in a diffuse field* (in Polish), Proc. XXI Seminar on Acoustics, Rzeszów, September 1974, 371-375 (with E. Glińska and M. Vogt).
56. *Acoustic and aerodynamic phenomena in exhaust of high-pressure gas installations*, Akustika 75, Varna, 207-210 (with M. Czechowicz).
57. *The principles of acoustic barrier use* (in Polish), Noise Control Conference, Katowice 1975.
58. *Noise control aspects inside industrial halls*, INTER-NOISE 75, Sendai, 183-193 (invited paper).
59. *Chamber-disk suppressors for high-pressure discharge installations* (in Polish), Proc. XXII Open Seminar on Acoustics, Wrocław–Świeradów Zdrój, September 1975, I, 254-259 (with M. Czechowicz).
60. *Noise control in industrial halls using acoustic barriers*, FASE 75, Proceedings, Paris, 321-326 (with E. Glińska).
61. *Acoustic silencers of exhaust in industrial installations* FASE 75, Proceedings, Paris, 346-362 (general paper).
62. *The analysis of action of acoustic barriers in rooms*, 19th Conference on Acoustics, Tatranska Łomnica 1975 (with E. Glińska).
63. *Electronic analog machinery* (in Polish), W. Sz. i P, Warsaw 1976 (chapters 11-13, pp. 236-270).
64. *Methods of phased cancellation of acoustic signals* (in Polish), Wibroakustyka, 2 (1976).
65. *Measurements of the sound power of a piston in the near field using the correlation method* (in Polish), Archiwum Akustyki, **11**, 3, 261-273 (1976) (with Z. Engel and R. Panuszka).
66. *Correlation method of measurements of sound power in the near field conditions*, Archives of Acoustics, **1**, 3, 201-213 (1976) (with Z. Engel and R. Panuszka).
67. *Model investigations of the efficiency of acoustic barriers in industrial halls and urban areas*, 76 Noise Control Conference, Proceedings, Warsaw 1976, 157-162 (with E. Kotarbińska).

68. *Attenuation of choked airflow by chamber-disk suppressor*, 76 Noise Control Conference, Proceedings, Warsaw 1976, 163-167 (with M. CZECHOWICZ).
69. *Near field measurements of sound power on an example of a piston in an infinite baffle*, 4th Conference on Acoustics, Budapest, April 1976 (with Z. ENGEL and R. PANUSZKA).
70. *Analysis of sound source phase cancellation conditions*, 76 Noise Control Conference Proceedings, Warsaw 1976, 409-413.
71. *Investigations of the properties of acoustic barriers with consideration given to the spatial conditions of the environment* (in Polish), Archiwum Akustyki, **11**, 4, 339-368 1976 (with E. KOTARBIŃSKA).
72. *Properties of acoustic barriers in a field of reflected waves*, Archives of Acoustics, **1**, 4, 269-278 (1976) (with E. KOTARBIŃSKA).
73. *Vibration and waves, Guide for construction engineer and technician* (in Polish), Arkady, Warsaw 1976, pp. 188-245.
74. *Suppressor of valve noise in the preheated steam installations*, INTER-NOISE 77, Zurich 1977, B210-B215.
75. *The cooperation of acoustic barriers with sound-absorbing surfaces in industrial halls* (in Polish), Proc. XXIII Seminar on Acoustics, Wisła 1977.
76. *Comparison of the correlation and pulse methods for identification of sound paths in industrial interiors*, 9th ICA Congress, Proceedings, Madrid 1977, N13.
77. *Sound absorbing surfaces as image sources*, 9th ICA Congress, Proceedings, Madrid 1977, D1.
78. *The effect of the diffraction phenomenon on the acoustic conditions in concert and industrial halls* (in Polish), Proc. XXIV Seminar on Acoustics, Cetniewo 1977.
79. *Consequences of limited applicability of reverberation theory for an acoustic treatment of industrial and residence interiors*, 16th Conference on Acoustics, Proceedings, Strbskie Pleso 1977.
80. *The principle of acoustic barrier use in industry* (in Polish), Institute of Construction Technology (ITB), Warsaw.
81. *Methods of noise control in industry and internal transportation means* (in Polish), Secura 78, Poznań 1978, pp. 58-86 (with Z. ENGEL, Cz. PUZYNA and J. SADOWSKI).
82. *Local means of traffic noise control inside residence interiors*, FASE 78, Proceedings, Warsaw 1978, 177-180 (with J. SZUBA).
83. *How to use the absorbing material in a shallow room for the optimal condition of noise reduction*, FASE 78, Proceedings, Warsaw 1978, **III**, 103-106.
84. *The paths of sound propagation through the barriers*, FASE 78, Proceedings, Warsaw 1978, **III**, 123-126 (with Z. ENGEL and A. MIELNICKA).
85. *Mirror image method of analyzing the combined effect of barriers and absorbing surfaces in industrial interiors and apartments*, Noise Control Engineering, **11**, 1, 18-30 (1978).
86. *Complex methods of noise control in urban areas*, Inter Noise 78, Proceedings, San Francisco, 1978, 535-540.
87. *The role of acoustic feedback in the mechanism of edge tone generation* (in Polish), Proc. XXV Open Seminar on Acoustics, Poznań 1978, 95-98 (with M. CZECHOWICZ and T. SOBOL).
88. *Reduction of piano noise in living apartments*, Inter Noise 79, Proceedings, Warsaw 1979, 929-932 (with J. SMURZYŃSKI, A. RAKOWSKI and A. RÓŻYCKI).
89. *Model investigations of noise barrier effectiveness for a chosen section of the freeway Trasa Łazienkowska in Warsaw*, Inter Noise 79, Proceedings, Warsaw 1979, 549-552 (with E. SŁAWIŃSKA and J. SZUBA).
90. *Influence of the shape and kind of acoustical treatment of ceiling for distribution of sound energy in a shallow rooms*, Inter Noise 79, Proceedings, Warsaw 1979, 397-402 (with R. JANCZUR).

91. *Aero-vibroacoustic feedback for the edgetone production,* Inter Noise 79, Proceedings, Warsaw 1979, 135-138 (with M. Czechowicz and T. Sobol).
92. *Noise control in Poland,* Inter-Noise 79, Proceedings, Warsaw 1979, 11-21.
93. *Estimation of equivalent surface area for determination of the acoustic power of a circular plate,* Inter Noise 79 Proceedings, Warsaw 1979, 67-70 (with Z. Engel and A. Mielnicka).
94. *Correlation and pulse techniques for identification of the path of diffracted and penetrating waves through barriers,* Archives of Acoustics, **4**, 4, 317-330 1979 (with Z. Engel and A. Mielnicka).
95. *Investigation of acoustical barriers used in the foundry industry,* Noise Con 79, Lafayette 1979, Proceedings, 345-352 (with Z. Engel and A. Mielnicka).
96. *The effectiveness of a barrier at the wall* (in Polish), ZN, Academy of Mining and Metallurgy, Electrification and Mechanization of Agriculture, 112, 79-86 (1979) (with A. Mielnicka and A. Siudyła).
97. *Perception of transition states, quasi-nonlinear transient distortions* (in Polish), Proc. XXVI Open Seminar on Acoustics, PTA, Wrocław—Oleśnica 1979 (with B. Osiecki).
98. *Methods, possibilities and prognosis of the protection of the environment against noise and vibration in the central macroregion,* in: *Protection and shaping of the environment in terms of social and economic development plans and town and country planning in the central macroregion* (in Polish), Scientific Session of the Planning Committee of the Council of Ministers and the Scientific Committee of the Polish Academy of Sciences "Man and the Environment", Piotrków Trybunalski, October 1979, pp. 482-507.
99. *The methods for analyzing of acoustic field in industrial halls and urban areas,* International Science Symposium, Volos, Greece, June 1980.
100. *Calculation methods of noise control in industrial halls,* NAS-80, Proceedings, 10-12 June 1980, Turku, Finland.
101. *Differences between insertion loss and transmission loss measurements for various acoustical systems,* 3 Seminar on Noise Control, Szekesfehervar, 1980, 16-28.
102. *Model investigations on the identification of airborne and structureborne sounds,* Inter Noise 80, Proceedings, Miami, Florida, 1980, 2, 1125-1128 (with Z. Engel, A. Gawlik and H. Łopacz).
103. *Gradient method of sound power measurements in situ,* 10th ICA, Sidney 1980, 2, C1-71 (with Z. Engel, R. Panuszka and A. Gawlik).
104. *The transmittance method in the evaluation of the effect of the conditions of the environment on the barrier efficiency* (in Polish), Proc. XXVII Open Seminar on Acoustics, Warsaw—Puławy 1980, **IV**, 9-12.
105. *The effect of the external factors on the effectiveness of barriers and suppressors* (in Polish), Proc. XXVIII Open Seminar on Acoustics, Warsaw—Puławy 1980, **IV**, 53-56 (with R. Janczur, E. Kotarbińska and E. Walerian).
106. *The problem of the determination of the aeroacoustic parameters of microphone windscreens* (in Polish), Proc. XXVII Open Seminar on Acoustics, Warsaw—Puławy 1980, **IV**, 57-60 (with A. Lipowczan and Z. Niczyporuk).
107. *Mechanical-aerodynamic feedback in the process of sound generation,* Archives of Acoustics, **5**, 4, 289-303 (1980) (with M. Czechowicz and T. Sobol).
108. *Model investigations as the method for prognosis and optimization of planning systems in terms of external noise* (in Polish), Scientific and Technological Symposium on the Protection of the Environment against the External Noise, Warsaw, 25-26 November, 1980, NOT.
109. *Application of a gradient method for approximate estimation of a sound directivity in situ,* Inter Noise 81, Proceedings, Amsterdam 1981 (with Z. Engel, R. Panuszka and A. Gawlik).

110. *Sound power and radiation efficiency of a circular plate*, Archives of Acoustics, **6**, 4, 339-357 (1981) (with Z. ENGEL and R. PANUSZKA).
111. *Nonlinear properties of the sound absorption coefficient of resonance plate systems* (in Polish), Proc. XXVIII Open Seminar on Acoustics, Gliwice 1981 (with M. CZECHOWICZ and F. SUJKOWSKI).
112. *Methods of additional stimulation in diagnostics* (in Polish), Proc. VII Conference on Diagnostics of Machinery, Wisła 1981, IFTR and the Silesian Technical University.
113. *A comparison of identification of sources of noise and sound propagation paths*, Summer Workshop, Jabłonna 1981.
114. *Quasi-nonlinear distortion of signals in closed space for an unsteady state*, Archives of Acoustics, **7**, 2, 83-106 1982 (with W. WYGNAŃSKI).

Patents

1. No. 59040 (2 September, 1975)
Method for selective absorption of acoustic waves
Co-authors: Michał VOGT and Mieczysław CZECHOWICZ
Patentee: Institute of Applied Cybernetics, Polish Academy of Sciences, Warsaw.
2. No. 143305 (26 June, 1981)
Sound absorbing and insulating acoustic barrier
Co-authors: Michał VOGT, Jerzy BOROWIAK, Ewa GLIŃSKA, Ryszard JANKOWIAK, Henryk JAŻDŻYK, Tadeusz MARGANIEC, Marian STEFANIAK and Czesław TRUSZCZYŃSKI
Patentees: Institute of Fundamental Technological Research, Polish Academy of Sciences, Warsaw, and Poznań Cable Products Company, Poznań.

ARCHIVES OF ACOUSTICS
8, 3, 185-204 (1983)

FOCUSING OF AN ULTRASONIC BEAM BY MEANS OF A PIEZOELECTRIC ANNULAR ARRAY

T. WASZCZUK, T. KUJAWSKA

Department of Ultrasound, Institute of Fundamental Technological Research, Polish Academy of Sciences
(00-049 Warsaw, ul. Świętokrzyska 21)

J. C. SOMER

University of Limburg, Biophysics Department
(6200 MD Maastricht, Holland)

The lateral resolution of ultrasonographs for the investigation of the internal structures of the body depends on the diameter of the ultrasonic beam. A decrease in the diameter of the beam can be achieved by the use of multi-element annular ultrasonic probe controlled by the electronic system described in the present paper. This paper also presents a method for the calculation of the distribution of the radiated acoustic field and two experimental methods which permit the measurement of the field distribution, with focusing during transmission only. The analytical results were compared with the experimental results obtained by two measurement methods. This comparison indicates that over the major part of the range there is agreement between the analytical and experimental results. Some differences between them occur mainly at the ends of zone 2 (focal point 60 mm) and in zone 4 (focal point 110 mm).

1. Introduction

One of the fundamental methods of investigation in ultrasonic medical diagnosis is *B*-mode echography. In this mode the reflected echoes, which correspond to the distribution of anatomical structures of the body, are shown as bright points on the screen of the CRT. The brightness and diameter of these points depend on the amplitude of the echoes and the diameter of the electron beam of the CRT. In good quality CRT, echoes with mean amplitude are shown

as points of 0.5 mm diameter [4]. This diameter can be taken as the criterion in *B*-mode ultrasonographs for the investigation of the internal structures, in order that a good resolution may be achieved.

The resolution of the ultrasonograph is defined by the longitudinal and lateral resolution of the ultrasonic probe, the accuracy of deflection and focusing of the electron beam in the CRT, the mechanical stability of the system which transforms the motion of the probe into the motion of the time base on the screen and by variations in the velocity of the ultrasonic beam in investigated structures. In addition to variations in the velocity of the ultrasonic beam in the structures, other parameters result from the design and accomplishment of the equipment.

In the present state of ultrasonic technology the most negative effect on the resolution of the ultrasonograph is exerted by the lateral resolution of the ultrasonic probe. The other parameters permit the achievement of the resolution which results from the size of a spot on the CRT screen.

The lateral resolution is defined as the minimum distance between two elements reflecting the ultrasonic beam. The signals reflected from these elements should be displayed as two independent echoes on the screen of the CRT. The lateral resolution of the ultrasonic probe is a function of the observation depth and depends on the geometry of the radiating surface and the radiated wave length.

The aim of the present paper is to indicate the possibilities of decreasing the width of the ultrasonic beam, i.e. to improve the lateral resolution of *B*-mode ultrasonic equipment.

2. Method

The well known method of reducing the diameter of the radiated ultrasonic beam is the use of a lens superimposed on the ultrasonic probe or the use of probes with appropriately profiled concave transducers [1]. This kind of focusing is efficient only over a short depth range. This is a serious disadvantage of this method.

It is possible to focus over the whole observation range when a multi-element ultrasonic probe, controlled by an appropriate electronic system, is used [3, 4, 7]. A multi-element annular ultrasonic probe consists of co-axial elements: a disc and the surrounding rings. The disc and the rings are excited to vibrate by transmitters attached to them. The excitation time of a successive element in the probe is related to the curvature of the radiated ultrasonic wave front, which is focused on the axis of the transducer at a desired distance from its surface (Fig. 1). When the successive elements of the probe are excited to work with various delays, the ultrasonic waves generated by these elements reach at the same time the point P, where summing up they give the effect

of the focusing of the ultrasonic beam. At transmission the wave front can be focused only at one depth. When at transmission the ultrasonic beam is to have a small diameter over the whole range of investigation, it is necessary to generate ultrasonic waves of different curvatures of the wave front radiated.

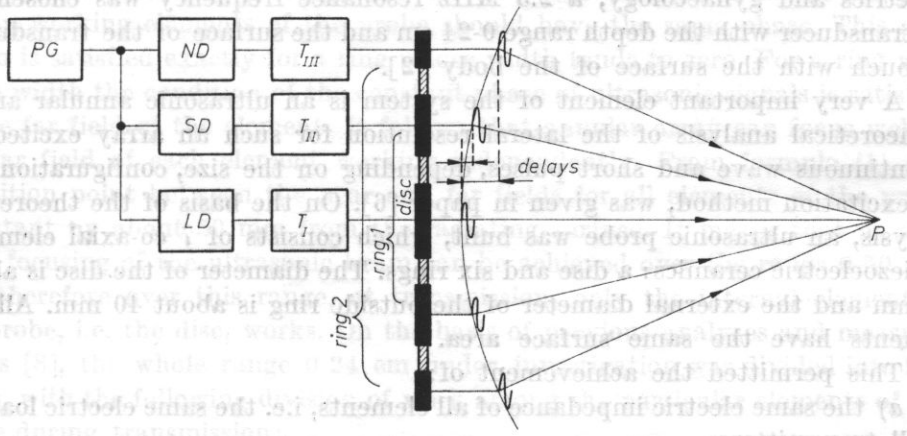

Fig. 1. Focusing during transmission. *PG* — pulse generator, *ND* — transmitter triggering without delay, *SD* — transmitter triggering with small delay, *LD* — transmitter triggering with large delay, *T* — transmitters

This corresponds to several foci over the investigated range. Unlike the focusing at several points during transmission, in the case of detection it is possible to achieve continuous focusing, by a continuous change of the delay of the signals received. The delay changes at a velocity equal to the ultrasonic wave propagation velocity in the body investigated (Fig. 2). This kind of focusing is called dynamic focusing and has a substantial effect on the improvement in the lateral resolution. Focusing using an annular array can be achieved

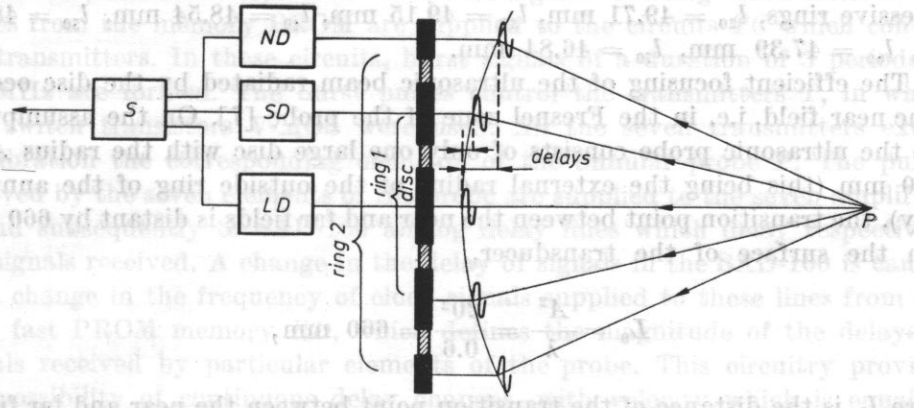

oiig. 2. Focusing during reception, *LD* — circuit with large delay in received signal, *SD* — Frcuit with small delay in received signal, *ND* — circuit without delay in received signal, *S* — summator

only along the axis of the transducers and therefore, in order to achieve a cross-section of the body investigated, the ultrasonic probe has to be moved mechanically.

In view of the expected use of the ultrasonic beam focusing system in obstetrics and gynaecology, a 2.5 MHz resonance frequency was chosen for the transducer with the depth range 0-24 cm and the surface of the transducers in touch with the surface of the body [2].

A very important element of the system is an ultrasonic annular array. A theoretical analysis of the lateral resolution for such an array excited by a continuous wave and short pulses, depending on the size, configuration and the excitation method, was given in paper [6]. On the basis of the theoretical analysis, an ultrasonic probe was built, which consists of 7 co-axial elements of piezoelectric ceramics: a disc and six rings. The diameter of the disc is about 10 mm and the external diameter of the outside ring is about 40 mm. All the elements have the same surface area.

This permitted the achievement of:

a) the same electric impedance of all elements, i.e. the same electric loading of all transmitters;

b) practically the same distance from the surface of the probe, of the transition point between the near and far fields for the disc and all the rings. This distance is given by formula (1) [7],

$$l_{n0} = \sqrt{\left(\frac{a_{nz}^2}{\lambda} - \frac{a_{nw}^2}{\lambda} - \frac{\lambda}{4}\right)^2 - a_{nw}^2}, \tag{1}$$

where l_{n0} is the distance of the transition point between the near and far fields for each element of the probe, a_{nz} is the external radius of the element, a_{nw} is the internal radius of the element (for the disc $a_{nw} = 0$), λ is the wave length radiated ($\lambda = 0.6$ mm for $f = 2.5$ MHz). For the disc $l_{10} = 50.05$ mm; for successive rings, $l_{20} = 49.71$ mm, $l_{30} = 49.15$ mm, $l_{40} = 48.54$ mm, $l_{50} = 48.27$ mm, $l_{60} = 47.39$ mm, $l_{70} = 46.84$ mm.

The efficient focusing of the ultrasonic beam radiated by the disc occurs in the near field, i.e. in the Fresnel zone of the probe [7]. On the assumption that the ultrasonic probe consists of only one large disc with the radius $A = 20$ mm (this being the external radius of the outside ring of the annular array), the transition point between the near and far fields is distant by 660 mm from the surface of the transducer,

$$L_0 = \frac{A^2}{\lambda} = \frac{20^2}{0.6} = 660 \text{ mm}, \tag{2}$$

where L_0 is the distance of the transition point between the near and far fields measured from the surface of the transducer and A is the external radius of the last ring in the probe.

Relation (2) defines the practical restriction of the range of the system described, with the size of the ultrasonic transducer given previously.

An additional condition for the focusing of the ultrasonic beam by means of the annular array is that signals received at the focus from all the independently working elements of the probe should have the same phase. This condition is satisfied exactly for a ring whose width tends to zero. For a ring with finite width the condition of the constant phase of ultrasonic signals is satisfied in the far field of the element. It follows that annular array can focus well in the far field of each element working independently. From formula (1), the transition point between the near and far fields for all elements of the probe is distant by about 50 mm from the radiating surface. It means that no efficient focusing of the ultrasonic beam can be achieved over the range 0-50 mm and therefore over this range, at transmission, only the internal element of the probe, i.e. the disc, works. On the basis of previous analyses and measurements [8], the whole range 0-24 cm under investigation was divided into five zones, with the following division of work among the particular elements of the probe during transmission:

zone 1: from 0 to 50 mm, with only the disc transmitting;

zone 2: from 50 to 70 mm, with the focus at a distance of 60 mm, three elements: the disc and two internal rings, transmitting;

zone 3: from 70 to 90 mm, with the focus at a distance of 80 mm;

zone 4: from 90 to 140 mm, with the focus at a distance of 110 mm;

zone 5: from 140 to 240 mm, with the focus at a distance of 180 mm.

In zones 3, 4 and 5 all the seven elements of the probe transmit.

The annular array works with an electronic system whose schematic diagram is given in Fig. 3. At transmission, signals from the pulse generator *PG* are supplied to seven memories PROM *TD*, which depending on the focus, set the respective relative time delays of signals exciting transmitters. The pulses from the memory PROM are supplied to the circuits *TC* which control the transmitters. In these circuits, burst signals of a duration of 3 periods of 2.5 MHz are formed. The burst pulses control the transmitters *T*, in which fast switch transistors V-MOS were used. All the seven transmitters excite to vibration the corresponding elements of the annular probe *P*. The pulses received by the seven elements of the probe are supplied to the seven amplifiers *R* and subsequently to SAD-100 analog delay lines which delay respectively the signals received. A change in the delay of signals in the SAD-100 is caused by a change in the frequency of clock signals supplied to these lines from the very fast PROM memory *RD*, which defines the magnitude of the delays of signals received by particular elements of the probe. This circuitry provides the possibility of continuous delay changes, with velocity which is equal to the ultrasonic wave propagation velocity in the human body, i.e. the possibility of dynamic focusing. After a respective delay, all the signals are fed to the summator *S*, where they are summed up. Since the SAD-100 delay lines work

using the signal sampling principle, it is necessary to filtrate signals at the sampling frequency. This is achieved by the filter F following the summator.

3. Calculation of the distribution of the radiated acoustic field

This problem consists in the calculation of the space and time distribution of the acoustic field generated by the radiating surfaces of the multi-element ultrasonic annular array. These surfaces are excited to vibration by signals

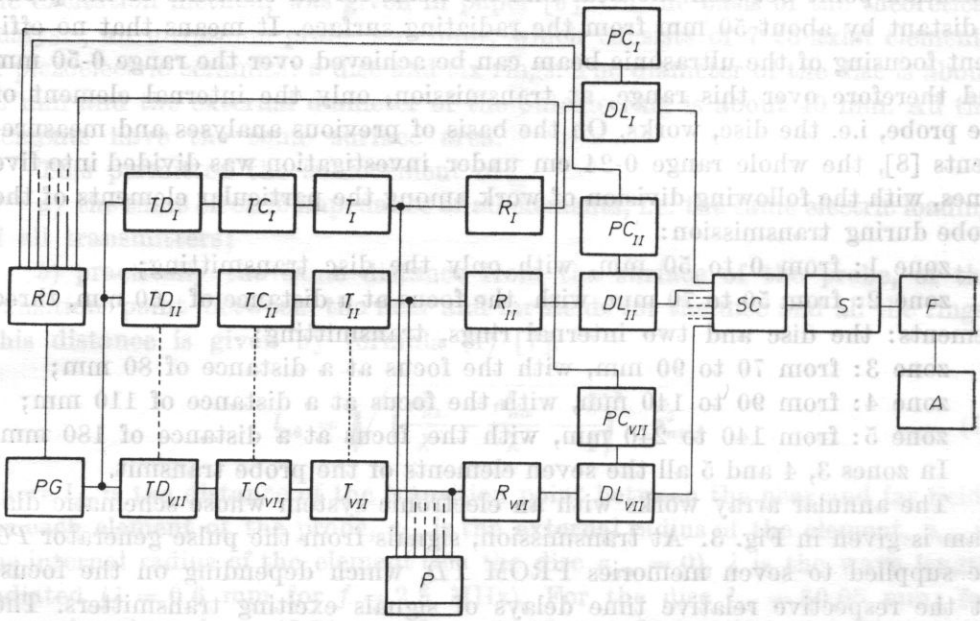

Fig. 3. A schematic diagram of the electronic system working with an annular array. PG — pulse generator, TD — PROM memories of the transmitted pulse delay, TC — transmitter control, T — transmitters, P — probe, R — receivers, DL — SAD-100 delay lines, RD — PROM memory (change in the received signal delay), PC — pulse control of the SAD-100 delay lines, SC — switch circuitry, S — summator, F — filter, A — amplifier

in the form of high-frequency pulses with delays so selected that the beam focuses at a desired point of the field. In the calculations, a pulse shape closest to one in practice was assumed. This pulse contains five sinusoidal high-frequency periods with the envelope $\sin^2(\pi t/2)$.

The theoretical method for the calculation of the acoustic field is based on analysis of transient fields generated by piston surfaces. This analysis consists in the determination of the pulse response of a radiating surface at a given point in space and subsequently in the convolution of this response with the exciting pulses.

The problem of the analytical determination of the distribution of the acoustic field as a function of time, at any point in a half-space, generated by the vibrating surface of an annular array, was considered in paper [5]. According to the formulae derived in this paper, analytical expressions for the calculation of the time behaviour of acoustic pressure, focused on the axis at the distance z from the radiating surface, become

$$P_{\Sigma}(\boldsymbol{r}, t) = P_0(\boldsymbol{r}, t) + \sum_{N} P_n(\boldsymbol{r}, t), \tag{3}$$

where $P_0(\boldsymbol{r}, t)$ is the time behaviour of the acoustic pressure generated by the central disc, $P_n(\boldsymbol{r}, t) = P_{nz}(\boldsymbol{r}, t) - P_{nw}(\boldsymbol{r}, t)$ is the time behaviour of the acoustic pressure generated by the nth ring with the external radius a_{nz} and the internal radius a_{nw};

$$P_{\Sigma}(\boldsymbol{r}, t) = \varrho\{\dot{h}_0(\boldsymbol{r}, t) * V_0(t) + \sum_{N} [\dot{h}_{nz}(\boldsymbol{r}, t) * V_n(t) - \dot{h}_{nw}(\boldsymbol{r}, t) * V_n(t)]\}, \tag{4}$$

where ϱ is the density of the medium, t is time, $\boldsymbol{r}$ is the vector of the distance between a point source and the observation point in the half-space, $V_0(t) = V[H(t) - H(t-\tau_0)]\sin^2(\pi t/2)\sin\omega t$ is the vibration velocity of the central disc, $V_n(t) = V[H(t-\Delta\tau_n) - H(t-\Delta\tau_n-\tau_0)]\sin^2[\pi/2(t-\Delta\tau_n)]\sin\omega(t-\Delta\tau_n)$ is the vibration velocity of the nth ring, $\Delta\tau_n$ is the time difference (acceleration) in the excitation of the nth ring with respect to the disc; $\dot{h}_0(\boldsymbol{r}, t)$, $\dot{h}_{nz}(\boldsymbol{r}, t)$ and $\dot{h}_{nw}(\boldsymbol{r}, t)$ are respectively the partial derivatives with respect to time of the pulse responses for the central disc and rings with the radii a_{nz} and a_{nw}.

The calculations were taken on a VAX computer at Limburg University (the Netherlands) in Fortran. From these calculations, the width of the ultrasonic beam was determined over the whole range for signal level decreases of respectively 3 dB, 6 dB and 10 dB. The 3 dB and 6 dB and 10 dB beam — widths determined analytically are shown in Fig. 15 (section 5) in the form of dotted curves, together with the experimental results.

4. Measurement methods

The measurements were taken on the acoustic pressure of the ultrasonic field of the annular array at transmission. The measurement conditions were the following:

zone 1: pulses transmitted only by the disc;

zone 2: pulses transmitted by three elements; disc and two internal rings;

zones 3, 4 and 5: pulses transmitted by all the elements of the probe.

All the elements of the probe were excited to vibration by a burst with a duration of three cycles of the 2.5 MHz signal. A hydrophone of piezoelectric pvdf (polyvinylidene fluoride) foil (with the diameter of the active part being

1 mm, the thickness 25 mm), manufactured by Marconi (Fig. 4), with a known directional response, was used as the measurement element. This hydrophone is characterized by a flat response of signals received as a function of frequency

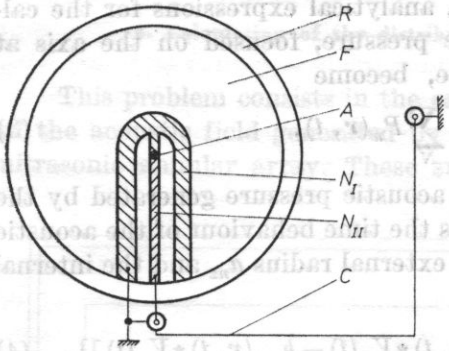

Fig. 4. The hydrophone of pvdf foil manufactured by Marconi, R – frame, F – pvdf foil, N_I – part of the upper foil surface covered with a gold layer, N_{II} – part of the lower foil surface covered with a gold layer, A – active region where the gold-covered parts of the upper and lower surfaces overlap, C – concentric cable

over the range 1-10 MHz and by its lack of effect on the distribution of the ultrasonic field at the measurement point.

As a confirmation of the validity of the parameters assumed for the exciting pulse in the calculation of the field distribution, Fig. 5 shows a pulse shape detected by the pvdf hydrophone at transmission by the disc. The signal detected

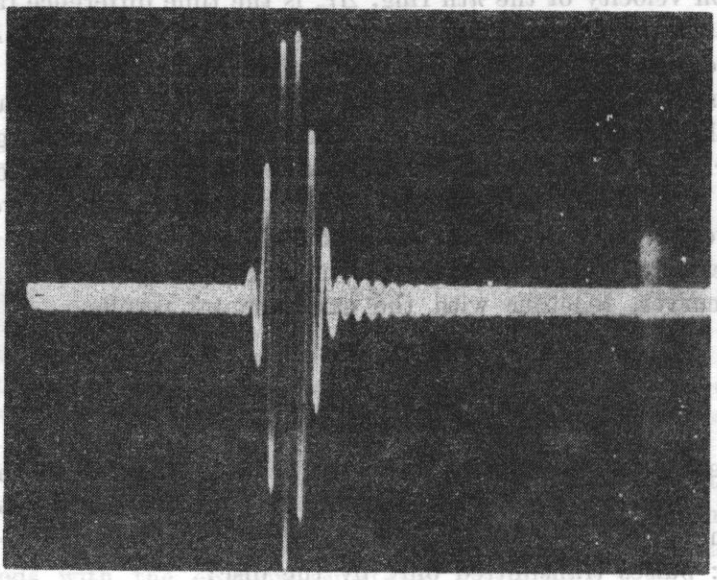

Fig. 5. The pulse shape received by the hydrophone at transmission by the disc

contains about five 2.5 MHz cycles modulated by a signal of the approximate shape $\sin^2(\pi t/2)$ of 2 μs duration.

The acoustic pressure distribution was measured by the system shown in Fig. 6. Ultrasonic waves radiated by particular elements of the array P are

received by the hydrophone H, transformed into electric pulses and fed to the amplifier A. After amplification the signals are fed to the oscilloscope O. The hydrophone can be moved in the direction x and y, with high shifting accuracy. On account of the symmetry of the system, measurements were

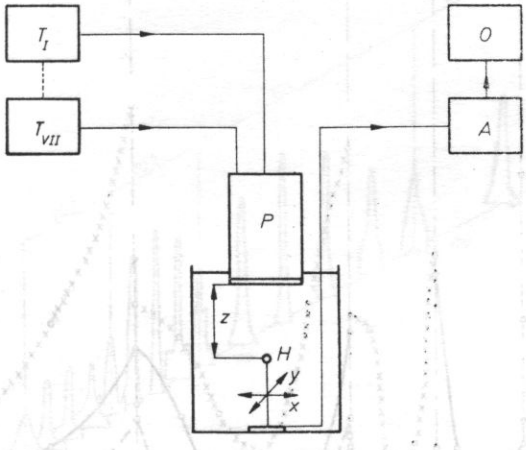

Fig. 6. The system for the measurement of the acoustic pressure. T — transmitters, P — probe, H — hydrophone, A — amplifier, O — oscilloscope, z — probe-hydrophone distance, x, y — directions of the hydrophone shift

taken only for a shift in one direction from the axis of the system. With individual work of each element of the probe, signals detected by the hydrophone were adjusted for the distance $z = 110$ mm (the focus of zone 4). The measured results are shown in Fig. 7.

Zone 1 is in the near field of the element and therefore measurements were taken only for two probe-hydrophone distances, 40 mm and 50 mm. For zones closer to the probe, 2 and 3, "point focusing", i.e. good focusing at the focus and worse at the ends of the zone, can distinctly be seen.

For farther zones, 4 and 5, slightly worse focusing can be seen at points close to the focus, at the expense of the more uniform focusing over the whole zone. For comparison, a half beamwidth is shown for respective 3 dB, 6 dB, 10 dB and 20 dB decreases in signal level. The determination of the 3 dB beamwidth does not take into account the effect of the side lobes. The determination of the 20 dB beamwidth is also inconvenient because of the overlarge effect of the side lobes on the response, e.g. in the case of the 20 dB beamwidth in zone 2. With focussing at transmission only, it is best to determine the beamwidth at a level of — 6 dB or — 10 dB. In addition, when focusing at the same points at reception, the curves for — 6 dB and — 10 dB (Fig. 7) define the respective beamwidths at signal level decreases to 12 dB and 20 dB with focusing both at transmission and detection. This is satisfied under the condition that the directional patterns are the same both at transmission and reception.

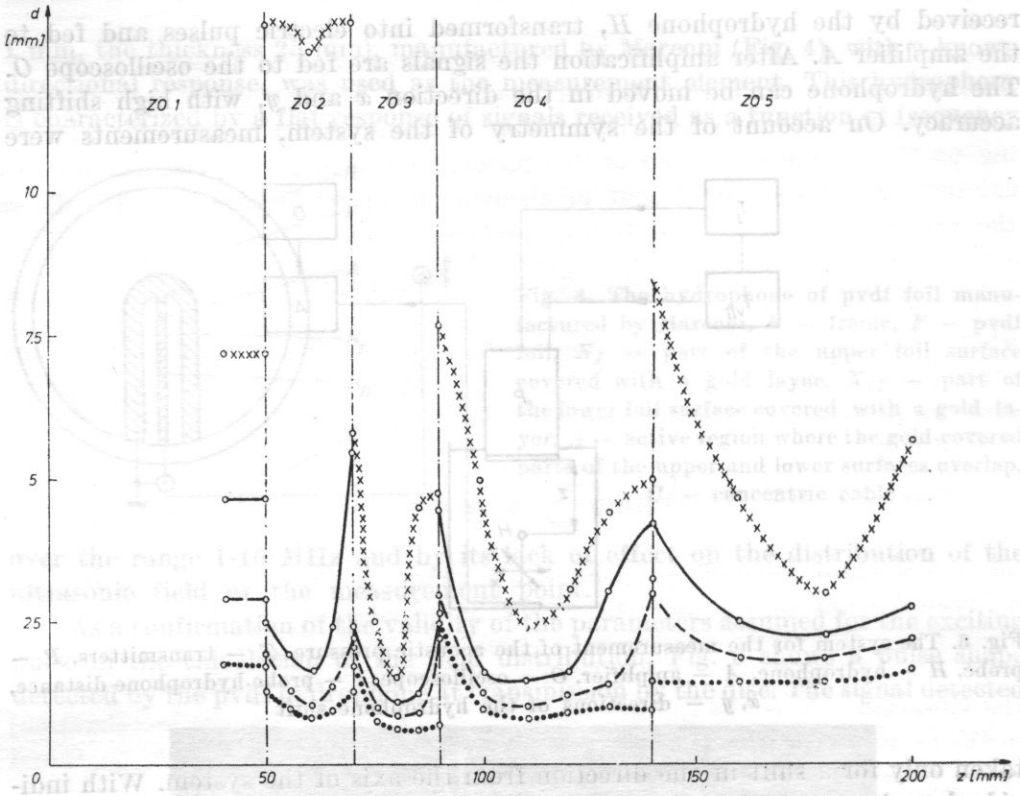

Fig. 7. Half beamwidth for different values of the drop in the signal received, d — half beamwidth, z — distance from the probe, ZO — zone division of the range, ... 3 dB half beamwidth, — — — 6 dB half beamwidth, ——— 10 dB half beamwidth, xxx 20 dB half beamwidth, 000 — measurement points

At reception the described system implements dynamic focusing, for which, over the whole zone under study, ultrasonic signals reflected from points on the axis of the system are focused.

The combination of dynamic focusing at reception with focusing in several zones at transmission causes a decrease in the ultrasonic beamwidth, with respect to focusing in zones both at transmission and detection. The improvement is particularly distinct at the ends of zones.

Fig. 8 shows the distribution of signal amplitudes over the whole range. Greater amplitudes occur in zones 3, 4 and 5; it should be mentioned, however, that all the elements transmit to these zones. At the ends of zones 2 and 3 there

is a distinct effect of the side lobes. It can be seen from the plots in the figure that the amplitude distribution is rather regular over the whole range under study.

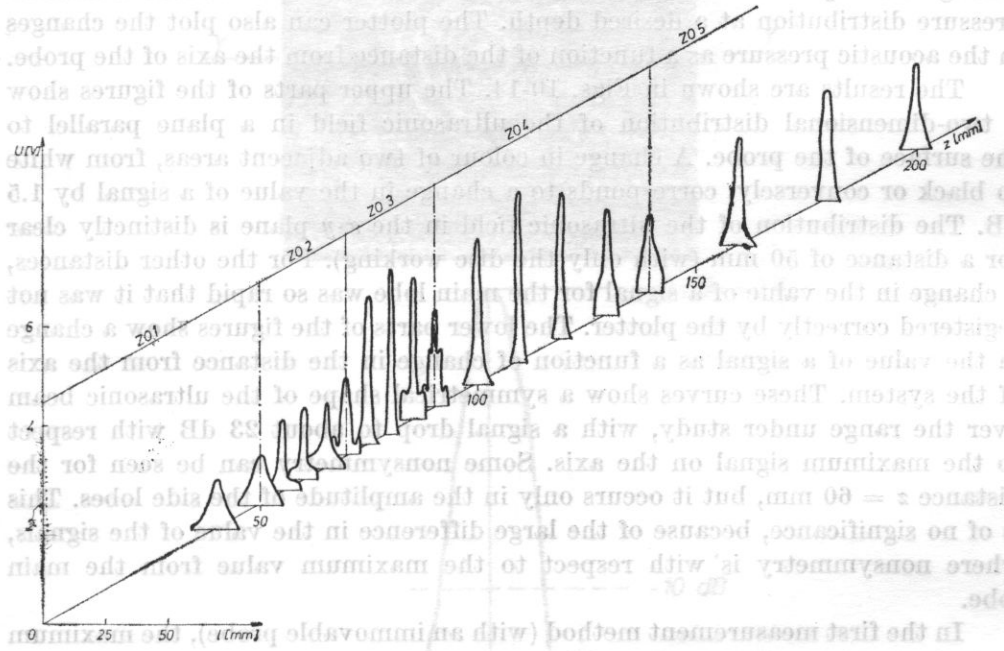

Fig. 8. The signal amplitude distribution over the whole range. U — measured signal value, z — distance from the probe, l — distance from the axis of the system

In the other investigation method, the pressure distribution of the ultrasonic field of the annular array was measured using an ultrasonic beam — scanner. This device was constructed at Limburg University, Maastricht. Fig. 9 explains the principle of work of this device. In this case the hydrophone

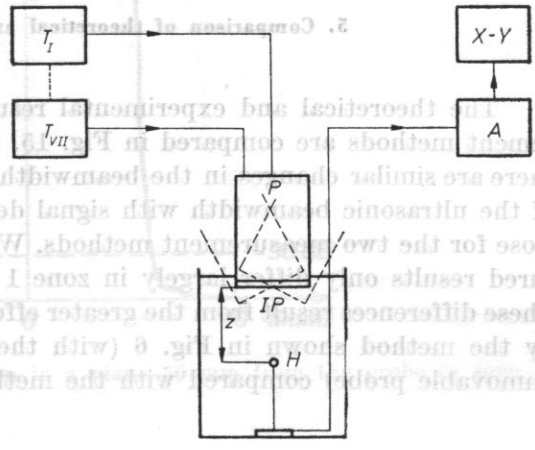

Fig. 9. The working principle of the beam scanner. T — transmitters, P — probe, H — hydrophone, A — amplifier, $X-Y$ — $x-y$ plotter, z — probe — hydrophone distance, IP — immovable point on the surface of the probe, round which the probe swings

is immovable and set on the axis of the system. The ultrasonic probe swings in all directions round the point *IP* which lies both on the axis of the system and on the surface of the transducer. Signals from the hydrophone are fed through an amplifier to a *x-y* plotter, which can plot a two-dimensional acoustic pressure distribution at a desired depth. The plotter can also plot the changes in the acoustic pressure as a function of the distance from the axis of the probe.

The results are shown in Figs. 10-14. The upper parts of the figures show a two-dimensional distribution of the ultrasonic field in a plane parallel to the surface of the probe. A change in colour of two adjacent areas, from white to black or conversely, corresponds to a change in the value of a signal by 1.5 dB. The distribution of the ultrasonic field in the *x-y* plane is distinctly clear for a distance of 50 mm (with only the disc working). For the other distances, a change in the value of a signal for the main lobe was so rapid that it was not registered correctly by the plotter. The lower parts of the figures show a change in the value of a signal as a function of change in the distance from the axis of the system. These curves show a symmetrical shape of the ultrasonic beam over the range under study, with a signal drop to about 23 dB with respect to the maximum signal on the axis. Some nonsymmetry can be seen for the distance $z = 60$ mm, but it occurs only in the amplitude of the side lobes. This is of no significance, because of the large difference in the value of the signals, where nonsymmetry is with respect to the maximum value from the main lobe.

In the first measurement method (with an immovable probe), the maximum probe-hydrophone distance for which measurements were taken was 200 mm. The lack of the measurement of the field distribution at a distance of 240 mm from the probe was caused by the absence of a measurement vessel at greater depth. The field distribution at a distance of 240 mm was measured using a beam scanner and it showed a slight broadening of the beamwidth with respect to the measurements at the 200 mm distance between probe and hydrophone.

5. Comparison of theoretical and experimental results

The theoretical and experimental results obtained using the two measurement methods are compared in Fig. 15. It can be seen that in all the cases there are similar changes in the beamwidth shape. The results of measurements of the ultrasonic beamwidth with signal decreases of 3 dB and 6 dB are very close for the two measurement methods. With a signal drop of 10 dB the measured results only differ largely in zone 1 and at the ends of zones 2 and 3. These differences result from the greater effect of the side lobes in measurements by the method shown in Fig. 6 (with the hydrophone being shifted and an immovable probe) compared with the method using the beam scanner.

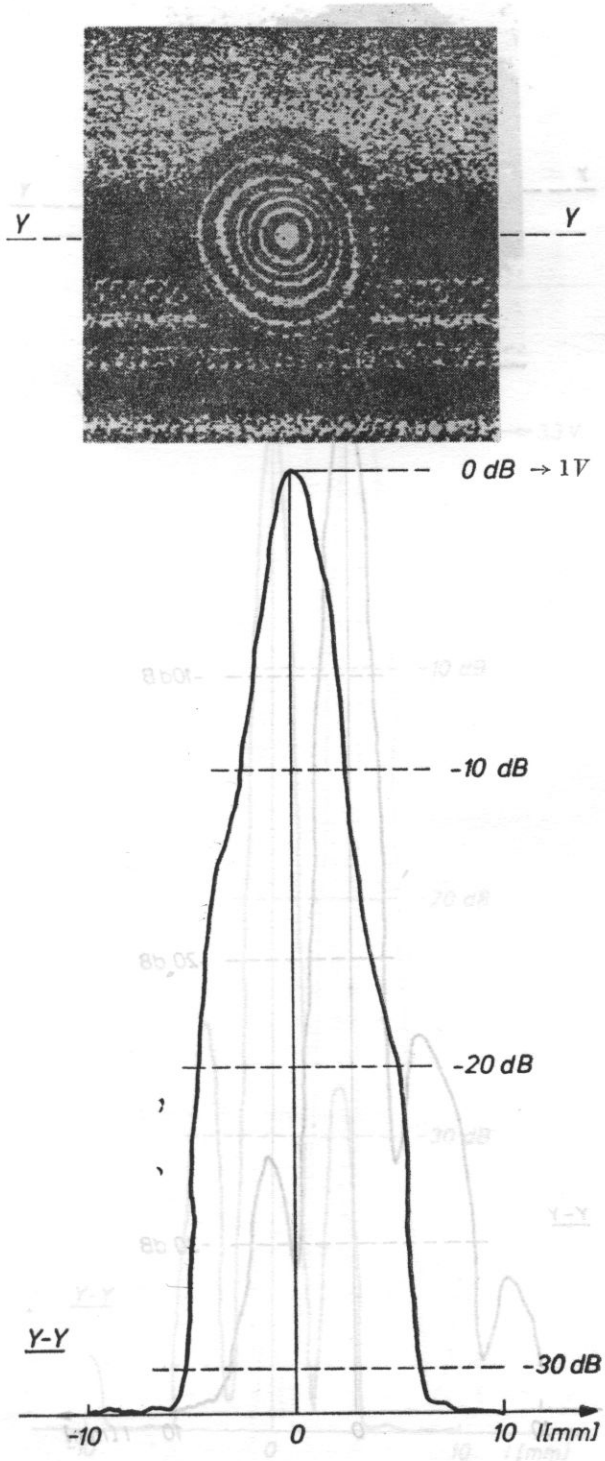

Fig. 10. The ultrasonic field distribution in a plane 50 mm from the probe in zone I

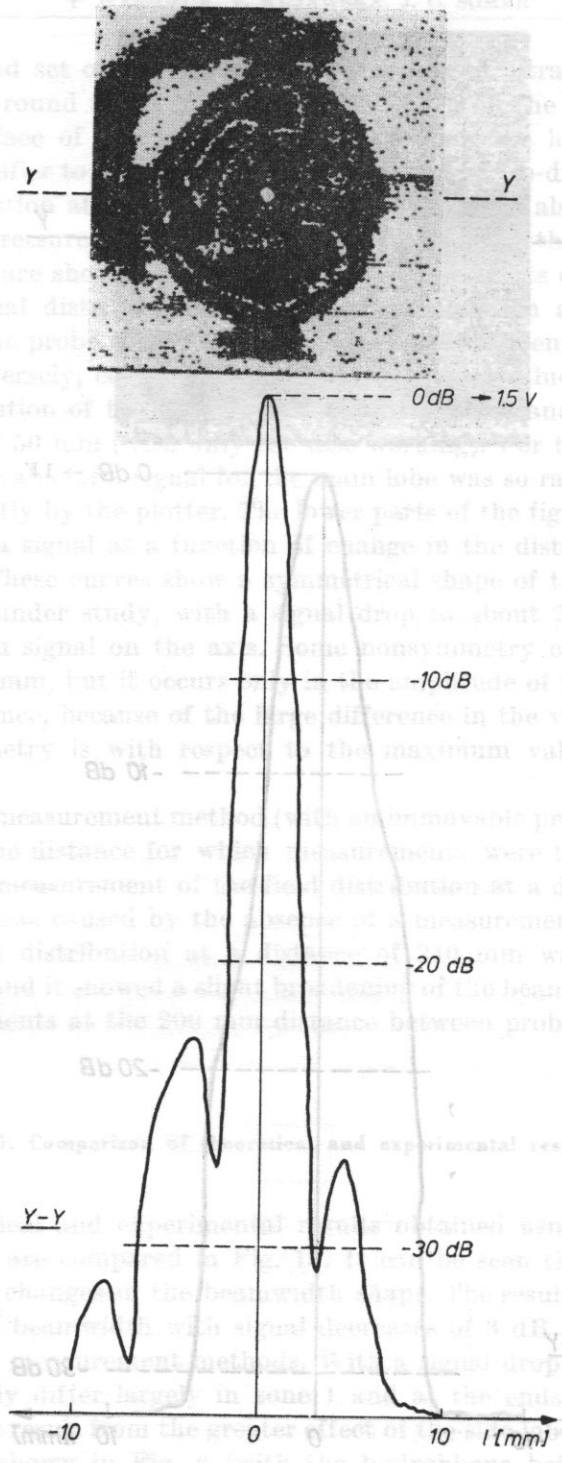

Fig. 11. The ultrasonic field distribution in a plane 60 mm from the probe in zone 2

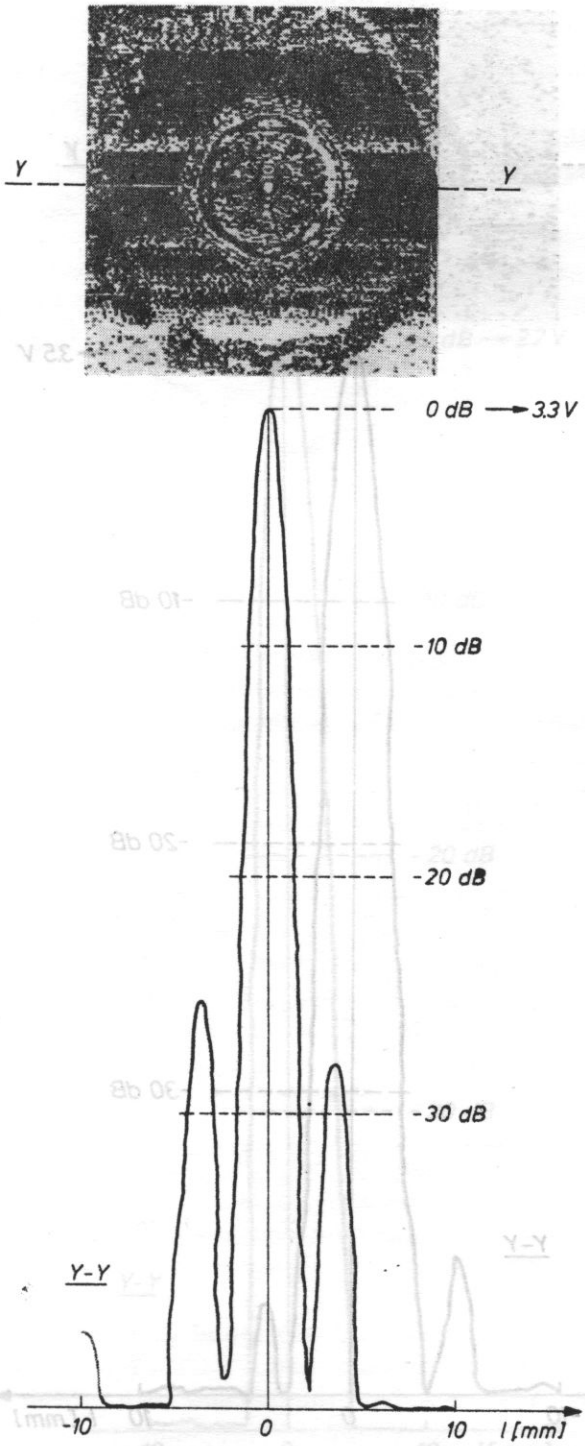

Fig. 12. The ultrasonic field distribution in a plane 80 mm from the probe in zone 3

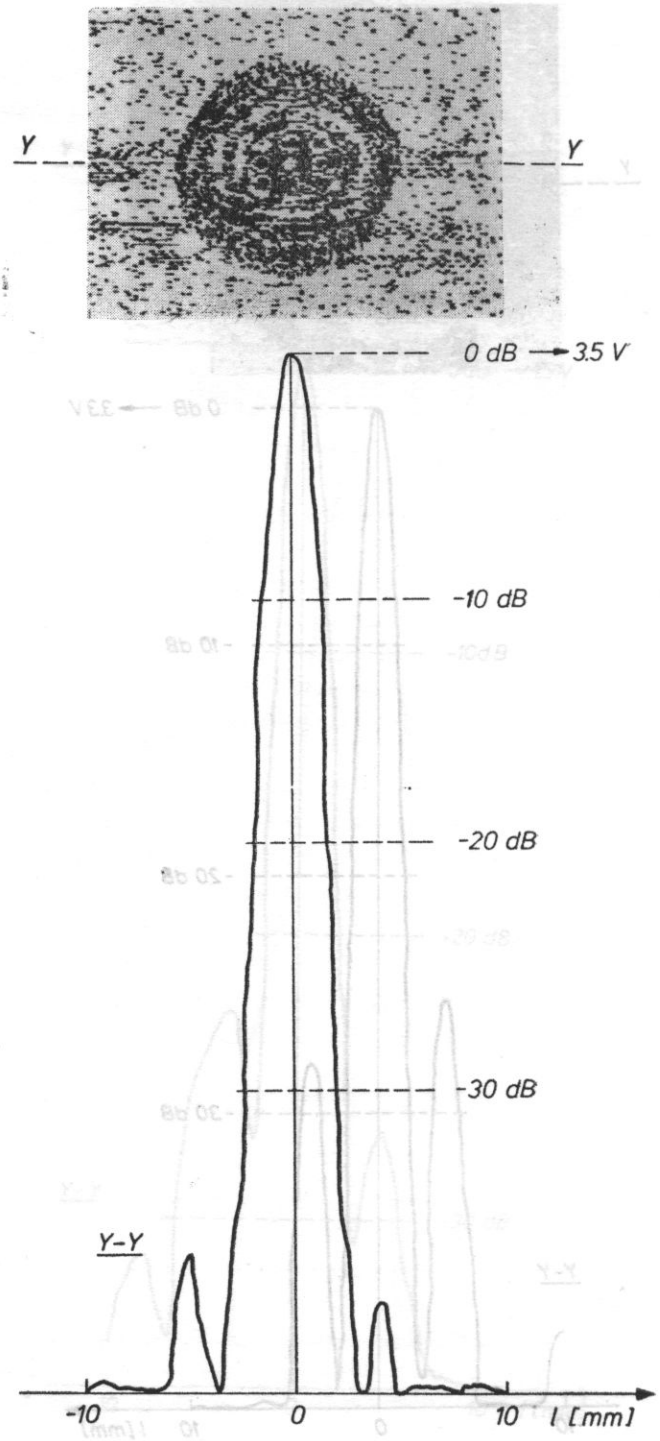

Fig. 13. The ultrasonic field distribution in a plane 110 mm from the probe in zone 4

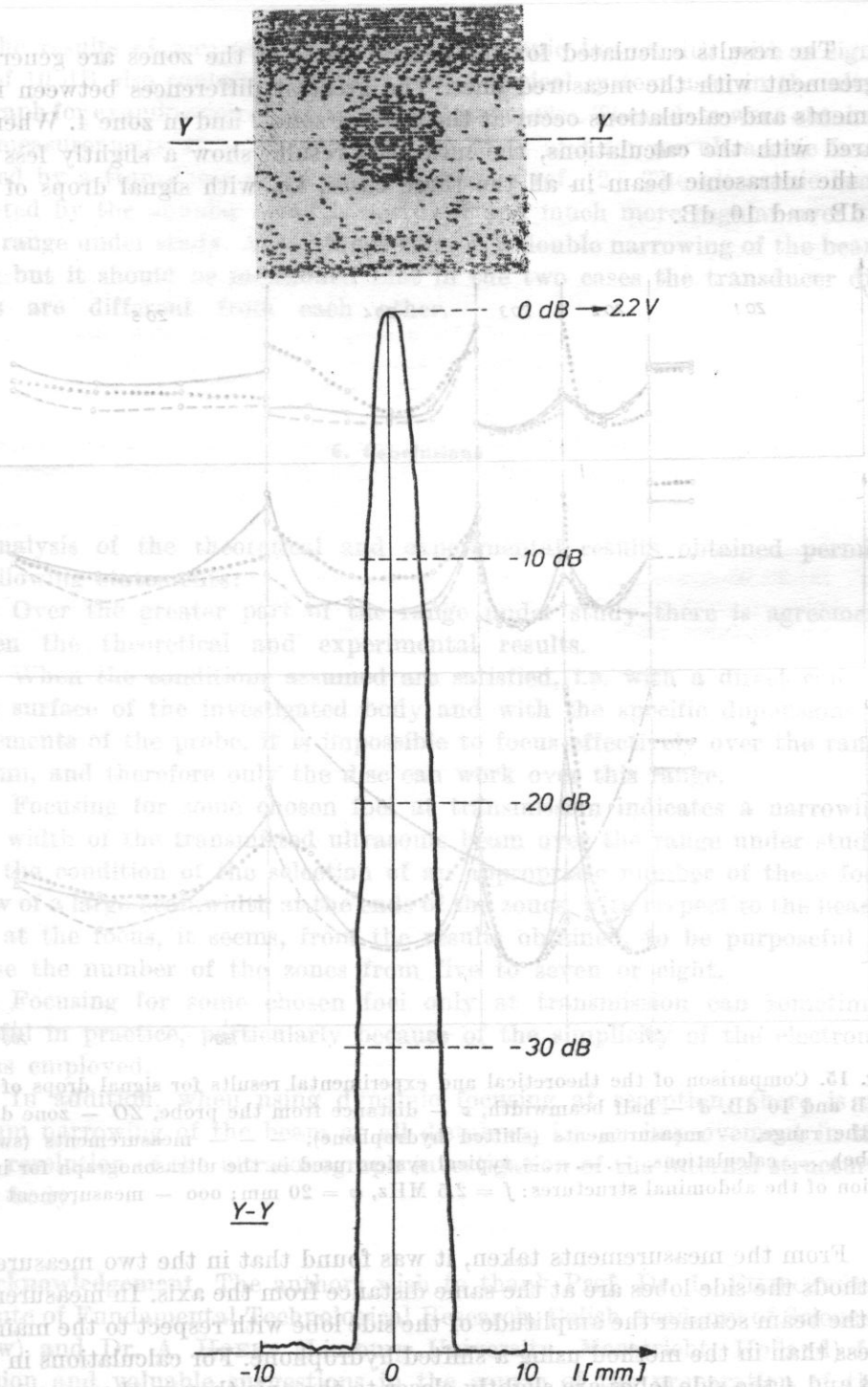

Fig. 14. The ultrasonic field distribution in a plane 180 mm from the probe in zone 5

The results calculated for the central parts of the zones are generally in agreement with the measured ones. The greatest differences between measurements and calculations occur at the ends of zone 2 and in zone 4. When compared with the calculations, the measured results show a slightly less width of the ultrasonic beam in all the three cases, i.e. with signal drops of 3 dB, 6 dB and 10 dB.

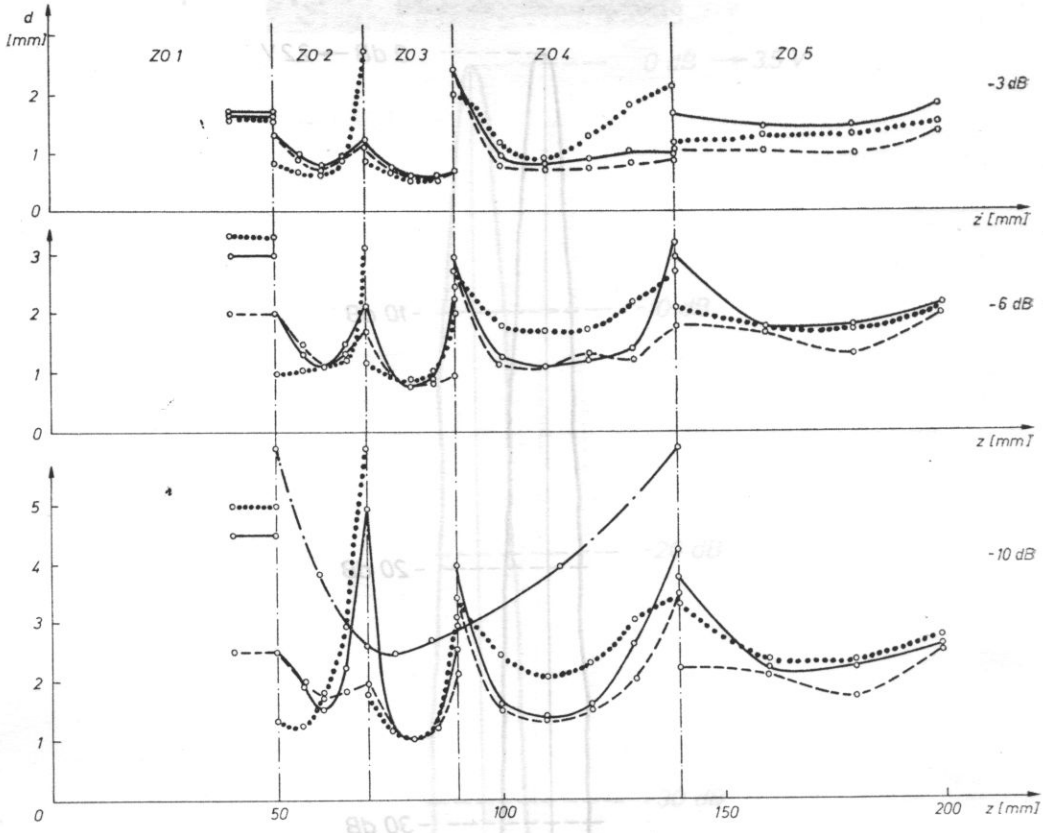

Fig. 15. Comparison of the theoretical and experimental results for signal drops of 3 dB, 6 dB and 10 dB. d — half beamwidth, z — distance from the probe, ZO — zone division of the range, — measurements (shifted hydrophone), — — — measurements (swinging probe), . . . calculations, —.—.—.— typical system used in the ultrasonograph for investigation of the abdominal structures: $f = 2.5$ MHz, $\varphi = 20$ mm; ooo — measurement points

From the measurements taken, it was found that in the two measurement methods the side lobes are at the same distance from the axis. In measurements by the beam scanner the amplitude of the side lobe with respect to the main lobe is less than in the method using a shifted hydrophone. For calculations in zones 2, 3 and 4 the side lobes are slightly closer to the axis than in the experimental results.

The results of measurements of the ultrasonic beamwidth with a signal drop of 10 dB also contain the response of a typical system used in the ultrasonograph for examination of the abdominal structures. These data were obtained from measurements at a frequency of 2.5 MHz and for an ultrasonic beam radiated by a transducer of 20 mm diameter in ref. [2]. The ultrasonic beam generated by the annular array is narrower and much more regular over the whole range under study. At the focus there is a double narrowing of the beamwidth, but it should be mentioned that in the two cases the transducer diameters are different from each other.

6. Conclusions

Analysis of the theoretical and experimental results obtained permits the following statements:

1. Over the greater part of the range under study there is agreement between the theoretical and experimental results.

2. When the conditions assumed are satisfied, i.e. with a direct contact to the surface of the investigated body and with the specific dimensions of the elements of the probe, it is impossible to focus effectively over the range 0-50 mm, and therefore only the disc can work over this range.

3. Focusing for some chosen foci at transmission indicates a narrowing of the width of the transmitted ultrasonic beam over the range under study, under the condition of the selection of an appropriate number of these foci. In view of a large beamwidth at the ends of the zones, with respect to the beamwidth at the focus, it seems, from the results obtained, to be purposeful to increase the number of the zones from five to seven or eight.

4. Focusing for some chosen foci only at transmission can sometimes be useful in practice, particularly because of the simplicity of the electronic systems employed.

5. In addition, when using dynamic focusing at reception, there is an optimum narrowing of the beam at all distances, i.e. an improvement in the lateral resolution of the ultrasonograph investigation of the internal structures of the body.

Acknowledgement. The authors wish to thank Prof. Dr. L. FILIPCZYŃSKI (Institute of Fundamental Technological Research, Polish Academy of Sciences, Warsaw) and Dr. A. HOEKS (Limburg University, Maastricht, Holland) for discussion and valuable suggestions in the course of the preparation of this paper.

References

[1] L. FILIPCZYŃSKI, G. ŁYPACEWICZ, J. SAŁKOWSKI, T. WASZCZUK, *Automatic eye vizualization and ultrasonic intensity determination in focused beams by means of electrodynamic and capacitance methods*, Ultrasonics in Medicine, ed. KATZNER *et al.*, Excerpta Medica, Amsterdam – Oxford 1975.

[2] L. FILIPCZYŃSKI, I. ROSZKOWSKI, *Ultrasonic diagnosis in obstetrics and gynaecology* (in Polish), PZWL, Warsaw 1977.

[3] M. HUBELBANK, O. J. TRETIAK, *Focused ultrasonic transducer design*, M. I. T. Res. Lab. Elec. Q. P. R. 1971, 169-177 (1971).

[4] G. KOSSOFF *et al.*, *Annular phased arrays in ultrasonic obstetrical examinations*, Advanced Study Institute, Ultrasonic Diagnostics, Milan, June 1974.

[5] T. KUJAWSKA, *Dynamic focusing of an ultrasonic beam by a phased array using the pulse method*, Archives of Acoustics (in press).

[6] T. MARUK-KUJAWSKA, *Dynamic focusing of an ultrasonic beam by annular transducers* (in Polish), doct. diss., Institute of Fundamental Technological Research, Polish Academy of Sciences, Warsaw 1980.

[7] H. E. MELTON, F. L. THURSTONE, *Annular array design and logarithmic processing for ultrasonic imaging*, Ultrasound in Biology and Medicine, 4, 1-12 (1978).

[8] T. WASZCZUK, J. SOMER, *System for dynamic focusing of an ultrasonic beam using annular array, practical implementation*, Proc. XXVII Open Seminar on Acoustics, Warsaw – Puławy, September 1980.

Received on 10 March, 1983.

ARCHIVES OF ACOUSTICS
8, 3, 205-222 (1983)

DETECTABILITY OF CALCIFICATIONS IN BREAST TISSUES BY THE ULTRASONIC ECHO METHOD

LESZEK FILIPCZYŃSKI

Department of Ultrasound, Institute of Fundamental Technological Research, Polish Academy of Sciences
(00-049 Warsaw, ul. Świętokrzyska 21)

The tumour processes in breasts involve calcifications which can be detected using ultrasonic methods. The aim of the present paper is to determine the minimum size of these calcifications which can be detected by the ultrasonic echo method.

The models of the calcification which was assumed in this paper are a rigid and an elastic sphere onto which a plane wave is incident. Such density and longitudinal wave velocity were assumed here as are characteristic of the skull bone, and it is for these values that the far field form function $f_\infty(ka)$ was determined for different values of the Poisson's ratio.

On the basis of these calcification models, the detectability of the calcification by the echo method was evaluated, showing that, when a typical ultrasonograph at a frequency of 3 MHz is used, sphere-shaped calcifications with radii from 4 μm to 52 μm, depending on the depth at which they occur, give signals at the level of the electronic noise of the ultrasonograph.

Experimental research has shown that the detectability by the echo method is restricted by breast tissue heterogeneities which cause the interfering background to occur. The level of these interference signals was determined at a frequency of 3 MHz. At 4 cm depth this level was higher by 31 dB than the electronic noise level. From these results, the present author determined the radii of calcifications detectable by the echo method at a level higher by 20 dB (ten times higher) than the level of the tissue interference signal. The radii are 0.05, 0.15 and 1 mm long at the respective depths of 2, 4 and 6 cm. Their dependence on the depth results mainly from the wave attenuation in tissues, which increases as the depth at which a given calcification is, grows. A linear receiver should be used for calcification detection.

Notation

A — attenuation loss on the path of the wave
a — radius of the sphere
c — wave velocity in soft tissue

c_m — expansion coefficients
m — natural number
c_L — longitudinal wave velocity in the calcification
c_T — transverse wave velocity in the calcification
c — wave velocity in the medium which constitutes the tissue reflector
D — level increase caused by tissue interference (Fig. 10)
$f_\infty(ka)$ — far field form function
$h^{(2)}$ — spherical Hankel function of the second kind
$h^{(2)'}$ — derivative of the function $h^{(2)}$ with respect to the argument
j — $\sqrt{-1}$
j_m — spherical Bessel function
j'_m, j''_m — derivatives of the function j_m with respect to the argument
$k = \omega/c$ — wave number
n_m — spherical Neumann function
n'_m — derivative of the function n_m with respect to the argument
N — electronic noise level
P_m — Legendre polynomial
p_i — pressure of the plane wave incident on the sphere
p_0 — pressure amplitude of the plane wave
p_s — pressure of the wave scattered by the sphere
p_{s0} — pressure amplitude of the wave scattered by the sphere
R — depth at which the calcification occurs
r — radial component of the polar coordinate system
T — double electroacoustic transducing loss
t — time
U_r — electric sensitivity of the ultrasonograph receiver
U_t — output voltage of the ultrasonograph transmitter in a pulse
W — electric dynamics of the ultrasonograph
x, x_1, x_2 — auxiliary quantities (see formulae (12a b, c))
α — pressure attenuation coefficient
η_m — phase angle of partial spherical waves reflected
θ — angular coordinate of the polar coordinate system
ν — Poisson's ratio
ϱ — density of the tissue medium
ϱ_s — density of the sphere
ϱ' — density of the tissue reflector
φ_m — auxiliary quantity (see formula (11))
ω — angular frequency

1. Introduction

The ultrasonic method is one of the more recent ways of detecting breast tumours [14]. Despite the intensive research performed on it in a large number of scientific centres, the possibilities of the ultrasonic diagnosis of breast tumours are far from exhausted. One example of the developments in this field is the Doppler ultrasonic methods which permit the observation of changes in the blood supply to the tumour when it is malignant [15].

Another problem in the diagnosis of breast tumours is the detection of calcifications by the ultrasonic echo method. The reactions which proceed

in breast tissue cells and which cause calcifications when the cancer occurs are present in a very early stage of its development. They usually occur prior to the infiltrative phase, which is visible in a mammogram or an X-ray microgram preparation [16].

The detection of the microcalcifications is therefore fundamentally significant in the early diagnosis of breast tumours. In view of this, the question arises as to what are the possibilities of detecting small calcifications by the ultrasonic method.

The recent papers on the problems in ultrasonic investigations of the breast report on microcalcifications being detected only by mammographic methods; they cannot be detected, however, by ultrasound [21].

This paper presents an attempt to explain this problem and to determine the minimum calcification size which can be detected by ultrasonic echo method.

2. Assumptions of the analysis

Fig. 1 shows the ultrasonic system used here for detecting calcifications by the echo method. The first stage of these considerations consists in an evaluation of the magnitude of the ultrasonic wave reflected from a sphere-shaped calcification with a radius a.

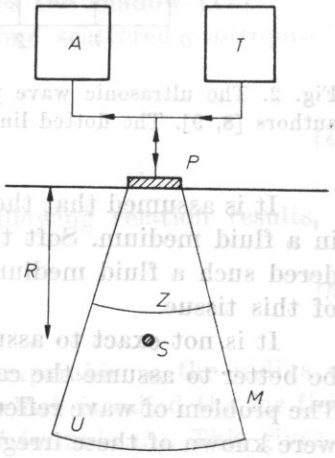

Fig. 1. The ultrasonographic system used in the investigations. T – transmitter, A – receiver, P – piezoelectric transducer swinging over an angle of 30°, M – medium investigated, S – calcification, U – area of the medium covered by the ultrasonic beam, Z – electronic distance indicator, R – depth at which the calcification occurs

It is assumed that the acoustic parameters of this calcification are the same as those of bone tissue. This assumption is justified by that about 66 per cent of the bone mass consists of inorganic matter, including mainly calcium salts [19]. The acoustic properties of bone tissue have been investigated by a large number of authors, who have obtained a rather considerable scatter

of the measured values. Fig. 2 shows the results of ultrasonic wave velocity measurements, drawn from the available literature [8, 9]. The present considerations are based on the results of the measurements of WHITE *et al.* [23], who, working on rather ample experimental material, obtained the following data for the skull bones: the longitudinal wave velocity $c_L = 3.2$ km/s, the density $\varrho = 2.23$ g/cm^3, the specific acoustic impedance $c_L = 7.1 \times 10^5$ g cm^{-2} s^{-1}. Neither these authors nor any other have given data on the transverse wave velocity.

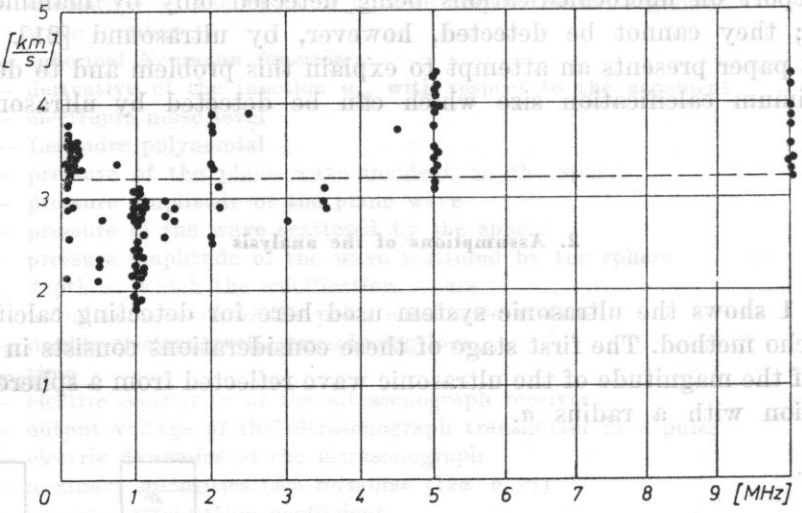

Fig. 2. The ultrasonic wave propagation velocity in bone tissue, measured by different authors [8, 9]. The dotted line indicates the value assumed in the present considerations

It is assumed that the calcification has the shape of a sphere and is placed in a fluid medium. Soft tissue can with rather good approximation be considered such a fluid medium and water, in turn, can be a good approximation of this tissue.

It is not exact to assume that the calcification is sphere-shaped. It would be better to assume the calcification as a solid with irregularly shaped surface. The problem of wave reflection from such a solid could be solved if the statistics were known of these irregularities [24]. These data are not available, however, there is also a lack of the simpler information on the density, the elastic properties of the calcifications etc. There is also no information on the heterogeneity of these calcifications which occur in the breast.

In view of this, the present problem must be considered with approximation, by assuming two calcification models: in the form of an ideal rigid sphere and an ideal elastic one. The analysis will be performed for steady-state (continuous wave).

3. Ultrasonic wave reflection from a rigid sphere

The acoustic pressure of a plane wave incident in a fluid onto the sphere can be represented, in a polar coordinate system whose centre coincides with the centre of the sphere, in the form of the infinite series [20, 17]

$$p_i = p_0 \exp(j\omega t + kr\cos\theta) = p_0 \exp(j\omega t) \sum_{m=0} j^m (2m+1) P_m(\cos\theta) j_m(kr). \tag{1}$$

The acoustic pressure of the wave scattered by the sphere is in the form

$$p_s = \sum_{m=0}^{\infty} c_m P_m(\cos\theta) h_m^{(2)}(kr) \exp(j\omega t), \tag{2}$$

where the expansion coefficients c_m are determined from the boundary conditions on the surface of the sphere. When the sphere is rigid and immovable, these coefficients take the form

$$c_m = j^m (2m+1) \frac{j_m'(ka)}{h_m^{(2)}(ka)}. \tag{3}$$

When the wavelength is very short with respect to the radius of the rigid sphere, the power scattered by the sphere is $\pi a^2 I_0$, where I_0 is the intensity of the incident plane wave; the same power is concentrated into a narrow beam which interferes with the primary beam and causes the shadow [17].

Comparison of the incident power with the one scattered isotropically by the sphere gives the equation

$$\frac{\pi a^2 p_0^2}{2\varrho c} = \frac{4\pi r^2 p_{s0}^2}{2\varrho c}, \tag{4}$$

where the distance $r \gg a$. Hence, directly the following relation results,

$$p_{s0} = p_0 \frac{a}{2r}. \tag{5}$$

In a general case, when the wavelength is comparable to the radius of the sphere or longer, the additional factor $f_\infty(ka)$, which is called the far field form function, is introduced into the right side of formula (5). This gives

$$p_{s0} = p_0 \frac{a}{2r} f_\infty(ka). \tag{6}$$

For the rigid sphere the function $f_\infty(ka)$ takes the form of the curve S shown in Fig. 3 [13]. The undulations in the curve result from the wave interference around the sphere, since, in view of its ideal rigidity, the wave does

not penetrate inside. In real calcifications, whose surface is irregular and whose shape is only similar to a sphere, the curve is not so regular as in Fig. 3.

The previous considerations were concerned with an immovable sphere. When affected by the incident wave, the sphere can move freely. This problem was investigated by HICKLING and WANG [13], who showed that a rigid sphere

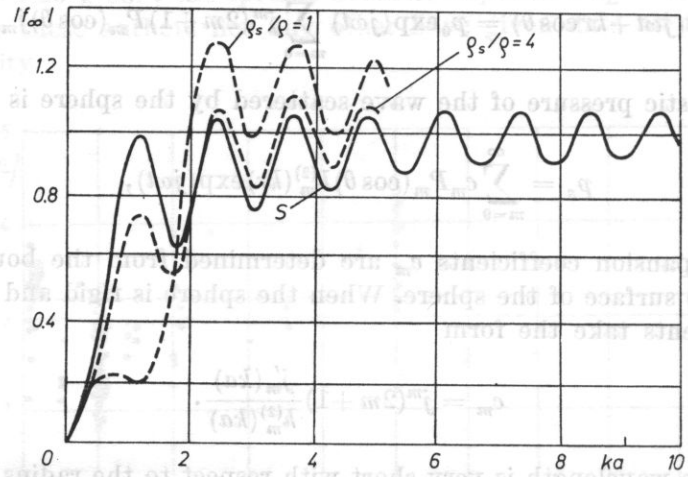

Fig. 3. The function $f_\infty(ka)$ for a rigid sphere in a fluid, according to HICKLING and WANG [13]

vibrates when acoustic pressure acts on it. In view of this, the form of the function $f_\infty(ka)$ changes, particularly over the range $ka < 5$. The magnitude of this change depends on the density of the sphere and on the density of the surrounding medium. Fig. 3 shows curves calculated by HICKLING and WANG for the ratios $\varrho_s/\varrho = 1$ and 4.

For the calcifications of interest here, whose density is about twice as large as that of the surrounding tissue, the real curve of $f_\infty(ka)$ should be close to both curves in Fig. 3.

4. Ultrasonic wave reflection from an elastic sphere

In the case of an ideal elastic sphere the problem of reflection becomes more complex [2, 3, 12, 18]. In addition to reflected waves, longitudinal and transverse waves penetrate inside the sphere. The latter waves arise at the interface of the fluid medium and the sphere. The expansion coefficients (2) take then the form

$$c_m = -p_0(-j)^{m+1}(2m+1)\sin\eta_m \exp(j\eta_m). \tag{7}$$

The angle η_m is a function of the velocity of longitudinal and transverse waves within the sphere and of longitudinal waves in the surrounding medium,

and of the radius of the sphere and frequency. The way of determining the angles η_m was given in paper [3] and subsequently verified in papers [12, 22].

With backscattering ($\theta = 180°$) the Legendre polynomials disappear from expression (2), since $P_m(-1) = (-1)^m$. For long distances a spherical Hankel function can be represented by the asymptotic expression [20]

$$h_m^{(2)}(kr) = \frac{1}{kr} \exp\left[-j\left(kr - \frac{m+1}{2}\pi\right)\right]. \tag{8}$$

Thus, when coefficients (7) are taken into account and the time factor neglected, formula (2) becomes [18]

$$p_s = p_0 \frac{a}{2r}\left[\frac{-2}{ka}\sum_{m=0}^{\infty}(2m+1)(-1)^m \sin\eta_m \exp(j\eta_m)\right] = p_0 \frac{a}{2r} f_\infty(ka), \tag{9}$$

where

$$\tan\eta_m = -\frac{j_m(x)}{n_m(x)}\left[\tan\varphi_m - x\frac{j_m'(x)}{j_m(x)}\right]\left[\tan\varphi_m - x\frac{n_m'(x)}{n_m(x)}\right]^{-1} \tag{10}$$

and

$$\tan\varphi_m = \frac{\varrho}{\varrho_s}\left[\frac{x_2^2}{2}\frac{\dfrac{x_1 j_m''(x_1)}{x_1 j_m'(x_1) - j_m(x_1)} - \dfrac{2(m^2+m)j_m(x_2)}{(m^2+m-2)j_m(x_2) + x_2^2 j_m''(x_2)}}{\dfrac{x_1^2\{[\nu/(1-2\nu)]j_m(x_1) - j_m''(x_1)\}}{x_1 j_m'(x_1) - j_m(x_1)} - \dfrac{2(m^2+m)[j_m(x_2) - x_2 j_m'(x_2)]}{(m^2+m-2)j_m(x_2) + x_2^2 j_m''(x_2)}}\right]. \tag{11}$$

Expressions (10) and (11) include the quantities

$$x = ka = \frac{\omega}{c}a, \quad x_1 = k_1 a = \frac{\omega}{c_L}a, \quad x_2 = k_2 a = \frac{\omega}{c_T}a \tag{12a,b,c}$$

and the Poisson's ratio ν which is related to the velocity of longitudinal and transverse waves by the relation

$$c_T = c_L\sqrt{\frac{1-2\nu}{2(1-\nu)}}. \tag{13}$$

Fig. 4 gives the values of the Poisson's ratio for different materials, depending on the ratio of the transverse wave velocity to the longitudinal wave velocity. This ratio increases as the material becomes in terms of elasticity increasingly similar to a fluid, for which it reaches the value $\nu = 0.5$. In view of their elastic properties, it seems that calcifications should be assigned to the group of materials close to glass, porcelain or molten quartz, for which the Poisson's ratio ν varies between 0.17-0.26.

Taking as the basis the theory of wave reflection from an ideal elastic sphere, from formulae (9), (10) and (11), the far field form function $f_\infty(ka)$ was

determined for the parameters of calcifications given in point 3, with different values of the Poisson's ratio $\nu = 0$; 0.1; 0.2; 0.3 and 0.4. These calculations were carried out on a Cyber 70 (IBM) computer and their results are shown in Figs. 5 and 6. It follows from the curves obtained that a distinct effect of

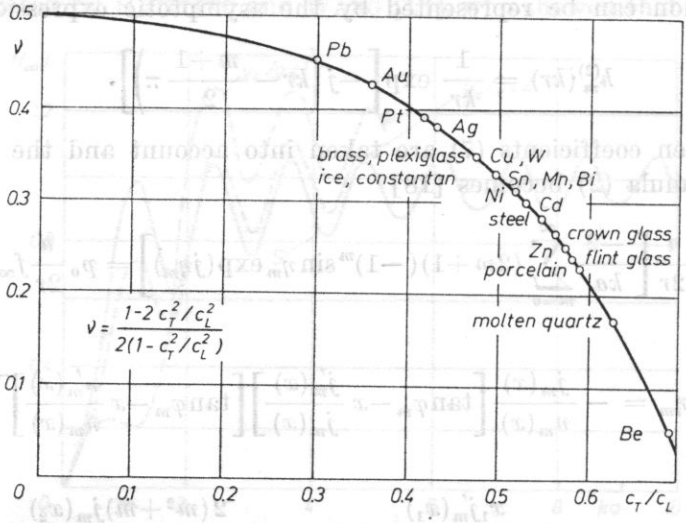

Fig. 4. The Poisson's ratio ν for different materials, depending on the ratio of the transverse wave velocity c_T to the longitudinal wave velocity c_L

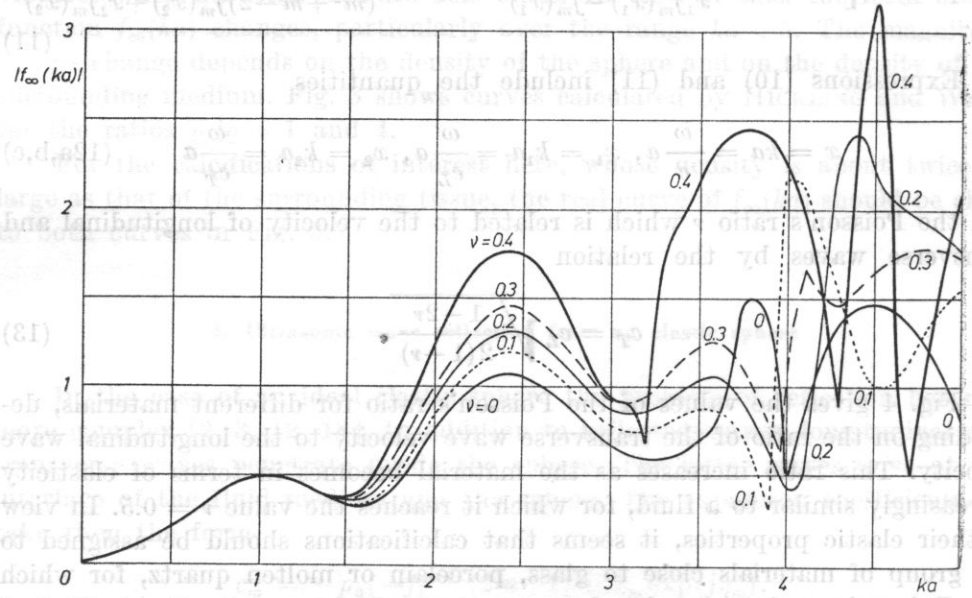

Fig. 5. The function $f_\infty(ka)$ of the sphere (in the calcification for $c_L = 3.2$ km/s, $\varrho_s = 2.23$ g/cm^3, in the tissue for $c_L = 1.5$ km/s, $\varrho = 1$ g/cm^3) determined for various values of the Poisson's ratio ν

the Poisson's ratio on the behaviour of the function $f_\infty(ka)$ does not occur until the value $ka > 1.5$.

It is interesting to note that the existing theories of wave scattering by elastic spheres apply to immovable spheres. It should not be excluded that, as for rigid spheres, the phenomenon of scattering will behave in a slightly

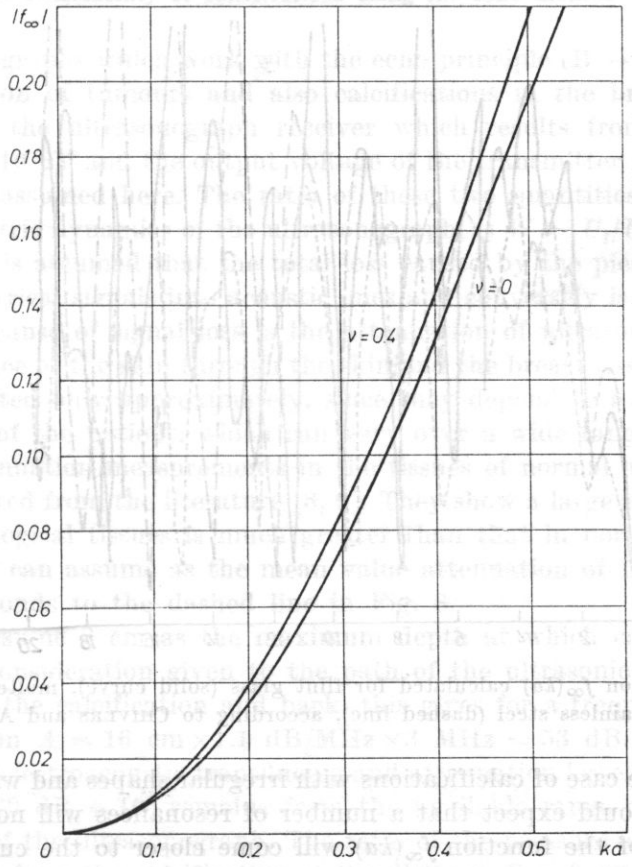

Fig. 6. The function $f_\infty(ka)$ of the sphere as in Fig. 5 but for small arguments of ka

different way, when the possibility of spheres being movable under the effect of pressures acting on their surfaces is taken into account.

Fig. 7 shows the functions $f_\infty(ka)$ calculated for flint glass, molten silica and stainless steel by CHIVERS and ANSON [1], which all show similar behaviour. Their maxima and minima result from the interference of waves around the sphere and also from resonances within it.

In their investigations of the scattering phenomenon, FLAX *et al.* [7] used a formalism drawn from nuclear reaction theory. They showed that in the case of bodies with density and wave velocities greater than those of the surro-

unding fluid, scattering is a result of the superposition of the phenomenon of wave scattering by a rigid body and a number of resonances which occur in these bodies. These resonances differ in character, since they correspond to different wave types, including, for example, also surface waves and waves of the "whispering gallery" type.

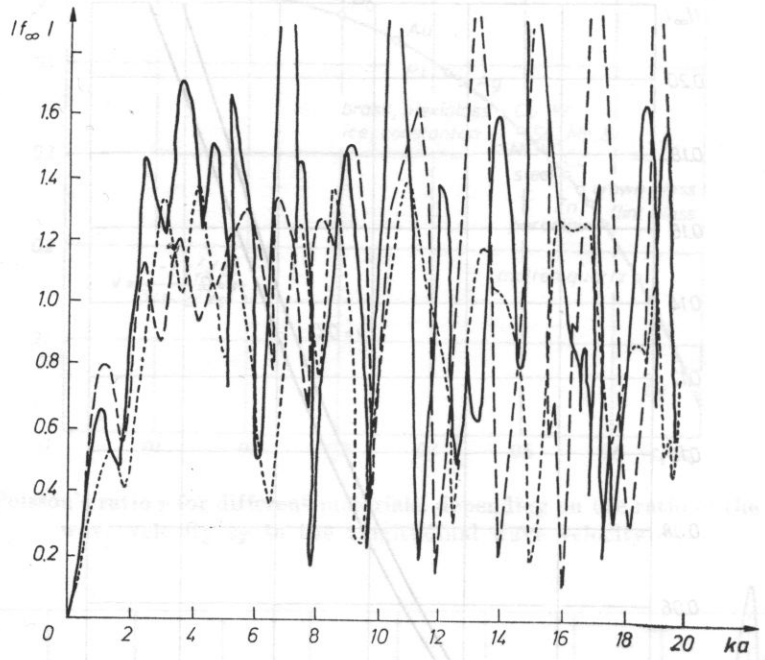

Fig. 7. The function $f_\infty(ka)$ calculated for flint glass (solid curve), molten silica (dotted line) and stainless steel (dashed line), according to CHIVERS and ANSON [1]

Thus, in the case of calcifications with irregular shapes and with corrugated surfaces, one should expect that a number of resonances will not occur at all and the curve of the function $f_\infty(ka)$ will come closer to the curve of a rigid body. From Fig. 7, it can thus be assumed that the maxima and minima will smooth out about the mean value, which for $ka > 3$ can be taken as $f_\infty(ka) = 1$. A similar conclusion can be drawn for rigid spheres (Fig. 3).

Extensive experimental investigations of the scattering of acoustic waves by metal (aluminium and brass) spheres submerged in water were carried out by HAMTON and MCKINEY [11] over the range 4.1 — 57 of the product ka. They showed that for large values of ka, backscattering is constant as a function of scattering and slightly less than follows from theoretical data for a rigid sphere. The present assumption of the constant value of the function $f_\infty(ka)$ was thus confirmed experimentally. It is, however, necessary to note that the conclusion formulated above for large values of ka only applies to the amplitudes of pulses reflected from the surface of the sphere and is not valid for those

which arise as a result of multiple reflection within the sphere. This condition corresponds to a lack of resonances, i.e. such a situation which is expected with calcification of irregular shape and unsumooth surface.

5. Detectability of calcifications using the echo method

Ultrasonographs which work with the echo principle (B – mode) are used in the detection of tumours and also calcifications in the breast. A typical sensitivity of the ultrasonograph receiver which results from its electronic noise is $U_r = 10$ μV and the output voltage of the transmitter in a pulse $U_t = 250$ V are assumed here. The ratio of these two quantities, which will be called the electric dynamics of the ultrasonograph, is $W = U_t/U_r = 2.5 \times 10^7 = 148$ dB. It is assumed that the total loss caused by the piezoelectric transducing of electrical signals into acoustic ones and conversely is $T = 15$ dB [5].

Another cause of signal loss is the attenuation of ultrasound on its path from the surface of the skin through the skin and the breast tissue. These losses can be evaluated only approximately, since they depend to a large extent on the anatomy of the patient, which can vary over a wide range. Fig. 8 shows values of attenuation measurements in the tissues of normal and pathological breasts, collected from the literature [8, 9]. They show a large scatter; attenuation in pathological tissues is much greater than that in normal tissues. For the latter one can assume as the mean value attenuation of 1.1 dB/MHz cm, which corresponds to the dashed line in Fig. 8.

Let us assume 8 cm as the maximum depth at which calcifications can occur. With consideration given to the path of the ultrasonic wave from the transducer to the calcification and back, this gives for a frequency of 3 MHz the attenuation $A = 16$ cm $\times 1.1$ dB/MHz $\times 3$ MHz $= 53$ dB.

After the electroacoustic transducing and attenuation losses are subtracted, $W - T - A = 80$ dB $\doteq 10^4$ remains from the available range of the electrical dynamics W of the ultrasonograph. The ratio of the pressure amplitude of the wave reflected from the calcification at the distance $R = 8$ cm to the pressure amplitude of the wave incident on the calcification should be higher than a value of 10^{-4}. Only than the electrical signal detected by the ultrasonograph will be greater than the electronic noise level of the receiver.

When a rigid, immovable sphere is assumed as the calcification model, for $ka < 1$ it is possible to write, according to RSHEVKIN [20],

$$p_s = -p_0 \frac{(ka)^3}{3kr}\left(1 + \frac{3}{2}\cos\theta\right)\exp[j(\omega t - kr)]. \tag{14}$$

Hence, in the case of backscattering when $\theta = 0$ (Rshevkin [20]), unlike the papers cited above [3, 12, 22], the opposite incidence direction of the wave is assumed here; hence, the angle $\theta = 0$ and not 180°, and neglecting the phase

factor, for $ka < 1$,

$$\frac{p_s}{p_0} = \frac{5}{6}\frac{(ka)^3}{kr} > 10^{-4}. \tag{15}$$

The solution of inequality (15) gives the condition $ka > 0.5$.

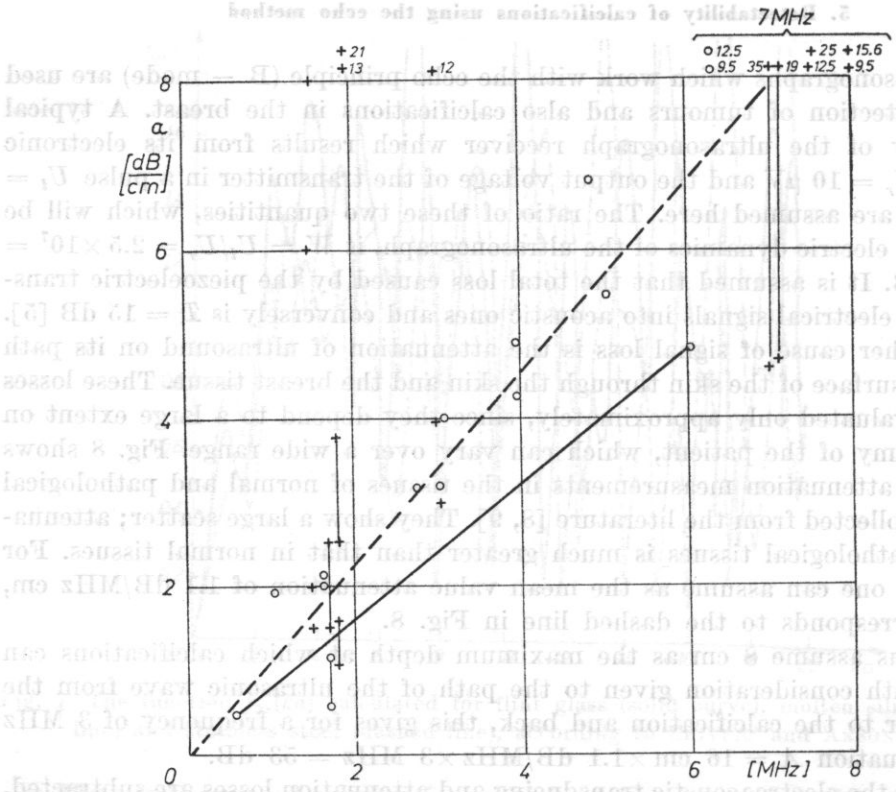

Fig. 8. Attenuation in the tissue of normal (points) and pathological (crosses) breasts, measured by different authors [8, 9]. The solid lines represent the measured value ranges given by the authors. (The values beyond the range of the diagram are given at the points and crosses). The dashed line represents the value of attenuation assumed in the present calcifications

When an elastic sphere is assumed as the calcification model, from formula (9),

$$\frac{p_s}{p_0} = \frac{ka}{2kr} f_\infty(ka) > 10^{-4}. \tag{16}$$

The value of the function $f_\infty(ka)$ can be read from Figs. 5 and 6. Inequality (16) is then satisfied for $ka > 0.65$; the effect of the Poisson's ratio ν can be neglected.

It follows that the two calcification models, the rigid and elastic spheres give a similar value of ka, satisfying inequality (15) or, alternatively, (16).

Assumption of $ka = 0.65$, at a frequency of 3 MHz, gives the radius of the sphere $a = 52$ μm. This sphere gives a signal received by the ultrasonograph; one, however, which is close to its electronic noise level.

For $ka > 3$, from Fig. 7, the function $f_\infty(ka)$ can, according to the conclusions in chapter 4, be assumed to have a value of about one.

Table 1 shows the results of calcifications of the expected radius of the calcification which gives a signal at the level of electronic noise of the ultrasonograph, depending on the depth at which the calcification occurs. Over the range of low values of ka, $ka < 0.65$, the assumption as the calcification model of an elastic sphere (formula (16)) or a rigid, stationary one (formula (15)) gives small differences; in the case of the rigid, stationary sphere model the sphere radii calculated are about 20 per cent smaller. The dependence of the smallest sphere radius on the depth at which the calcification occurs is striking; at depths of 8 and 1 cm these radii are different by an order of magnitude (Fig. 9).

Table 1. The expected radius of a sphere-shaped calcification which gives an electric signal on the electronic noise level, calculated as a function of the depth R at which the calcification occurs, at a frequency of 3 MHz

R [cm]	1	2	4	6	8
A [dB]	7	13	26	40	53
$-(W-T-A)$ [dB]	−126	−120	−107	−93	−80
$-(W-T-A)$ (lin)	5×10^{-7}	10^{-6}	4.5×10^{-6}	2.2×10^{-5}	10^{-4}
ka from (16)	0.05	0.08	0.17	0.34	0.65
ka from (15)	0.042	0.067	0.14	0.27	0.50
a from (16) [μm]	4.0	6.3	13	27	52
a from (15) [μm]	3.3	5.3	11	21	48

It follows from the analysis performed so far that even microcalcifications give signals detected by the ultrasonograph. It does not signify, however, that such signals can be recognized among the many signals obtained at the boundaries of fat, fibre and gland tissues and their heterogeneities. Microphotographs of the milk gland show discrete structures in the form of polygons with diagonals from 50 μm to 200 μm [19]. A lack of information on the value of the scattering coefficient of ultrasound in so heterogeneous breast tissue prevents an evaluation of the tissue interference whose level is much higher than the electronic noise level of the ultrasonograph. The magnitude of the tissue interference signal can be determined experimentally.

6. Experimental investigation of the tissue interference

The experimental investigations were performed using an USK 79/M ultrasonocardiograph, developed at the Department of Ultrasound, Institute of Fundamental Research [6], at a frequency of 3 MHz. This device is equipped

with a piezoelectric transducer of 15 mm diameter with a plastic lens which focuses an ultrasonic beam at a distance of 6 cm from the surface of the transducer. At this distance the width of the ultrasonic beam, measured between — 20 dB levels with respect to the maximum, is 9 mm. The piezoelectric transducer swings over an angle of 30°, thus exploring the area of the body under examination at a frequency of about 25 swings per second.

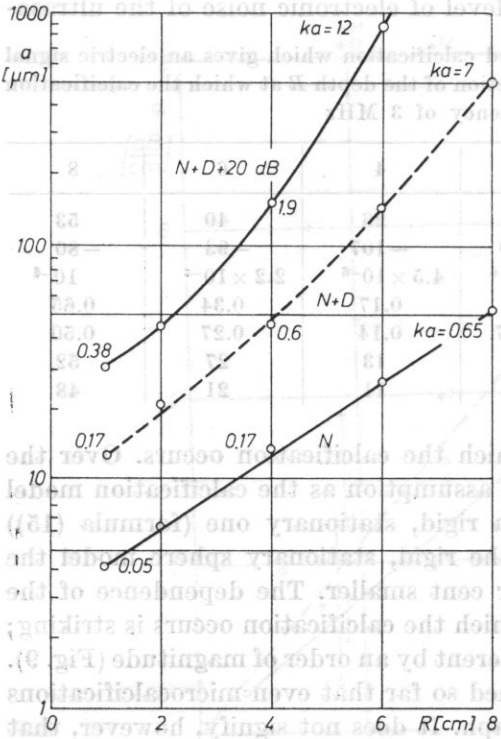

Fig. 9. The expected dependence of the detectability of calcifications on the depth at which they occur in the breast tissue, with the echo method at a frequency of 3 MHz. a — radius of the smallest detectable calcification which gives an electric signal on the electronic noise level (N), on the level of the tissue interference signals ($N+D$) and on a level higher by 20 dB than the tissue interference ($N+D+20$ dB), R — depth at which the calcification occurs. The respective values of ka are given at the points

In order to determine the magnitude of the tissue interference signal, the breasts of three women about 40 years old were examined using this device. The level of this interference signal was determined at a depth of 4 cm (Fig. 10). This level was higher by $D = 31 \pm 4$ dB than the level of the maximum sensitivity N of the ultrasonograph conditioned by the electronic noise.

A hypothetic reflector in the form of a half-space with the characteristic acoustic impedance $\varrho' c'$ can now be introduced. It can be assumed that the tissue interference results from the reflection of a plane wave incident perpendicularly at a flat surface limiting the present hypothetic reflector. The flat surface of the reflector is at the distance $R = 4$ cm from the surface of the probe, i.e. at the same distance at which the tissue interference signal in the women's breasts was measured.

The level of the amplitude of the wave incident on the surface of the hypothetic reflector is, with respect to the level of the electric signal of the transmit-

ter (Fig. 10),

$$-T/2-A/2 \quad [\text{dB}]. \tag{17}$$

Simplifying the problem, one can neglect the focusing of the ultrasonic beam, which in the present case is small, in view of the low ratio of the diameter of the transducer to the focal length, i.e. 0.25.

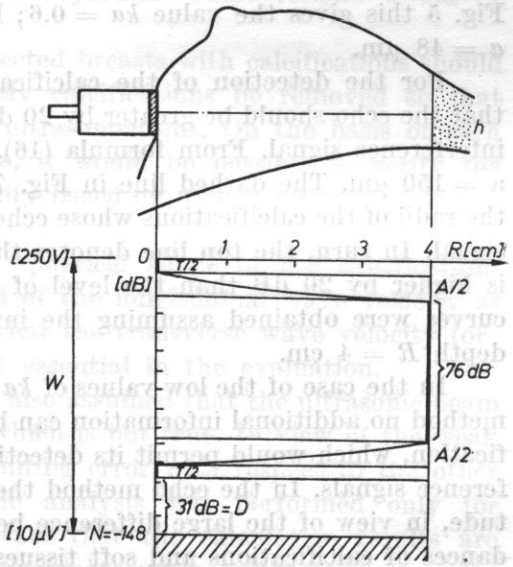

Fig. 10. The signal level as a function of the distance R in the determination of the tissue interference in the breast. 0 – level of the electric signal transmitted, T – electroacoustic transducing loss, A – wave attenuation loss, N – electronic noise level, D – experimentally determined increase in the level caused by the tissue interference signals, W – electrical dynamics of the ultrasonograph, h – hypothetic tissue reflector

The level of the amplitude of the wave reflected from the reflector is

$$N+D+T/2+A/2 \quad [\text{dB}]. \tag{18}$$

The difference between levels (18) and (17) corresponds to the amplitude ratio of the reflected wave to the one incident on the surface of the reflector. Consideration of the values $N = 148$ dB, $D = 31$ dB, $T = 15$ dB and $A = 26$ dB, gives

$$N+D+T+A = -76 \text{ dB} = 1.6\times10^{-4} = \frac{\varrho c-\varrho' c'}{\varrho c+\varrho' c'} \cong \frac{\Delta\varrho c}{2\varrho c}. \tag{19}$$

In expression (19) the amplitude ratio of these waves is equated to the reflection coefficient of the plane wave at the interface between the tissue medium and the hypothetic reflector. The tissue medium would then show very small changes in the acoustic impedance $\Delta\varrho c/\varrho c = 3.2\times10^{-4}$, which cause the tissue interference.

The present considerations were reduced to the equivalent (hypothetic) flat reflector. In reality the dimensions of the interfering tissue heterogeneities are comparable to the wavelength and, therefore, the scattering of the detected wave can be assumed and the amplitude of this wave decreases with increasing

distance. Real, local differences in the acoustic impedance of the tissue medium can then be greater by an order of magnitude than the value of (19).

On the basis of the value of relation (19), from formula (16), it is possible to determine the product ka of a sphere-shaped calcification which gives an echo at the level of the tissue interference signal. For the value of $f_\infty(ka)$ in Fig. 5 this gives the value $ka = 0.6$; hence, the radius of the calcification is $a = 48$ μm.

For the detection of the calcification to be certain, it can be assumed that the echo should be greater by 20 dB (10 times) than the level of the tissue interference signal. From formula (16), in this case $ka = 1.9$ and accordingly $a = 150$ μm. The dashed line in Fig. 7 represents as a function of the depth the radii of the calcifications whose echo is at the level of the tissue interference signal. In turn, the top line denotes the radii of the calcifications whose echo is higher by 20 dB than the level of the tissue interference signal. The two curves were obtained assuming the interference signal level measured at the depth $R = 4$ cm.

In the case of the low values of ka for calcifications detected by the echo method no additional information can be obtained, e.g. on the shape of a calcification, which would permit its detection from the background of tissue interference signals. In the echo method the only discriminator is the signal amplitude, in view of the large difference between the characteristic acoustic impedances of calcifications and soft tissues. It is therefore ill-advised in this case to use typical ultrasonographic equipment with a receiver of logarithmic characteristic, which introduces a compression of echoes detected. The receiver should show a linear relationship between the output and input voltages.

7. Conclusions

It was shown that in the echo method using a typical ultrasonograph at a frequency of 3 MHz sphere-shaped calcifications with radii from 4 μm to 52 μm, depending on the depth at which they occur, give signals at the electronic noise level.

The detectability by the echo method is restricted by breast tissue heterogeneities which constitute the background of the tissue interference signals. The level of these interference signals was determined by examinations of normal breasts in 3 women about 40 years old, at a depth of 4 cm. From these results, the radii of the calcifications were determined which give a signal level 20 dB higher than the level of the tissue interference signals. These radii are 0.05; 0.15 and 1 mm at the respective depths of 2, 4 and 6 cm (Fig. 9). Their dependence on the depth results mainly from the attenuation loss in the tissue which in turn depends on the path of ultrasonic waves.

In the examinations by the echo method it is desired that a receiver with a linear relationship between the output and input signals should be used, since the use of logarithmic receivers causes signals to be compressed. This results in the loss of information on the signal amplitude which distinguishes the echo from a calcification from the echoes constituting the tissue interference background signals. A receiver with an adjustable characteristic would be the best.

It is recommended that tumour-affected breasts with calcifications should be examined clinically and subsequently calcifications be removed so that their size may be correlated with the ultrasonograms. On the basis of such clinical and experimental investigations, it would be possible to verify the present conclusions, which are of neccesity based on a large number of approximations.

These approximations include the spherical shape of the calcifications and the same values of its density and of the longitudinal wave velocity as those of the skull bone. It was shown that the transverse wave velocity (or the value of the Poisson's ratio) is not essential in the evaluation.

In the present considerations it was also assumed that the ultrasonic beam is a parallel homogeneous plane wave, which is not true. In view of the weak focusing of the beam, however, the resulting error with respect to the other approximations can be neglected. The analysis was performed only for steady-state (continuous wave). This means that the calculation results are exact for small radii a and become approximate when a increases.

Acknowledgement. The author is grateful to Dr. G. ŁYPACEWICZ for her measurements in breasts and to Dr. T. KUJAWSKA for her elaboration of computer programs.

References

[1] R. C. CHIVERS, L. W. ANSON, *Calculations of the backscattering and radiation force functions of spherical targets for use in ultrasonic beam assessment*, Ultrasonics, **20**, 1, 1, 25-34 (1982).

[2] L. DRAGONETTE, M. VOGT, L. FLAX, W. NEUBAUER, *Acoustic reflection from elastic spheres* II. *Transient analysis*, J. Acoust. Soc. Am., **55**, 1130-1137 (1974).

[3] J. FARAN, *Sound scattering by solid cylinders and spheres*, J. Acoust. Soc. Am., **23**, 4, 405-418 (1951).

[4] L. FILIPCZYŃSKI, I. ROSZKOWSKI (eds), *Ultrasonic diagnosis in obstetrics and gynaecology* (in Polish), PZWL, Warsaw 1977.

[5] L. FILIPCZYŃSKI, *Detectability of gas bubbles in blood by the ultrasonic method*, Archives of Acoustics (in press).

[6] L. FILIPCZYŃSKI, J. SAŁKOWSKI, *Attempts at the ultrasonic visualization of the heart in real time*, Archives of Acoustics, **2**, 225-230 (1977).

[7] L. FLAX, C. R. DRAGONETTE, H. UBERALL, *Theory of elastic resonance excitation by sound scattering*, J. Acoust. Soc. Am., **63**, 3, 723-731 (1978).

[8] S. Goss, E. Johnston, F. Dunn, *Comprehensive compilation of empirical ultrasonic properties of mammalian tissues*, J. Acoust. Soc. Am., **64**, 2, 423-457 (1978).

[9] S. Goss, E. Johnston, F. Funn, *Compilation of empirical properties of mammalian tissues*. II, J. Acoust. Soc. Am., **68**, 1, 93-107 (1980).

[10] B. J. Hackeloer, B. Huneke, V. Duda, R. Eulenburg, G. Lauth, R. Buchholz, *Sonografische Differentialdiagnose der Mammakarzinome*, Ultraschall in der Medizine, **2**, 129-134 (1981).

[11] L. D. Hampton, C. M. McKiney, *Experimental study of the scattering of acoustic energy from solid metal spheres in water*, J. Acoust. Soc. Am., **33**, 5, 664-673 (1961).

[12] R. Hickling, *Analysis of echoes from a solid elastic sphere in water*, J. Acoust. Soc. Am., **34**, 1582-1592 (1962).

[13] R. Hickling, N. Wang, *Scattering of sound by a rigid movable sphere*, J. Acoust. Soc. Am., **39**, 276-279 (1966).

[14] C. R. Hill, V. R. McCready, D. O. Cergrove (eds.), *Ultrasound in tumor diagnosis*, Pitman Medical, Kent 1978.

[15] G. Łypacewicz, T. Powałowski, K. Łukawska, *Ultrasonic examination of breast tumors with Doppler method*, Proc. of the 2nd Congress of the Federation of Acoustical Societes of Europe, PAN, Warsaw, II, 153-156, 1978.

[16] V. Menges, *Mammographie, die zuverlässigste Ultersuchungsmethode zur Brustkrebs-Früherkennung*, Electromedica, **2**, 42-49 (1979).

[17] P. Morse, K. Ingard, *Theoretical acoustics*, McGraw Hill, New York 1968.

[18] W. Neubauer, M. Vogt, L. Dragonette, *Acoustic reflection from elastic spheres*. I. *Steady-state signals*, J. Acoust. Soc. Am., **55**, 1123-1129 (1974).

[19] T. Pawlikowski, M. Karasek, M. Pawlikowski, *Histology handbook* (in Polish), PZWZ, Warsaw 1981.

[20] S. N. Rshevkin, *Kurs leksij po teorii zvuka*, Moscow 1980.

[21] *Second International Congress on the Ultrasonic Examination of the Breast*, London June 22-23, 1981, Abstracts, Institute of Cancer Research.

[22] T. Hasegawa, K. Yosioka, *Acoustic radiation force on a solid elastic sphere*, J. Acoust. Soc. Am., **46**, 5 (P2), 1139-1143 (1969).

[23] D. N. White, G. R. Curry, R. J. Stevenson, *The acoustic characteristic of the scull*, Ultrasound in Medicine and Biology, **4**, 3, 225-252 (1978).

[24] Y. N. Chen, S. J. Kim, *Scattering of acoustic waves by a penetrable sphere with statistically corrugated surface*, J. Acoust. Soc. Am., **42**, 1-5 (1967).

Received on 25 January, 1983.

ARCHIVES OF ACOUSTICS
8, 3,223-234 (1983)

AN ULTRASONIC METHOD FOR THE INVESTIGATION OF CORONARY GRAFT PATENCY

ANDRZEJ NOWICKI

Department of Ultrasound, Institute of Fundamental Technological Research, Polish Academy of Sciences
(00-049 Warsaw, ul. Świętokrzyska 21)

JOHN REID

Institute of Applied Physiology and Medicine, Seattle, USA
now at Drexel University, Philadelphia, PA 19104

A new method and system for the visualization of blood flow in coronary grafts is presented. This method is based on the technique of stationary echo cancellation (SEC), phase detection and integration of Doppler signals in real time, using broad-band analog CCD delay lines. Preliminary results of examinations of coronary graft patency for 15 patients are presented.

1. Introduction

Visualization of biological structures in real time is now the main direction in the development of ultrasonic diagnostic methods. With the unquestionable advantages of this new technique, particularly for dynamic imaging of the heart, it neglects the hemodynamic parameters related to the blood flow in the cavities of the heart, in the area of the mitral, aortic, pulmonary and tricuspid valves and in the coronary vessels.

The main aim of this paper is to develop a method and system for noninvasive visualization of blood flow in coronary grafts. At the same time, this method could be used in investigations of children's hearts.

2. Method and system

Of the many methods which are used for the measurement of the hemodynamic parameters, in practice only the so-called Doppler method permits transcutaneous noninvasive measurements of blood flow in the peripheral vessels and in the heart.

The position of the left, anterior coronary graft (LAD), which runs diagonally down from the aorta in the area of the right ventricle outflow track, causes the continuous wave method to be greatly unreliable, in view of the simultaneous effect of the flows in the two vessels (aorta + pulmonary artery) with the left-diagonal position of the probe in the second or third intercostal space and also in view of the motion of the pulmonary valve and, quite frequently, of the

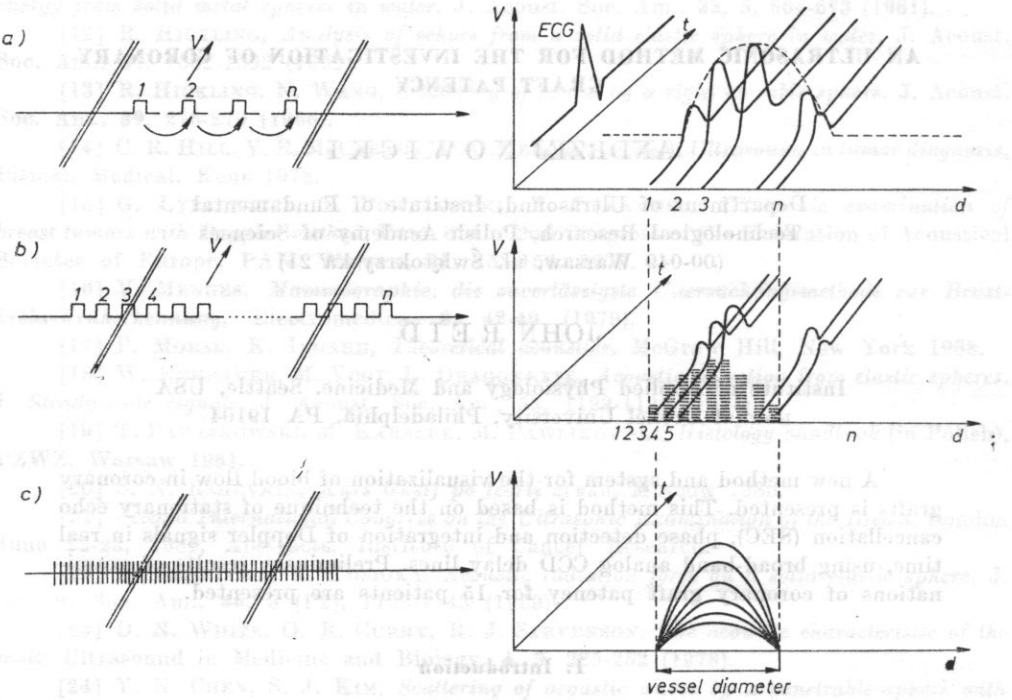

Fig. 1. The performance principle of pulse Doppler systems: *a*) single channel system with one analyzing gate, *b*) multichannel system with *n* parallel gates, *c*) system with stationary echo cancellation (SEC)

mitral valve. The discrimination of the low coronary signal from the large variety of signals from the heart, both from the systole and the diastole, seems to be quite difficult when using *C.W.* Doppler. However, a pulse Doppler method which combines the properties of the echo type and Doppler type equipment, thus providing both frequency and range resolution [2], offers a great promise in this field.

The recent years have brought large developments in Doppler pulse flowmeters, DPF, with three distinct varieties (Fig. 1),

a) Doppler pulse flowmeters with one analyzing gate [6] (e.g. UDP-30 produced by ZD Techpan);

b) Doppler pulse flowmeters with a large number of analyzing gates (e.g. FISH's system with 30 analyzing gates) or with serial digital data processing [1, 4, 5];

c) Doppler pulse flowmeters with stationary echo cancellation [7, 9]. The high cost of the multi-gate equipment, both analog and with serial digital data processing, has encouraged investigations of the third of the systems mentioned above. In addition this was to a large extent affected by the fact that the dynamics of stationary and Doppler signals from the motion of the heart and the blood flow frequently exceeds the range of the fast 8-bit A/D converters now available (with the real dynamics of the Doppler signals being evaluated at 60-90 dB).

The first model of equipment using stationary echo cancellation was developed in 1977-78; it had the coefficient of stationary echo cancellation > 50 dB and a range of $\simeq 5$ cm. Although the cancellation was sufficient, the range was too short for cardiological applications. It resulted from the use in the systems of stationary echo cancellers. They were periodic filters of the first order [7], of quartz delay lines with the delay $T = 64$ μs. This corresponds to a repetition frequency of 15.625 kHz and a range of $\simeq 5$ cm.

In order to increase the range, a new generation of the equipment was developed using CCD delay lines custom-made by Reticon USA in the construction of periodic filters, a phase detector, and an integrator with a positive feedback loop. Such a line consists of 295 "delay elements". The analog signal is controlled by a four-phase signal of the clock frequency f_c. The delay T_0 of the line is $295/f_c$.

The purpose of the equipment affected to a large extent the choice of the frequency f_n and the repetition interval T_p. These two parameters are related to the so-called ambiguity function [6] of Doppler pulse systems. This function describes the relations between the maximum range, resolution and the maximum measured velocity for given values of the parameters f_n and T_p.

In order to avoid the range "ambiguity", the repetition time T_p should be long enough so that the ultrasonic echoes could return to the receiver before the next pulse is transmitted. In view of this, the maximum penetration depth is defined by the expression $d = T_p c/2$, where c is the ultrasound propagation velocity in tissue.

In turn the minimization of the "ambiguity" in the measurement of the flow velocity $V_{\max}$ ($V = f_d c/2f_n$) imposes a converse condition. According to sampling theory, the maximum Doppler frequency f_d must be less than half the repetition frequency f_p ($f_p = 1/T_p$). These two conditions can be given by one expression which restricts the magnitude of the product of the maximum range $d_{\max}$ and the maximum velocity $V_{\max}$,

$$d_{\max} V_{\max} < c^2/8f_n. \tag{1}$$

In investigations of the heart the desired penetration depth should be greater than 10 cm. In a healthy heart the maximum flow velocity usually does not exceed several score cm/s, except the ascending aorta, where the flow velocity can exceed 1.5 m/s. In cases of heart defects this velocity increases greatly and can reach a value of several m/s, at the level of narrowed mitral

and tricuspid valves. In coronary grafts the flow velocity is much lower, not exceeding dozen-odd cm/s.

The technical difficulties related to the accurate measurement of low velocities (of Doppler frequencies < 200 Hz), which are in turn related to the effect of the external interference and the "masking" of signals corresponding to slow flow by those caused by the motion of the heart walls (with the amplitudes of the latter being greater by more than 40 dB than the signals scattered in blood), and the attenuation of ultrasound in blood (this attenuation increases linearly as the frequency increases) restrict the frequency range to be applied in cardiology to 2-5 MHz.

Lower frequencies are usually used on adults; higher, on children.

In the present system the transmitter frequency $f_n = 4$ MHz and the repetition time of transmitted pulses, $T_p = 147{,}5$ μs were chosen. For this repetition time the frequency of the generator controlling an analog CCD delay line is 2 MHz.

It should be noted that the repetition time of high-frequency pulses, the high-frequency signal and the clock signal of the CCD line should be coherent so as to prevent phase drift in the channel of Doppler frequency detection and the drift of the delay of the line with respect to the time of processing transmitted pulses. The repetition interval T_p corresponds to the range $d = 11.4$ cm, under the assumption that the mean velocity c of ultrasound propagation in the body is 1550 m/s. At the level of narrowed valves and in the aorta the permissible range of measured velocities (< 66 cm/s) is too short; it ensures, however, unambiguous measurements in coronary grafts.

In view of the more than hundredfold difference between the level of echoes reflected from the walls of the heart and signals scattered in the blood flowing in coronary vessels and the cavities of the heart, in the solution proposed here the stationary echo cancellation SEC should be greater than 40 dB. This imposes the condition that in the construction of periodic filters SEC of at least the second order should be used. Elements of a theory which describes the performance of such filters were given in a previous paper [9].

Fig. 2 shows a schematic diagram of the device. In view of its similarity to the diagram of the UDP-30 and UDP-30 SEC devices described previously [3, 9], only this part of the system which implements stationary echo cancellation and phase detection and the integrator with a positive feedback loop were described in greater detail.

For this purpose, Fourier analysis was used to give the transforms of time signals at the characteristic points of the system. The signals $f_1(t)$ and $f_4(t)$, whose Fourier transforms are given by the following expressions, are obtained at the output of all the mixers M.

$$F_1(f) = \tfrac{1}{2}[F(f-f_n)+F(f+f_n)]; \tag{2}$$

$$F_4(f) = -\tfrac{1}{2}j[F(f-f_n)-F(f+f_n)]. \tag{3}$$

For a single SEC filter

$$F_{\text{out}}(f) = F_{\text{in}}(f)\exp(-j2\pi fT). \tag{4}$$

For a double SEC filter

$$F_2(f) = F_1(f)[\exp(-j2\pi fT)-1]^2; \tag{5}$$

$$F_5(f) = F_4(f)[\exp(-j2\pi fT)-1]^2. \tag{6}$$

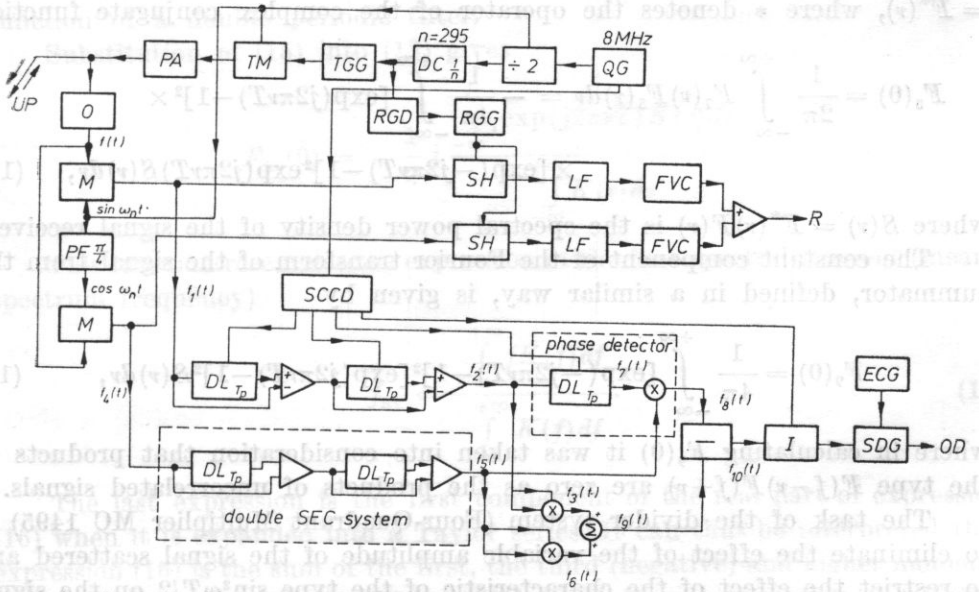

Fig. 2. A schematic diagram of the SEC device: *QG* — quartz generator, *DC* — frequency divider, *TGG* — transmitter gate generator, *TM* — transmitter modulator, *PA* — power amplifier, *UP* — ultrasonic probe, *RGD* — receiver gate delay, *RGG* — receiver gate generator, *SH* — sample and hold system, *LF* — low-pass filter, *FVC* — frequency/voltage converter, *R* — recorder, *O* — receiver, *M* — mixer, *PF* — phase shifter, *DL* — CCD delay line, *SCCD* — four-phase synchronization of CCD delay lines, *I* — integrator, *ECG* — ECG synchronization, *SDG* — systolic/diastolic gate, *OD* — oscilloscope display

According to the properties of Fourier transformation, the product of the signals in the time domain is equal to the convolution of its transforms in the frequency domain,

$$f_a(t)\cdot f_b(t) \leftrightarrow F_a(f) * F_b(f) = \frac{1}{2\pi}\int_{-\infty}^{+\infty} F_a(f-v)F_b(v)\,dv. \tag{7}$$

From (7),

$$F_3(f) = \frac{1}{2\pi}\int_{-\infty}^{+\infty} F_2(f-v)F_2(v)\,dv; \tag{8}$$

$$F_6(f) = \frac{1}{2\pi}\int_{-\infty}^{+\infty} F_5(f-v)F_5(v)\,dv. \tag{9}$$

The constant component of the Fourier transform of the signal at the output of the multiplier system (Four-Quadrant Multiplier IC 8013) has the form

$$F_8(f)_{DC} = F_7(f) * F_5(f) = \frac{1}{2\pi} \int_{-\infty}^{+\infty} F_7(f-\nu) F_5(\nu)\, d\nu. \tag{10}$$

Assuming the identity $F(f)_{DC} = F(0)$ and keeping in mind that $F(-\nu) = F^*(\nu)$, where $*$ denotes the operator of the complex conjugate function

$$F_8(0) = \frac{1}{2\pi} \int_{-\infty}^{+\infty} F_7(\nu) F_5(\nu)\, d\nu = -\frac{1}{4\pi} \int_{-\infty}^{+\infty} [\exp(j2\pi\nu T) - 1]^2 \times$$

$$\times [\exp(-j2\pi\nu T) - 1]^2 \exp(j2\pi\nu T) S(\nu)\, d\nu, \tag{11}$$

where $S(\nu) = F^*(\nu) F(\nu)$ is the spectral power density of the signal received.

The constant component of the Fourier transform of the signal from the summator, defined in a similar way, is given by

$$F_9(0) = \frac{1}{4\pi} \int_{-\infty}^{+\infty} [\exp(-j2\pi\nu T) - 1]^2 [\exp(j2\pi\nu T) - 1]^2 S(\nu)\, d\nu, \tag{12}$$

where in calculating $F_9(0)$ it was taken into consideration that products of the type $F(f-\nu)F(f+\nu)$ are zero as the products of uncorrelated signals.

The task of the divider system (Four-Quadrant Multiplier MC 1495) is to eliminate the effect of the variable amplitude of the signal scattered and to restrict the effect of the characteristic of the type $\sin^2 \omega T/2$ on the signal from the phase detector. Thus,

$$F_{10}(0) = \frac{F_8(0)}{F_9(0)} = -\frac{1}{2} j \frac{\int_{-\infty}^{+\infty} [\exp(j2\pi\nu T) - 1]^2 [\exp(-j2\pi\nu T) - 1]^2}{\int_{-\infty}^{+\infty} [\exp(j2\pi\nu T) - 1]^2 [\exp(-j2\pi\nu T) - 1]^2} \times$$

$$\times \frac{\exp(j2\pi\nu T) S(\nu)\, d\nu}{S(\nu)\, d\nu}. \tag{13}$$

Expression (13) can readily be reduced for one Doppler frequency only, i.e. in the case of one blood corpuscle or a group of corpuscles flowing at the same velocity. In such a case the signal received has the form $A \sin 2\pi\nu_1 t$, $S(\nu_1) = A^2$ and the product $[\exp(j2\pi\nu T) - 1]^2 [\exp(-(2\pi\nu T) - 1]^2 = 16 \sin^4 \pi\nu T$.

After successive simplifications, the real part of expression (13) becomes

$$\mathrm{Re}\, F_{10}(0) = \tfrac{1}{2} \sin 2\pi\nu T. \tag{14}$$

The SEC visualizer, described previously [9], has a similar characteristic: a quasi-monotonous frequency response over the range from $-1/4\, F_p$ to $+1/4 F_p$.

An essential difference, however, is the independence of the output signal of the amplitude of the signal received.

It is more difficult to interpret expression (13) for a wide spectrum of the Doppler frequency. Let

$$[\exp(j2\pi\nu T)-1]^2[\exp(-j2\pi\nu T)-1]^2\ S(\nu) = K(\nu), \tag{15}$$

where $K(\nu)$ is the product of the power density function and the transmission function of a double periodic filter.

Substitution of (15) into (13) gives

$$F_{10}(0) = -\frac{1}{2}j\frac{\int_{-\infty}^{+\infty}\exp(j2\pi\nu T)K(\nu)\,d\nu}{\int_{-\infty}^{+\infty}K(\nu)\,d\nu}. \tag{16}$$

This function resembles the expression of the first spectral moment (mean spectrum frequency)

$$f_{av} = \frac{\int_{-\infty}^{+\infty} fK(f)\,df}{\int_{-\infty}^{+\infty}K(f)\,df}. \tag{17}$$

The last expression is the first component of the real part of expression (16) when it is expanded into a Taylor series. It can thus be interpreted that expression (16) is the sum of the first, the third (negative) and higher moments of the Doppler spectrum. This signifies that in approximation (neglecting the terms of higher orders), a signal proportional to the mean flow velocity in all 295 gates is obtained at the output of the system. In other words, the signal at the oscilloscope *OD* corresponds to the "profiles" of the blood flow velocity.

The real frequency response of the system is shown in Fig. 3.

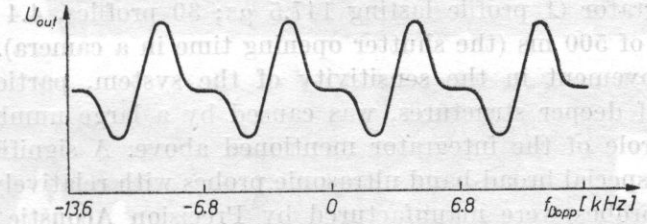

Fig. 3. The frequency response of the SEC device

The signal to noise ratio was greatly improved using an integrator with a feedback loop. The integrator also exerts a significant influence on the "legibility" of the dynamic flow profiles; it is known that instantaneous changes

in the intensity of a scattered Doppler signal, which result from a stochastic distribution of red blood corpuscles in the ultrasonic field, affect to a large extent the signal from the stationary echo canceller and the phase detector. The integrator smooths out these changes and its function can be compared to the role of analog output filters in Doppler flowmeters.

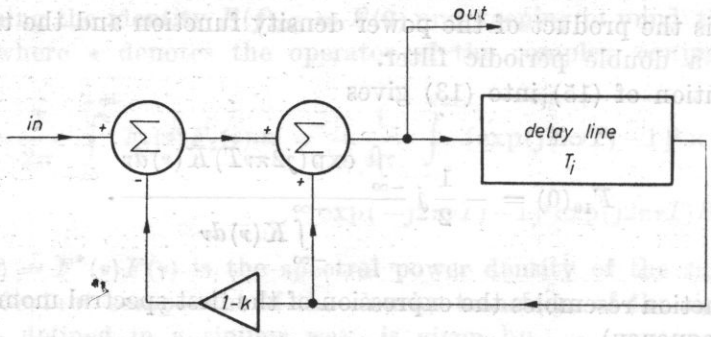

Fig. 4. A schematic diagram of the integrator

In this integrator the effective number of summed-up profiles is about $(1-k)^{-1}$, where $1-k$ is the amplification in the positive feedback loop. A stable performance of the integrator was achieved for a large value of the coefficient k, $k = 0.97$; i.e. about 30 profiles were integrated, increasing the signal to noise ratio by a factor of $\sqrt{30}$ [8].

The delay T_i of the CCD delay line in the integrator is shorter by about 350 ns than the respective delay in SEC systems. The difference results from the fact that the signal in the feedback loop is delayed in addition by the above values in the compensation filters, the operational amplifier $(1-k)$ and the summators.

Fig. 6 shows the performance of the system in the presence of large stationary echoes. The upper curve shows the superposition of more than 100 profiles from the integrator (1 profile lasting 147.5 μs; 30 profiles, 4.4 ms), received for a duration of 500 ms (the shutter opening time in a camera).

The improvement in the sensitivity of the system, particularly in the investigation of deeper structures, was caused by a large number of factors, including the role of the integrator mentioned above. A significant fact was also the use of special broad-band ultrasonic probes with relatively low internal losses. These probes were manufactured by Precision Acoustic Device; they provide multilayered, quarter-wave matching to the medium and very low, or none, damping by the back surface of the transducer.

In turn the identification of flow in coronary grafts was achieved using an electronic gate SDG controlled by the ECG signal of the patient. The performance of the system lies in the letting through or blocking of the output signal

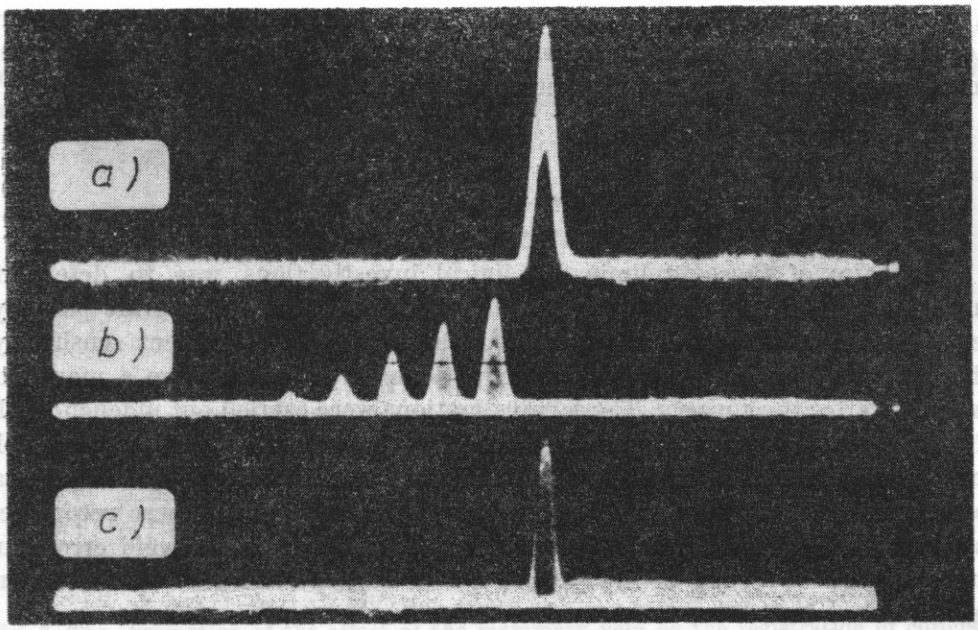

Fig. 5. The performance principle of the integrator: *a*) flow signal "profile" at the output of the integrator, $k = 0.97$; *b*) successive profiles under integration for a delay of the delay line less than the repetition time ($T_{\text{int}} < T_p$); *c*) signal at the input of the integrator for $T_{\text{int}} = T_p$

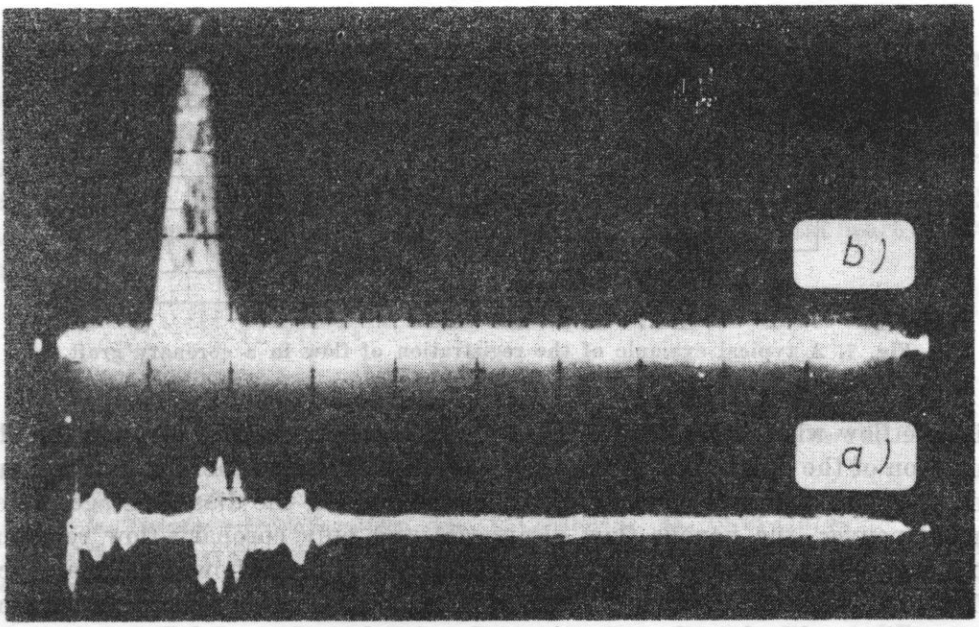

Fig. 6. Ultrasonic echoes: *a*) at the input of the SEC system; *b*) flow "profile" in the carotid artery. Stationary echo cancellation > 60 dB

in particular phases of the heart cycle. In the left, anterior coronary artery most flow occurs in the diastole, whereas the flows in the surrounding vessels (mammary, pulmonary artery) show a distinct systole component.

3. Results of clinical investigations

The aim of these preliminary clinical investigations was to determine the usefulness of the device for the investigation of coronary graft patency, i.e. a class of cases which require the highest possible equipment sensitivity. The examinations were carried out on patients with grafts, from a month to two years after the surgery. These investigations were carried out independently of arteriographic coronographic studies. In view of their readily accessible anatomical situation to the left of the chest in the second or third intercostal space, only left, anterior grafts were examined. Such grafts were recognized as patent which showed a distinct diastole flow. In order to avoid erroneous interpretation of results in the case of a flow superposition in the chest vein, the Valsalva maneuver was used.

After the identification of dynamic flows along the ultrasonic beam simultaneously at 295 gates, the flow velocity was registered at one gate located at a point where a distinct diastole flow occurred on the oscilloscope. An example of the registration of the coronary flow is shown in Fig. 7, where a distinct

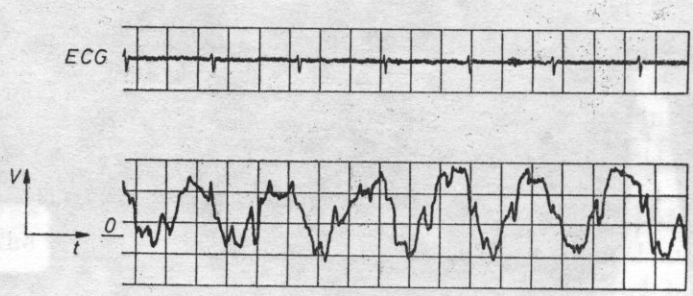

Fig. 7. A typical example of the registration of flow in a coronary graft

diastole flow with respect to the ECG signal can be seen. Fig. 8 shows the elimination of the flow signal in the mammary vein. Prior to the Valsalva maneuver, the signal consists of two distinct components in the diastole stage. After the maneuver, the venous flow disappears and only coronary flow remains. In a group of 15 patients examined arteriographically, 10 showed graft patency whereas 5 did not. In turn an ultrasonic examination showed graft patency in 6 patients; for the other 4 patients the signals registered failed to indicate a distinct diastole flow component.

It should be noted, however, that three of these patients were examined in the early stage of the verification of the method when the integrator, which improves greatly the sensitivity of the method, was not used.

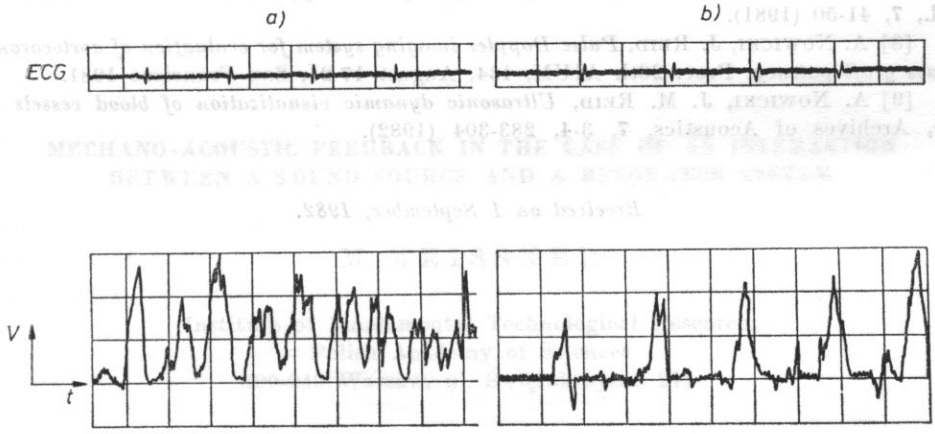

Fig. 8. The elimination of the effect of the mammary vein on the registration of coronary flow: signal before (*a*) and after (*b*) the Valsalva maneuver was used

4. Conclusions

The preliminary investigations of the present method have indicated its potential usefulness in direct evaluation of the dynamics of blood flows in real time both in small vessels and in the cavities of the heart. The noninvasive nature of the ultrasonic investigations makes them very attractive, particularly in the postoperational observation of coronary graft patency. A separate group of applications is the investigations of congenital heart defects in children.

References

[1] M. Brandestini, *Topoflow, a digital full range Doppler velocity meter*, IEEE Trans on Sonics and Ultrasonics, **SU-25**, 287 (1978).

[2] B. Diebold *et al.*, *Noninvasive assessment of aortocoronary bypass graft patency using pulse Doppler echocardiography*, Am. J. Cardiology, **43**, 10-43 (1979).

[3] L. Filipczyński, R. Herczyński, A. Nowicki, T. Powałowski, *Blood flows: hemodynamics and ultrasonic Doppler measurement methods* (in Polish), PWN, Warsaw—Poznań 1980.

[4] P. J. Fish, *Multi-channel, direct resolving Doppler angiography*, Proc. 2nd European Congress on Ultrasonics in Medicine, Munich 12-16 May, publ. Excerpta Medica Amsterdam, 1975.

[5] A. P. G. HOEKS *et al.*, *A multi gate pulse Doppler system with serial data processing*, IEEE Trans. on Sonics and Ultrasonics, **SU-28**, 4, 242-247 (1981).

[6] A. NOWICKI, *Ultrasonic pulse Doppler method in blood flow measurement*, Archives of Acoustics, **2**, 4, 305-323 (1977).

[7] A. NOWICKI, J. REID, *An infinite gate pulse Doppler*, Ultrasound in Med. and Biol., **7**, 41-50 (1981).

[8] A. NOWICKI, J. REID, *Pulse Doppler imaging system for evaluation of aortocoronary bypass graft patency*, Proc. 26th AIUM, 134, August 17-21, San Francisco 1981.

[9] A. NOWICKI, J. M. REID, *Ultrasonic dynamic visualization of blood vessels and flow*, Archives of Acoustics, **7**, 3-4, 283-304 (1982).

Received on 1 September, 1982.

ARCHIVES OF ACOUSTICS
8, 3, 235-248 (1983)

MECHANO-ACOUSTIC FEEDBACK IN THE CASE OF AN INTERACTION BETWEEN A SOUND SOURCE AND A RESONANCE SYSTEM

M. MEISSNER

Institute of Fundamental Technological Research,
Polish Academy of Sciences
(00-049 Warsaw, ul. Świętokrzyska 21)

This paper presents an analysis of the mechano-acoustic feedback between a sound source and a resonance system. In the theoretical part, the change in the mechanical impedance of the sound source which occurs when the source is affected by the external acoustic field is determined; and subsequently, using the image source method, the distribution of the standing pressure wave between the source and the resonator is given. The combination of the relations thus derived permits the distribution of the standing pressure wave between the source and the resonator to be determined, with consideration given to changes in the radiation impedance of the source and the mechanical parameters of the resonator. The experimental part gives the results of measurements of the dependence of the mean value of the modulus of the pressure amplitude of the standing wave on frequency for different resonance frequencies of the resonator and a comparison of the experimental and theoretically determined results in the case of an interaction between a sound source and a rigid baffle.

1. Introduction

In some aerodynamic problems, such as gas flow over a resonance cavity [1] or a mutual interaction between a resonance system and a sound source which occurs when gas flows on to a sharp edge [2], there is the necessity of using a physical model of the phenomenon which accounts for the interaction of mechanical, aeroacoustic and acoustic factors [2]. The process of sound generation due to the existence of the mechano-aerodynamic feedback is so complex that it has not been given an exact mathematical description; theory, in turn, is restricted to experimental formulae and relationships [3]. There is, however, the possibility of analyzing individually all the kinds of feedbacks which occur in flow phenomena.

The present paper gives a theoretical analysis of the mechano-acoustic interaction between a sound source, i.e. a loudspeaker and a resonance system with uniformly distributed surface impedance. The considerations are concerned with the frequency range over which the loudspeaker generates a plane wave.

2. Theoretical analysis

2.1. *Change in the radiation impedance of a dynamic loudspeaker caused by the introduction of reflecting surfaces or sound sources in its environment*

A dynamic loudspeaker as an electromechanical transducer of the magnetic type can be represented by an equivalent circuit where a gyrator with the impedance Z_s is the element which couples the electric and mechanical parts.

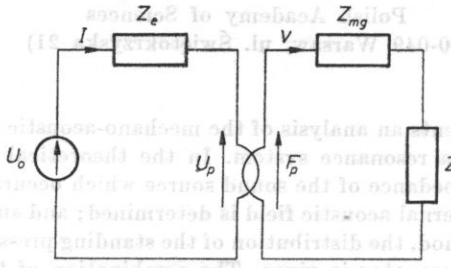

Fig. 1. A mechano-electrical equivalent circuit of an excited loudspeaker. U_0 – the rms value of the voltage supply to the loudspeaker, U_p – the rms value of the voltage at the gyrator, I – the rms value of the current intensity, F_p – the rms value of the force at the gyrator, V – the rms value of the mechanical velocity, Z_e – the impedance of the electrical part of the loudspeaker, $Z_{mg}+Z_{mp}$ – the impedance of the mechanical part of the loudspeaker, Z_{mp} – the radiation impedance

The properties of an ideal gyrator as part of the transducing part of the transducer can be defined from the matrix [1]

$$\begin{bmatrix} U_p \\ F_p \end{bmatrix} = \begin{bmatrix} 0 & -Z_s \\ -Z_s & 0 \end{bmatrix} \begin{bmatrix} \mathrm{I} \\ \mathrm{V} \end{bmatrix}, \tag{1}$$

where U_p is the rms value of the electric voltage at the gyrator, I is the rms value of the current intensity, F_p is the rms value of the mechanical force at the gyrator, V is the rms value of the mechanical velocity, $Z_s = Bl$; where B is the magnetic field induction in the slit and l is the winding length of the loudspeaker coil.

Using relation (1) the mechano-electric equivalent circuit of the transducer can be replaced with one which contains only mechanical or electric quantities. When on the electrical side the loudspeaker is supplied from a source with the voltage U_0, in its mechanical equivalent circuit the loading of the force

source F_z with the internal impedance $Z_{mw} = Z_s^2/Z_e + Z_{mg}$ is the mechanical radiation impedance Z_{mp}, where Z_{mg} is the impedance of the mechanical system of the loudspeaker without the radiation impedance, whereas Z_s^2/Z_e is an equivalent to the electric impedance of the loudspeaker in the mechanical circuit (Fig. 2).

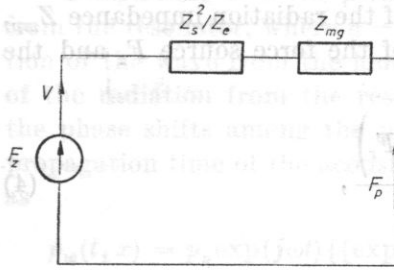

Fig. 2. A mechanical equivalent circuit of a loudspeaker radiating into unbounded space. F_z — the rms value of the force at the force source, equivalent to the voltage source U_0 in the mechanical circuit, F_p — the rms value of the mechanical force corresponding to the loading of the loudspeaker by an unbounded medium, Z_s^2/Z_e — the equivalent of the electric impedance of the loudspeaker in the mechanical equivalent circuit, Z_s — the coupling impedance of the gyrator, $Z_{mg}+Z_{mp}$ — the impedance of the mechanical part of the loudspeaker, Z_{mp} — the radiation impedance, V — the rms value of the mechanical velocity

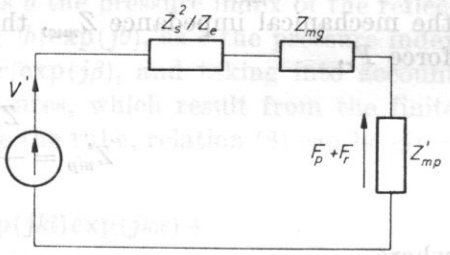

Fig. 3. A mechanical equivalent circuit of a loudspeaker acted upon by a reflexive acoustic wave. F_z — the rms value of the force of the force source which is the equivalent of the voltage source U_0 in the mechanical circuit, F_p — the rms value of the mechanical force corresponding to the loading of the loudspeaker by an unbounded medium, F_r — the rms value of the mechanical force which describes the additional loading of the loudspeaker by the reflexive acoustic field, V' — the rms value of the mechanical velocity, Z_s^2/Z_e — the equivalent of the electric impedance of the loudspeaker in the mechanical equivalent circuit, Z_s — the coupling impedance of the gyrator, $Z_{mg}+Z'_{mp}$ — the impedance of the mechanical part of the loudspeaker, Z'_{mp} — the radiation impedance

When only the wave radiated by the loudspeaker occurs in the medium, it follows from the third principle of dynamics that the medium acts on the loudspeaker with the force $-F_p = -Z_{mp}\,V$. When in the space surrounding the loudspeaker fed there are reflecting surfaces or sound sources, the additional force $-F_r$, which results from the existence of the reflexive or external acoustic field, acts on the loudspeaker. At a constant value of the supply voltage U_0 the additional force acting on the loudspeaker causes a change in its radiation impedance (Fig. 3). Considering the relationship resulting from the circuit in Fig. 3,

$$V' = \frac{F_p + F_r}{Z'_{mp}} = \frac{F_z}{Z'_{mp} + Z_{mw}}, \tag{2}$$

and the expression of the magnitude of the force F_p from Fig. 2,

$$F_p = Z_{mp} \frac{F_z}{Z_{mp}+Z_{mw}}, \tag{3}$$

after some transformations, the value of the new radiation impedance of the loudspeaker, Z'_{mp}, can be obtained as a function of the radiation impedance Z_{mp}, the mechanical impedance Z_{mw}, the efficiency of the force source F_z and the force F_r,

$$Z'_{mp} = \frac{Z_{mw}\left(\frac{F_z Z_{mp}}{Z_m}+F_r\right)}{\frac{F_z Z_{mw}}{Z_m}-F_r}, \tag{4}$$

where

$$Z_m = Z_{mp}+Z_{mw}; \tag{5}$$

$$Z_{mp} = R_{mp}+jX_{mp}; \tag{6}$$

$$Z'_{mp} = R'_{mp}+jX'_{mp}. \tag{7}$$

2.2. *The value of the acoustic pressure inside the Kundt tube*

Over the frequency range at which the acoustic wave length is at least twice as large as the diameter of the Kundt tube, the wave radiated by the loudspeaker can be replaced with a plane wave [4], whereas the membrane of the loudspeaker can be regarded as a plane, circular vibrating piston [5]. The origin of the axis of the coordinate x, which defines the propagation of acoustic perturbations in space, lies on the surface of this piston. Inside the tube, at the distance l from the source, there is a resonance system with uniformly distributed surface impedance and dimensions corresponding to the

ed by it and the wave radiated by the system have the form of plane waves with the same propagation directions as that of the incident wave.

For plane waves propagating in a direction parallel to the walls of the tube the instantaneous value of the sound pressure at all points of the cross-section of the tube is the same and the image source method can be used to analyze the resultant pressure inside the tube. In a steady state the resultant sound pressure is the sum of four kinds of pressure, i.e.

1. the pressure radiated by the loudspeaker, $p_0 \exp[j(\omega t - kx)]$,
2. the pressure radiated by the resonator, $p_1 \exp[j(\omega t + kx)]$,
3. the pressure being the sum of an infinite number of reflections from the resonator and the loudspeaker of the wave radiated by the loudspeaker, $p_2(t, x)$,

4. the pressure being the sum of an infinite number of reflections from the resonator and the loudspeaker of the wave radiated by the resonator, $p_3(t_x)$, i.e.

$$p_w(t, x) = p_0 \exp[j(\omega t - kx)] + p_1 \exp[j(\omega t + kx)] + p_2(t, x) + p_3(t, x). \quad (8)$$

Designating as a the pressure index of the reflection of the acoustic wave from the resonator, where $a = |a| \exp(j\phi)$, as b the pressure index of the reflection of the wave from the loudspeaker, $b = |b| \exp(j\theta)$, as c the pressure index of the radiation from the resonator, $c = |c| \exp(j\beta)$, and taking into account the phase shifts among the particular pressures, which result from the finite propagation time of the acoustic wave inside the tube, relation (8) can be given as

$$\begin{aligned} p_w(t, x) = p_0 \exp(j\omega t) \{ & [\exp(-jkx) + c \exp(jkl) \exp(jkx) + \\ & + a \exp(jkl) \exp(jkx) + ab \exp(j2kl) \exp(-jkx) + \\ & + a^2 b \exp(j3kl) \exp(jkx) + a^2 b^2 \exp(j4kl) \exp(-jkx) + \ldots] + \\ & + [cb \exp(j2kl) \exp(-jkx) + cab \exp(j3kl) \exp(jkx) + \\ & + cab^2 \exp(j4kl) \exp(-jkx) + ca^2 b^2 \exp(j5kl) \exp(jkx) + \ldots]\}; \end{aligned} \quad (9)$$

which after transformations becomes

$$\begin{aligned} p_w(t, x) = p_0 \exp(j\omega t) \{ & \exp(-jkx)[1 + bc \exp(j2kl)] + \\ & + \exp(jkx)[a \exp(jkl) + c \exp(jkl)]\} \Big\{ 1 + \sum_{n=1} [ab \exp(j2kl)]^n \Big\}. \end{aligned} \quad (10)$$

Since $|b| < 1$ and $|a| \leqslant 1$, the infinite series which occurs in formula (10) is convergent and the use of the formulae

$$1/2 + \sum_{n=1}^{\infty} D^n \cos nz = 1/2 \, \frac{1 - D^2}{1 - 2D \cos z + D^2}; \quad |D| < 1; \quad (11)$$

$$\sum_{n=1}^{\infty} D^n \sin nz = \frac{D \sin z}{1 - 2D \cos z + D^2};$$

and some simple transformations give the relation

$$1 + \sum_{n=1}^{\infty} [ab \exp(j2kl)]^n = \frac{1}{1 - ab \exp(j2kl)}; \quad (12)$$

thus the final expression of the resultant pressure inside the tube becomes

$$\begin{aligned} p_w(t, x) = \frac{p_0 \exp(j\omega t)}{1 - ab \exp(j2kl)} \{ & \exp(-jkx)[1 + bc \exp(j2kl)] + \\ & + \exp(jkx)[a \exp(jkl) + c \exp(jkl)]\}. \end{aligned} \quad (13)$$

From relation (12), the maximum and minimum values of the modulus of the pressure $p_w(t, x)$,

$$|p_w(t, x)|_{\min}^{\max} = |p_0| \frac{1 \pm |a| \pm |c| \pm |bc|}{[1 - 2\,|ab| \cos(2kl + \phi + \theta) + |ab|^2]^{1/2}}; \tag{14}$$

and, from equations (14), the mean value of the pressure modulus

$$\frac{|p_w(t, x)|\max + |p_w(t, x)|\min}{2} = \frac{p_0}{[1 - 2|ab| \cos(2kl + \phi + \theta) + |ab|^2]^{1/2}}. \tag{15}$$

can thus be obtained.

Equation (15) indicates that, depending on the frequency and the mechanical parameters of the loudspeaker and the resonator, the mean value of the modulus of the pressure in the tube varies greatly. This is related to the resonance of the Kundt tube itself, whose frequencies can shift as the reflection properties of the loudspeaker and the resonator change. The denominator of expression (15) reaches its minimum value of $1 - |ab|$ at frequencies for which the relation

$$2kl + \phi + \theta = 2n\pi, \quad n \in N; \tag{16}$$

is satisfied, and its maximum value $1 + |ab|$ when

$$2kl + \phi + \theta = (2n + 1)\pi, \quad n \in N. \tag{17}$$

Since, however, because of the mutual interaction between the loudspeaker and the resonator, the value of the modulus of the pressure radiated by the loudspeaker, $|p_0|$, varies depending on the frequency, the maximum and minimum mean values of the modulus of the pressure in the tube can occur for frequencies different from those for which relations (16) and (17) are satisfied.

2.3. *Mutual interaction between the dynamic loudspeaker as a sound source and the resonance system in the Kundt tube*

As a result of the presence of a resonance system in the effective range of the loudspeaker, part of the energy radiated by the loudspeaker in the form of acoustic waves returns to the source and, depending on the phase shifts, the conditions of sound radiation improve or worsen. The value of the amplitude of the sound pressure acting on the membrane of the loudspeaker can be obtained from formula (13), by the substitution $x = 0$, i.e.

$$p_{wa}(x = 0) = \frac{p_0}{1 - ab \exp(j2kl)} [1 + bc \exp(j2kl) + a \exp(jkl) + c \exp(jkl)]. \tag{18}$$

The amplitude of the pressure which occurs at the loudspeaker as a result of multiple reflections of the acoustic wave from the resonator and loudspeaker and as a result of the radiation from the resonator is thus defined by the relation

$$p_{ra} = p_{wa}(x = 0) - p_0. \tag{19}$$

Substitution of mechanical forces for the pressures gives the expression of the force F_r acting on the loudspeaker (point 2.1.),

$$F_r = F_w(x=0) - F_0 = F_0(A_0 - 1), \tag{20}$$

where

$$A_0 = \frac{1 + bc\exp(j2kl) + a\exp(jkl) + c\exp(jkl)}{1 - ab\exp(j2kl)}. \tag{21}$$

It should be noted that the force F_0, which corresponds to the pressure of the acoustic wave emitted by the loudspeaker, occurs in the condition of the bounded radiation field of the loudspeaker, and therefore

$$F_r = 1/2 R'_{mp} V'(A_0 - 1) = 1/2 \frac{R'_{mp} F_z}{Z_{mw} + Z'_{mp}}(A_0 - 1). \tag{22}$$

The introduction of the factor 1/2 accounts for the fact that only one side of the membrane of the loudspeaker emits acoustic waves into the tube. Substitution of relation (22) into formula (4) and some transformations give the relationship

$$Z_{mw}(Z'_{mp} - Z_{mp}) = 1/2\, R'_{mp}(A_0 - 1)(Z_{mw} + Z_{mp}), \tag{23}$$

and accordingly the expressions of the values of the radiation impedance and the impedance of the mechanical system of the loudspeaker, Z'_m,

$$R'_{mp} = \frac{R_{mp}}{1 - 1/2\, Re\left[(A_0 - 1)\left(1 + \dfrac{Z_{mp}}{Z_{mw}}\right)\right]}; \tag{24}$$

$$Z'_m = Z_m + \frac{1/2\, R_{mp}(A_0 - 1)\left(1 + \dfrac{Z_{mp}}{Z_{mw}}\right)}{1 - 1/2\,\mathrm{Re}\left[(A_0 - 1)\left(1 + \dfrac{Z_{mp}}{Z_{mw}}\right)\right]}. \tag{25}$$

Like the loudspeaker with changing working conditions, the resonator, when excited to vibration, changes the mechanical parameters. Analogously to the case of the loudspeaker, the mechanical force F_{rR} acting on the resonator can be determined with respect to the work of the resonator in a reflectionless environment,

$$F_{rR} = F_w(x = l) - F_{0R}, \tag{26}$$

where the force F_{0R} corresponds to the pressure radiated by the resonator. Thus, from Fig. 4,

$$F_{0R} = R'_{mpR} V_R = F_0 \frac{R'_{mpR}(1 - a)}{Z_{mwR} + Z'_{mpR}}. \tag{27}$$

and finally

$$F_{rR} = F_0\left[B_0 - \frac{R'_{mpR}(1-a)}{Z_{mwR}+Z'_{mpR}}\right]; \tag{28}$$

where

$$B_0 = \frac{\exp(-jkl)+bc\exp(jkl)+a\exp(j2kl)+c\exp(j2kl)}{1-ab\exp(j2kl)}. \tag{29}$$

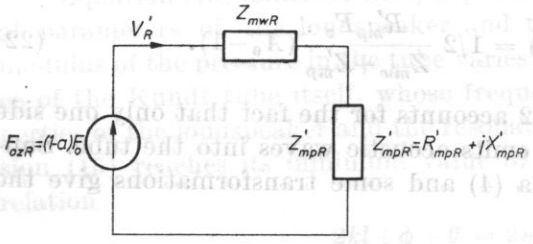

Fig. 4. The equivalent circuit of an excited resonator. F_{0zR} – the rms value of the mechanical force exciting the resonator system, F_0 – the rms value of the force corresponding to the acoustic pressure generated by the loudspeaker, a – the index of acoustic wave reflection from the resonator, V'_R – the mechanical velocity of vibrations in the resonator system, $Z_{mwR}+Z'_{mpR}$ – the mechanical impedance of the resonator system, Z'_{mpR} – the radiation impedance of the resonator

The use of formula (4), but in relation to the parameters of the resonator, and of relation (28) give the relationships

$$Z'_{mR} = \frac{Z_{mR}}{Z_{mwR}-Z_{mR}C_0}(Z_{mwR}-R'_{mpR}); \tag{30}$$

$$R'_{mpR} = \frac{\mathrm{Re}\left(\dfrac{Z_{mwR}Z_{mR}}{Z_{mwR}-Z_{mR}C_0}-R_s\right)}{\mathrm{Re}\left(1+\dfrac{Z_{mR}}{Z_{mwR}-Z_{mR}C_0}\right)}, \tag{31}$$

where $C_0 = B_0/(1-a)$ and R_s is the loss resistance of the resonator.

Since the quantities A_0 and C_0 are related to the mechanical parameters Z_m, Z_{mR}, R_{mp} and R_{mpR} by a system of implicit functions (see **Appendix**), Z'_m, Z'_{mR}, R'_{mp} and R'_{mpR} can be determined by solving numerically equations (24), (25), (30) and (31). This method is efficient, i.e. there is a solution and only one solution when the functions of the variables Z'_m and Z'_{mR} which occur on the right side of equations (25) and (30) satisfy the Banach principle, being converging functions [6]. According to this principle, irrespective of the selection of the initial data, the iteration series converges to one and only one solution.

From formula (13) and Fig. 3,

$$p_{wa}(x) = Ap_0 = A\frac{R'_{mp}F_z}{Z'_m} = A\frac{R'_{mp}}{Z'_m}\frac{R_{mp}F_z/Z_m}{R_{mp}/Z_m}, \tag{32}$$

where

$$A = \frac{\exp(-jkx)[1+bc\exp(j2kl)]+\exp(jkx)[a\exp(jkl)+c\exp(jkl)]}{1-ab\exp(j2kl)}. \tag{33}$$

Since, however, $p_1 = R_{mp}F_z/Z_m$ is the pressure radiated by the loudspeaker into unbounded space, the ratio p_{wa}/p_1 represents the pressure transmittance of the mechanical system loudspeaker-tube-resonator. Thus,

$$p_{wa}/p_1 = G_p = A\frac{R'_{mp}/R_{mp}}{Z'_m/Z_m} = A\left(1+\frac{\Delta R_{mp}}{R_{mp}}\right)\left(1+\frac{\Delta V}{V}\right) = A\frac{1+(\Delta R_{mp}/R_{mp})}{1+(\Delta Z_m/Z_m)}; \tag{34}$$

where $\Delta R_{mp} = R'_{mp}-R_{mp}$; $\Delta V = V'-V$; $\Delta Z_m = Z'_m-Z_m$.

It can be seen that the transmittance G_p depends on the product of two factors, the first of which defines the distribution of the standing pressure wave inside the tube and is a function of the variable x which takes values from the interval $\langle 0, l\rangle$ and of the mechanical quantities Z_m, Z_{mR}, R_{mp} and R_{mpR}; the second being related to changes in the parameters of the loudspeaker itself. It follows from its form that the relative pressure changes are in direct proportion to changes in the velocity and resistance of radiation, i.e. proportional to changes in the radiation resistance, but in inverse proportion to changes in the mechanical impedance of the loudspeaker. Since the mechanical parameters of the source and the phase shifts (the coefficients A and A_0) which occur in formulae (24), (25) and (33) depend on frequency, the transmittance G_p is also a function of it.

3. Experimental investigations

The measurements were carried out in a 4002 Brüel and Kjaer Kundt tube of 10 cm diameter, which permitted a plane wave shape, radiated by the loudspeaker over the frequency range 90-1800 Hz, to be obtained [4]. The

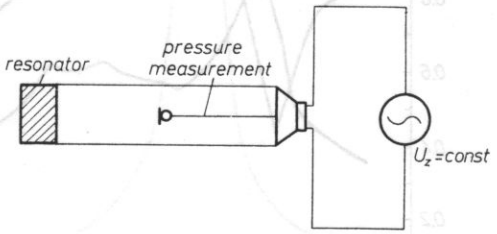

Fig. 5. A schematic diagram of the measurement system
U_z – the value of the voltage supply to the loudspeaker

resonator used had the form of a cylindrical chamber filled with air and closed at one end by an ideally rigid surface, i.e. with the impedance $Z = \infty$, and at the other, by a thin ($d = 1$ mm), perforated membrane clamped rigidly on the circumference (Fig. 5). The aim of the measurements was to determine

the mean value of the modulus of the pressure amplitude inside the tube. Figs. 6 and 7 show the results of the measurements for two different resonance frequencies of the resonator, whereas Fig. 8 gives the results obtained in the case when the resonator was replaced with an ideally rigid plate. The results obtained were referred to the quantities measured when the loudspeaker radiated into unbounded space. The value of the impedance Z_m used in the calculations was determined from the list of typical mechanical and electric parameters

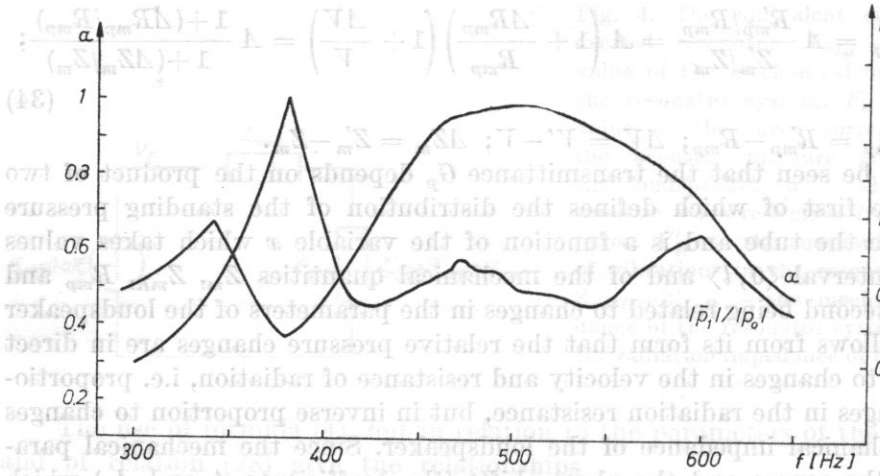

Fig. 6. The relative mean value of the modulus of the pressure amplitude $|\bar{p}_1|/|p_0|$ as a function of the frequency f and the behaviour of the absorption coefficient of the resonator, α, for the main resonance frequency $f_r = 500$ Hz.

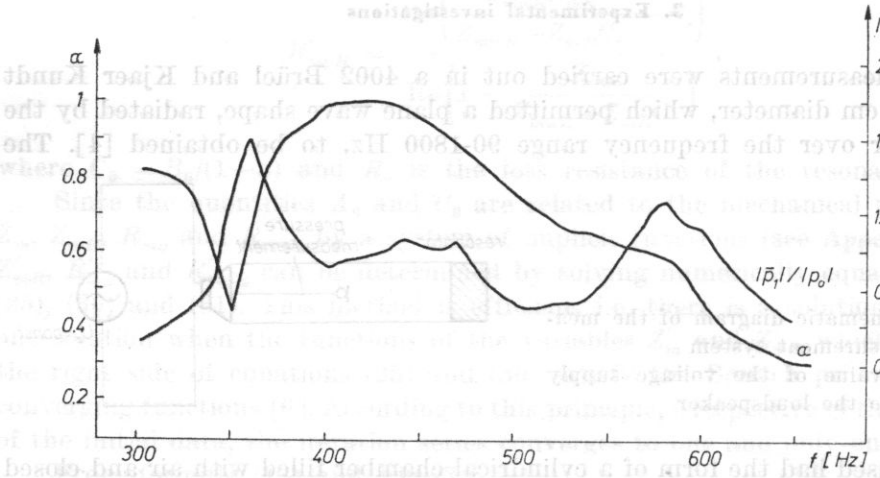

Fig. 7. The relative mean values of the modulus of the pressure amplitude $|\bar{p}_1|/|p_0|$ as a function of the frequency f and the behaviour of the absorption coefficient of the resonator, α, for the main resonance frequency $f_r = 420$ Hz.

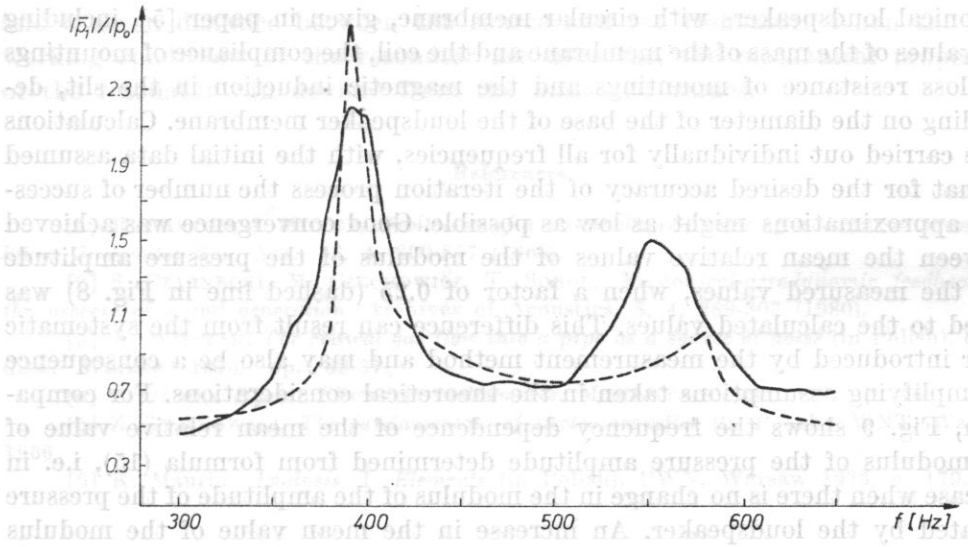

Fig. 8. The measured (solid line) and calculated (dashed line) relative mean values of the modulus of the pressure amplitude $|\bar{p}_1|/|p_0|$ as a function of the frequency f in the case when the tube is closed by a rigid surface.

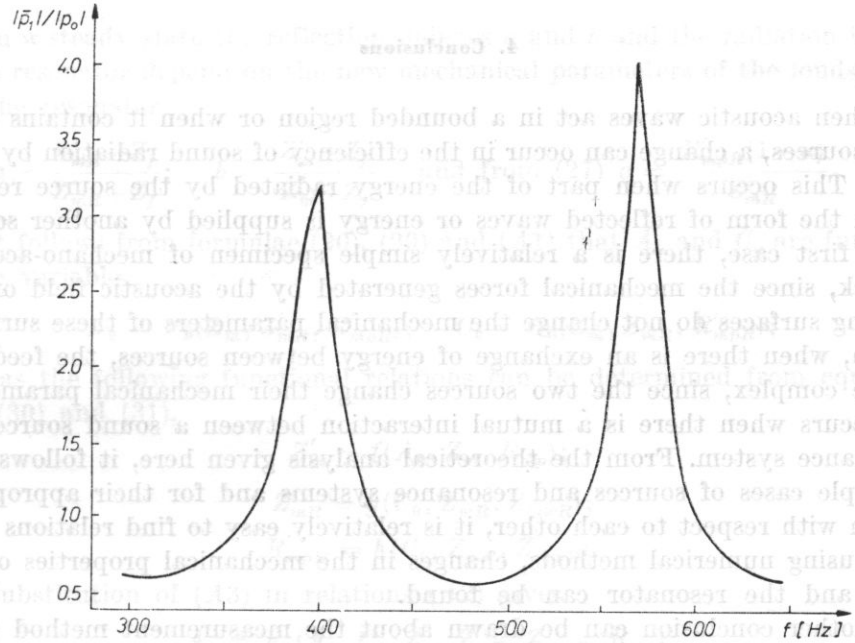

Fig. 9. The relative mean values of the modulus of the pressure amplitude $|\bar{p}_1|/|p_0|$ as a function of the frequency f obtained from formula (15), i.e. under the assumption of a lack of change in the mechanical parameters of the source.

of conical loudspeakers with circular membrane, given in paper [5], including the values of the mass of the membrane and the coil, the compliance of mountings the loss resistance of mountings and the magnetic induction in the slit, depending on the diameter of the base of the loudspeaker membrane. Calculations were carried out individually for all frequencies, with the initial data assumed so that for the desired accuracy of the iteration process the number of successive approximations might as low as possible. Good convergence was achieved between the mean relative values of the modulus of the pressure amplitude and the measured values, when a factor of 0.25 (dashed line in Fig. 8) was added to the calculated values. This difference can result from the systematic error introduced by the measurement method and may also be a consequence of simplifying assumptions taken in the theoretical considerations. For comparison, Fig. 9 shows the frequency dependence of the mean relative value of the modulus of the pressure amplitude determined from formula (15), i.e. in the case when there is no change in the modulus of the amplitude of the pressure radiated by the loudspeaker. An increase in the mean value of the modulus of the pressure amplitude results in all the cases presented from the resonance of the Kundt tube itself, whose frequency depends on the length of the tube and on the mechanical parameters of the loudspeaker and the resonator.

4. Conclusions

When acoustic waves act in a bounded region or when it contains other sound sources, a change can occur in the efficiency of sound radiation by their source. This occurs when part of the energy radiated by the source returns to it in the form of reflected waves or energy is supplied by another source. In the first case, there is a relatively simple specimen of mechano-acoustic feedback, since the mechanical forces generated by the acoustic field on the bounding surfaces do not change the mechanical parameters of these surfaces. In turn, when there is an exchange of energy between sources, the feedback is more complex, since the two sources change their mechanical parameters. This occurs when there is a mutual interaction between a sound source and a resonance system. From the theoretical analysis given here, it follows that for simple cases of sources and resonance systems and for their appropriate position with respect to each other, it is relatively easy to find relations from which, using numerical methods, changes in the mechanical properties of the source and the resonator can be found.

Another conclusion can be drawn about the measurement method using the Kundt tube. The measurement by this method, e.g. of the absorption coefficient or the resonance frequency of a resonance system, gives correct results only under some specific measurement conditions, i.e. a specific sound source

and a given distance between the source and the resonator. When the real working conditions of the resonator are different, the mechanical properties of the resonator can deviate from the measured values.

References

[1] R. PANTON, J. MILLER, *Excitation of a Helmholtz resonator by a turbulent boundary layer*, J. Acoust Soc. Am., **58**, 4, 800-857 (1965).

[2] S. CZARNECKI, M. CZECHOWICZ, T. SOBOL, *Mechanical-aerodynamic feedback in the process of sound generation*, Archives of Acoustics, **5**, 4, 289-303 (1980).

[3] K. WITCZAK, *The critical gas flow into a pipe as a source of noise* (in Polish), doct. diss., Warsaw 1975, pp. 32-37.

[4] *Brüel and Kjaer, Electronic instruments*, Master catalogue, 1977, p. 469.

[5] Z. ŻYSZKOWSKI, *The fundamentals of electro-acoustics* (in Polish), WNT, Warsaw 1966.

[6] K. Maurin, *Analysis*, I. *Elements* (in Polish), PWN, Warsaw 1973, p. 179.

Received on 18 October, 1982,

Appendix

In a steady state the reflection indexes a and b and the radiation index c of the resonator depend on the new mechanical parameters of the loudspeaker and the resonator:

$$a = \frac{Z'_{mR} - Z_f}{Z'_{mR} + Z_f}; \quad b = \frac{Z'_m - Z_f}{Z'_m + Z_f} \quad \text{and from (27)} \quad c = \frac{R'_{mpR}(1-a)}{Z'_{mR}}. \tag{A1}$$

It follows from formulae (20), (29) and (A1) that A_0 and C_0 are functions of the variables

$$A_0 = F_0(Z'_m, Z'_{mR}, R'_{mpR}); \quad C_0 = G_0(Z'_m, Z'_{mR}, R'_{mpR}); \tag{A2}$$

whereas the following functional relations can be determined from equations (25), (30) and (31),

$$\begin{aligned} Z'_m &= f(A_0, Z_m, R_{mp}); \\ Z'_{mR} &= g(C_0, Z_{mR}, Z_{mwR}); \\ R'_{mpR} &= h(C_0, Z_{mR}, Z_{mwR}). \end{aligned} \tag{A3}$$

Substitution of (A3) in relations (A2) gives

$$\begin{aligned} A_0 &= F_1(A_0, C_0, Z_m, Z_{mR}, Z_{mwR}, R_{mp}); \\ C_0 &= G_1(A_0, C_0, Z_m, Z_{mR}, Z_{mwR}, R_{mp}). \end{aligned} \tag{A4}$$

Thus, system (A4) represents a pair of functions implicit in terms A_0 and C_0.

ARCHIVES OF ACOUSTICS
8, 3, 249-254 (1983

OPTICAL GENERATION OF ACOUSTIC WAVES

ANDRZEJ MLECZKO, ROMAN BUKOWSKI,
ZYGMUNT KLESZCZEWSKI

Institute of Physics, Silesian Technical University
(44-101 Gliwice, ul. B. Krzywoustego 2)

This paper discusses optical generation of acoustic waves and gives preliminary results of experimental research. The acoustic wave was generated as a result of the interaction of two laser light beams of very high intensity and slightly different frequencies. The change in the frequency of the laser beams ($\Delta f = 116$ MHz) was achieved using the Bragg diffraction of laser light by the acoustic wave.

1. Introduction

The use of very powerful lasers in investigations of the acousto-optical interactions has permitted the study of a number of interesting nonlinear effects which occur in the diffraction of laser light by acoustic waves. From the large class of these phenomena, the effect of optical generation of coherent elastic waves, which KASTLER has predicted theoretically, is distinguished. The phenomenon was investigated preliminarily by American research workers [2, 3]. At present, in view of the large developments in theory [1], experimental research in this field has been resumed.

2. Short description of the phenomenon

When two electromagnetic waves with angular frequencies ω_1 and ω_2 propagate in a medium, the mutual interaction of these waves causes a periodic strain of the angular frequency $\omega_1 - \omega_2$ to occur. The coupling of these waves is a result of the electrostrictive effect.

The geometry of the phenomenon can be analysed on the basis of the principle of energy and momentum conservation in the photon — photon scattering.

$$\hbar\omega_1 - \hbar\omega_2 = \hbar\Omega; \tag{1a}$$

$$\hbar\boldsymbol{k}_1 - \hbar\boldsymbol{k}_2 = \hbar\boldsymbol{q}; \tag{1b}$$

where ω_1, ω_2, $\boldsymbol{k}_1$, $\boldsymbol{k}_2$ are respectively the angular frequencies and wave vectors of the interacting electromagnetic waves; Ω and $\boldsymbol{q}$ are the analogous quantities for the generated acoustic wave.

When the frequencies ω_1 and ω_2 of electromagnetic waves are not greatly different (which is most frequently the case), $|\boldsymbol{k}_1| \approx |\boldsymbol{k}_2|$. The angle which must be formed by the wave vectors $\boldsymbol{k}_1$ and $\boldsymbol{k}_2$ can be determined from equation (1*b*),

$$\psi = 2\theta_B = 2\sin^{-1}\frac{\lambda_0\Omega}{4\pi n v}, \tag{2}$$

where θ_B is the Bragg angle, λ_0 is the electromagnetic wave length in vacuum; and n and v are respectively the light refraction coefficient and the acoustic wave propagation velocity for the medium considered.

Fig. 1. shows the system of wave vectors for the photon — photon scattering (photon creation).

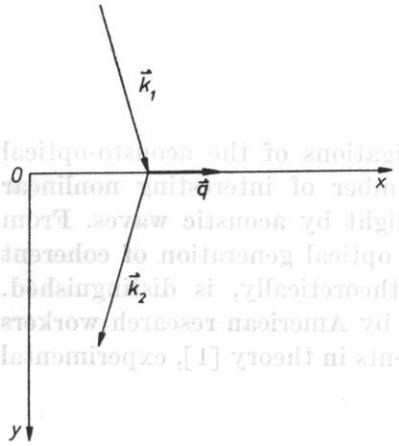

Fig. 1. The system of wave vectors $\boldsymbol{k}_1$ and $\boldsymbol{k}_2$ of the waves involved in the photon — photon scattering which generated an acoustic wave with the wave vector $\boldsymbol{q}$.

Theory [1, 2] also predicts that the power density P_s of the acoustic wave generated is proportional (in first approximation) to the product of the power densities of the interacting electromagnetic waves,

$$P_s = \frac{n^6 p^2}{8\varrho v^3 c^2}\,\Omega^2 L^2 P_1 P_2, \tag{3}$$

where L, P_1 and P_2 are respectively the interaction path length and the intensities of the electromagnetic waves, p is the photoelastic constant, ϱ is the density of the medium, and c is the light velocity in vacuum.

3. Experimental system. Discussion of the results

The investigation set-up which served for the observation of the generation of acoustic waves by the optical method is shown schematically in Fig. 2. The source of electromagnetic waves was a ruby laser working in a pulsed mode

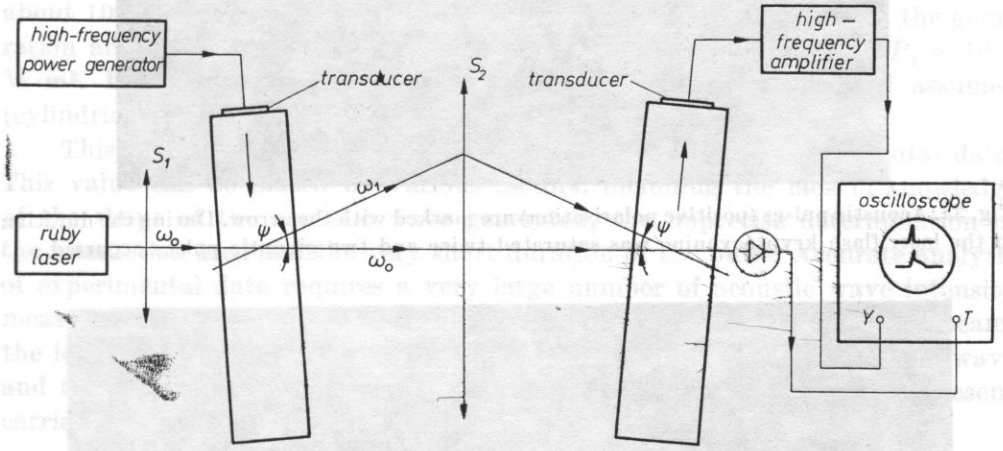

Fig. 2. A schematic diagram of the investigation system for the observation of the generation of acoustic waves by the optical method. ψ – the angle formed by the wave vectors $\boldsymbol{k}_1$ and $\boldsymbol{k}_2$, S_1 and S_2 – lenses, T – synchronisation

with an adjusted quality factor. In the acoustooptical modulator the beam was split into two parts of different frequency. In this experiment the frequency change was 116 MHz. The diffraction efficiency was about 10 per cent. The lens S_1 served to focus the laser beam in the modulator. The lens S_2 refocused the two beams in the material where they interacted. The geometry of the system was chosen so that the laser beam intersected at the angle $2\,\theta_B$. The material was glass SF – 14 for which $n = 1.76$, $\varrho = 4.35 \times 10^3$ kg/m^3, $v = 3.57 \times 10^3$ m/s and $p = 0.1$.

For these values $2\,\theta_B$ is 11.8 mrad. The acoustic wave generated was detected by a $LiNbO_3$ piezoelectric transducer, glued directly to the end of the sample. The signal from the transducer was amplified (selectively) and registered on the oscilloscope. An ultrasonic wave of the frequency $f = 116$ MHz was observed in the form of single pulses about several score nanoseconds long.

Fig. 3 shows the oscillograms registered.

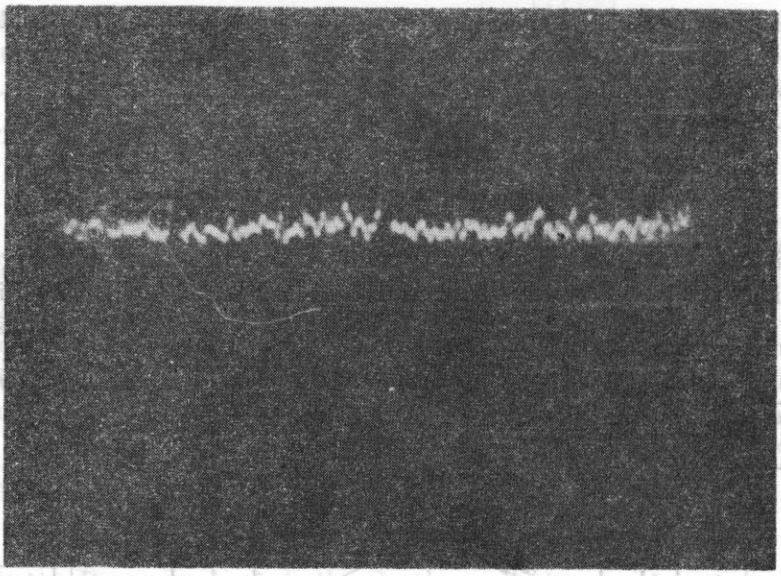

Fig. 3a. Acoustic pulses (positive polarisation) are marked with the arrow. During the duration of the laser flash kryptocyanine was saturated twice and two gigantic pulses occurred

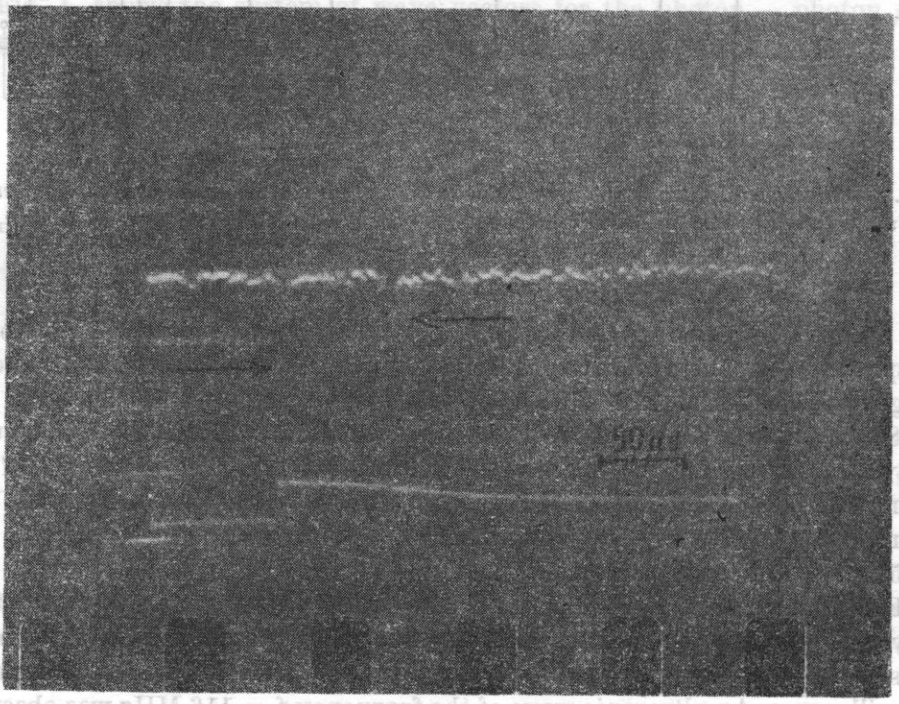

Fig. 3b. Acoustic pulses (negative polarisation) are marked with the arrow. The lower part represents the voltage at the photodiode; as a result of inertia, the second optical pulse is not visible and the back slope of the first is much widened

The high-frequency voltage amplitude on the receiving transducer varied from 40-80 μV, depending on the light intensity. For control, a signal from the photodiode illuminated by a laser flash was supplied to the time base B of the oscilloscope (Fig. 3*b*). The time correlation of the two pulses confirms the authenticity of the effect obtained. (The back slope of the laser pulse is greatly widened as a result of the inertia of the photodiode). Approximate calculations of the power flux of the acoustic wave generated were carried out. The generation area is the focus of the lens [4], i.e. a cylinder of a diameter of about 8×10^{-5} m and height of about 3×10^{-3} m (for the focal length of the lens S_1 being 15.8×10^{-2} m).

For the distance of the generation area from the lens assumed here at about 10^{-2} m, the approximate value of the wave amplitude close to the generation area is 3×10^{-14} m, which corresponds to the power density $P_s = 10^{-4}$ W/m². In view of the measurement method and approximations assumed (cylindrical waves), this value is rather underestimated.

This value is slightly higher than one estimated from experimental data. This value can be biased by various factors, including the lack of knowledge of the shape of the acoustic wave generated, the imprecise determination of the interaction area and the very short duration of the pulse. Accurate analysis of experimental data requires a very large number of acoustic wave intensity measurements to be carried out, depending on the power of the laser beam, the length of the interaction area, the angular frequency of the acoustic wave and the material constants of the medium. Such measurements are at present carried out by the authors.

References

[1] R. Bukowski, A. Mleczko, Z. Kleszczewski, *Nichtlineare Bragg'sche diffraktion und optische Erregung von Ultraschallwellen*, Acustica **52**, 3, 179–185 (1983).

[2] D. E. Cadden, C. F. Quate, C. D. W. Wilkinson, *Conversion of light to sound by electrostrictive mixing in solids*, Appl. Phys. Lett. **8**, 12, 309-311 (1966).

[3] A. Korpel, R. Adler, B. Alpiner, *Direct observation of optically induced generation and amplification of sound*, Appl. Phys. Lett., **5**, 4, 86-88 (1964).

[4] F. Kaczmarek, *Introduction to laser physics* (in Polish), PWN, Warsaw 1977, pp. 436-437.

Received on 10 May, 1982.

ARCHIVES OF ACOUSTICS
8, 3, 255-268 (1983)

ULTRASONIC INVESTIGATIONS OF 2-ETHYLHEXADIOLE-1.3. IN THE REGION OF VISCOELASTIC RELAXATION

MAREK WACIŃSKI

Institute of Chemistry, Silesian University
(40-006 Katowice, ul. Szkolna 6)

RYSZARD PŁOWIEC

Institute of Fundamental Technological Research, Polish Academy of Sciences
(00-049 Warsaw, ul. Świętokrzyska 21)

This paper gives the results of measurements of mechanical shear impedance in 2-ethylhexadiole-1.3., at frequencies of 0.520, 29.9 and 500 MHz. Measurements carried out with transverse waves in the region of viscoelastic relaxation permitted the determination of viscoelastic relaxation times and the characteristic constant quantities such as the modulus of elasticity, mechanical compliance and dynamic viscosity.

1. Introduction

The interest in shear transverse waves results from the fact that they can be used to measure the dynamic properties of a fluid, and thus to investigate the nature and character of the processes of change in the molecular structure.

The developments in the phenomenological theory of viscoelasticity have been inspired by investigations of the properties of construction materials and problems of elastohydrodynamic lubrication. The classical investigations of TOBOLSKY *et al.* [1, 2] and a number of other authors have shown that the viscoelastic behaviour of an elastomer undergoing rapidly changing shear deformations is related to the chemical degradation of long molecular chains with covalent bonds. They have thus pointed out the "chemical" aspect of viscoelasticity which results from the relationship between a macroscopic

deformation and the molecular structure and molecular displacements in the medium being deformed.

The further developments in the theory of viscoelasticity were instigated by the interest in problems related to elastohydrodynamic lubrication, e.g. in the investigations of BARLOW, LAMB *et al.* [3, 4]. The non-Newtonian behaviour of fluids under such conditions is related to the translational and configurational molecular processes.

The chemical aspect of viscoelasticity of fluids was given attention by the investigations of LITOVITZ, HERZFELD, DAVIES *et al.* [5, 6].

In the present investigations, measurements of the mechanical impedance of shear waves were carried out over a large frequency and temperature range. The use of suitably high frequencies permitted not only the relaxation range in a given fluid but also its limiting shear elasticity to be determined.

2. Theoretical analysis

According to the theory of linear viscoelasticity, the following generally known relations occur [4, 5, 7],

$$G = G_\infty \frac{\omega^2\tau^2}{1+\omega^2\tau^2} + iG_\infty \frac{\omega\tau}{1+\omega^2\tau^2} = G' + iG''$$

$$= G_\infty \frac{\omega^2\tau^2}{1+\omega^2\tau^2} + i\omega \frac{\eta}{1+\omega^2\tau^2} = G_\infty \frac{\omega^2\tau^2}{1+\omega^2\tau^2} + i\omega\eta(\omega), \tag{1}$$

where G' is a dynamic modulus of elasticity, G'' is a dynamic modulus of viscosity, G_∞ is the limiting modulus of shear elasticity, $\eta(\omega)$ is dynamic viscosity, τ is the relaxation time and ω is the angular frequency.

In view of the large attenuation of the transverse wave and the impossibility of measuring the attenuation and velocity over a given path, as in the case of the longitudinal wave, the complex mechanical shear impedance Z (i.e. the ratio of the strain (σ) to the displacement velocity ($\partial u/\partial t$)) must first be measured,

$$Z = -\frac{\sigma}{\left(\frac{\partial u}{\partial t}\right)} = R + iX, \tag{2}$$

where σ is the shear strain, R and X are mechanical resistance and shear reactance.

The relationship between G and Z can readily be found, since

$$Z = (\varrho G)^{1/2}, \tag{3}$$

$$Z = (\varrho/J)^{1/2}. \tag{4}$$

hence

$$G' = \frac{R^2 - X^2}{\varrho}, \tag{5}$$

$$G'' = \frac{2RX}{\varrho}, \tag{6}$$

$$J' = \frac{\varrho(R^2 - X^2)}{(R^2 + X^2)^2}, \tag{7}$$

$$J'' = \frac{2\varrho RX}{(R^2 + X^2)^2}. \tag{8}$$

It follows that the experimental determination of the two components of any of the complex functions given above (impedance Z, modulus G, compliance J) permits the calculation of the other two quantities, irrespective of the molecular base, i.e. of what molecular processes determine the macroscopic behaviour of the body. From the form of the relations of $G'(\omega)$, $G''(\omega)$ and $\eta(\omega) = G''(\omega)/\eta_s$, where η_s is stationary viscosity and $\tau = \eta_s/G_\infty$,

$$G' = G_\infty \frac{\omega^2\tau^2}{1 + \omega^2\tau^2}, \tag{9}$$

$$G'' = G_\infty \frac{\omega\tau}{1 + \omega^2\tau^2}, \tag{10}$$

$$\eta(\omega) = \frac{G_\infty\tau}{1 + \omega^2\tau^2} = \frac{\eta_s}{1 + \omega^2\tau^2}, \tag{11}$$

it follows that:

1. ω always occurs in the form of the product $\omega\tau$, and therefore it can be regarded as a function of the variable $x = \omega\tau$, provided it is normalised in the following way: G'/G_∞, G''/G_∞, $\eta(\omega)/\eta_s$;

2. when $\omega\tau \ll 0$, i.e. $\omega\tau \to 0$, the region is viscous, $\eta(\omega) = \eta_s$ and $G' = 0$;

3. when $\omega\tau \gg 0$, i.e. $\omega\tau \to \infty$, the region is elastic, $G' = G_\infty$;

4. when $\omega\tau = 1$, the region is viscoelastic, $G' = 0.5\ G_\infty$, $G'' = 0.5,\ G_\infty$, i.e. $G' = G''$ and $\eta(\omega) = 0.5\ \eta_s$;

5. $G'/G'' = \omega\tau$, since $\tan\delta = G''/G'$, $\tan\delta = 1/\omega\tau$;

6. G', G'' and $\eta(\omega)$ are symmetrical with respect to the scale $\log\omega\tau$, τ has its time dimension and can therefore be regarded as the inverse of some frequency characteristic of the relaxation $\omega_{\text{rel}} = \tau^{-1}$. Hence, $\omega\tau = \omega/\omega_{\text{rel}}$ and the scale $\omega\tau = \omega/\omega_{\text{rel}}$ or $\log\omega\tau = \log\omega/\omega_{\text{rel}}$ can be regarded as the characteristic frequency scale of the relaxation (or simply the relaxation frequency ω_{rel}). At the same time, G' and G'' can also be normalized, by dividing these quanties

by G_∞ and $\eta(\omega)$ by η_s,

$$\frac{\eta(\omega)}{\eta_s} = \frac{1}{1+\omega^2\tau^2} \to 0 < \frac{\eta(\omega)}{\eta_s} \leqslant 1;$$

$$\frac{G'}{G_\infty} = \frac{\omega^2\tau^2}{1+\omega^2\tau^2} \to 0 < \frac{G'}{G_\infty} \leqslant 1;$$

$$\frac{G''}{G_\infty} = \frac{\omega\tau}{1+\omega^2\tau^2} \to 0 < \frac{G''}{G_\infty} \leqslant \frac{1}{2}.$$

The behaviour of the shear moduli in the relaxation region is usually represented in the form of such normalised diagrams (provided G_∞ and η_s can be measured), which has an enormous advantage: since $x = \omega\tau$, this parameter can be altered by changing the frquency (ω) or temperature $(\tau = \tau(t))$. This permits investigations of the relaxation region at different frequencies and temperatures. Instead of the shear moduli, the relaxation region can also be represented graphically using the directly measured shear resistances and shear reactances (R and X), most frequently in the form of normalised $R/(\varrho G_\infty)^{1/2}$, $X/(\varrho G_\infty)^{1/2}$. Solution of the previous equations, which relate the components of the modulus to the components of the impedance with respect to R and X, gives

$$R^2 = \varrho \frac{G'}{2}\left\{\left[1+\left(\frac{G''}{G'}\right)^2\right]^{1/2}+1\right\}; \tag{12}$$

$$\frac{R^2}{\varrho G_\infty} = \frac{\omega^2\tau^2}{2(1+\omega^2\tau^2)}\left[\left(1+\frac{1}{\omega^2\tau^2}\right)^{1/2}+1\right]; \tag{13}$$

$$X^2 = \varrho \frac{G''}{2}\left\{\left[1+\left(\frac{G''}{G'}\right)^2\right]^{1/2}-1\right\}; \tag{14}$$

$$\frac{X^2}{\varrho G_\infty} = \frac{\omega^2\tau^2}{2(1+\omega^2\tau^2)}\left[\left(1+\frac{1}{\omega^2\tau^2}\right)^{1/2}-1\right]. \tag{15}$$

Thus, the normalised resistances and reactances are only functions of $\omega\tau$ and give normalised curves on a half-logarithmic scale, on which points corresponding to the frequency and temperature of measurements arrange themselves.

Since a description of the behaviour of real fluids would, for a generalized Maxwell model, require an infinite number of elements, summation should be replaced by integration, giving a continuous spectrum of relaxation times,

$$G' = G_\infty \int_0^\infty \frac{g\left(\frac{\tau}{\tau_s'}\right)\omega^2\tau^2}{1+\omega^2\tau^2} \cdot d\left(\frac{\tau}{\tau_s'}\right) = G_\infty \int_0^\infty \frac{g(x)\,\omega^2\tau_s'^2x^2}{1+\omega^2\tau_s'^2x^2}\,dx; \tag{16}$$

$$G'' = G_\infty \int_0^\infty \frac{g\left(\frac{\tau}{\tau_s'}\right)\omega\tau}{1+\omega^2\tau^2} \cdot d\left(\frac{\tau}{\tau_s'}\right) = G_\infty \int_0^\infty \frac{g(x)\,\omega\tau_s' x}{1+\omega^2\tau_s'^2 x^2}\,dx, \tag{17}$$

where $g(\tau/\tau_s')$ is a function of the distribution of normalised relaxation times (i.e. referred to τ_s', which is the main time of a given distribution), whereas $g(\tau/\tau_s')\ d(\tau/\tau_s')$ is the share in the limiting modulus G_∞ of those moduli whose relaxation time lies in the interval $\tau+d\tau$ and which are normalised over the interval $(\tau/\tau_s')+d(\tau/\tau_s')$. Similarly, the components of the impedance are represented in the normalised form:

$$\frac{R}{(\varrho G_\infty)^{1/2}} \tag{18}$$

$$= \sqrt{\frac{1}{2}\int_0^\infty \frac{g(x)\,\omega^2\tau_0^2 x^2}{1+\omega^2\tau_0^2 x^2}\,dx \left\{1+\left[1+\left(\frac{\int_0^\infty \left(g(x)\,x/(1+\omega^2\tau_0^2 x^2)\right)dx}{\int_0^\infty \frac{g(x)\,\omega^2\tau_0^2 x^2}{1+\omega^2\tau_0^2 x^2}\,dx}\right)^2\right]^{1/2}\right\}^{1/2}};$$

$$\frac{X}{(\varrho G_\infty)^{1/2}} \tag{19}$$

$$= \sqrt{\frac{1}{2}\int_0^\infty \frac{g(x)\,\omega^2\tau_0^2 x^2}{1+\omega^2\tau_0^2 x^2}\,dx \left\{\left[1+\left(\frac{\int_0^\infty \left(g(x)\,x/(1+\omega^2\tau_0^2 x^2)\right)dx}{\int_0^\infty \left(g(x)\,\omega^2\tau_0^2 x^2/(1+\omega^2\tau_0^2 x^2)\right)dx}\right)\right]^{1/2}\right\}^{1/2}},$$

where $x = \tau_s/\tau_{s,0}$, $g(x) = (b/\eta^{1/2}x)\exp-[b\ln x]^2$, $0 < \tau_s < \infty$, b is a parameter which defines the width of the distribution of the relaxation times.

The viscoelastic properties of 2-ethylhexadiole are described by both the Maxwell model and by the *B-E-L* one [4]. In the Maxwell model with a Gaussian distribution of the relaxation times, the matching of the curve calculated from equation (18) to the experimental points requires that the theoretical coefficient $\exp-(-1/4b^2)$ should be replaced by an experimental one which relates the main time of the Gaussian distribution $\tau_{s,0}$ with the Maxwell relaxation time $\tau_s = \eta_s/G_\infty$, according to the equation $\tau_{s,0} = (\eta_s/G_\infty)\ a$ (a being some displacement with respect to the frequency axis). It can thus be seen that the Maxwell relaxation time is different from the mean time of the Gaussian distribution, in opposition to the theory (with the difference between these two times being about 10 per cent).

In order to make the interpretation of results independent from the arbitrarily assumed function of the distribution of the relaxation times and to achieve a more correct representation of the viscoelastic relaxation, the *B-E-L*

(BARLOW, ERGINSAV, LAMB) model of supercooled fluids was used to describe the relaxation curves.

The *B-E-L* model [4] is constructed of the parallel-linked acoustic impedances for a solid (Z_s) and a Newtonian fluid (Z_n),

$$\frac{1}{Z} = \frac{1}{Z_n} + \frac{1}{Z_s}. \tag{20}$$

Transformation of this equation gives a formula for the shear compliance of the fluid, J, depending on the characteristic constants of the medium under study,

$$\frac{J}{J_\infty} = \frac{1}{G_\infty} + \frac{1}{j\omega\eta} + 2k\left(\frac{1}{j\omega G_\infty}\right)^\beta. \tag{21}$$

The components of the acoustic shear impedance of the fluid, R and X, are, from formula (21),

$$\frac{R}{(\varrho G_\infty)^{1/2}} = \frac{(\omega\eta/2G_\infty)^{1/2}[1+(2\omega\eta/G_\infty)^{1/2}]}{[1+(\omega\eta/2G_\infty)^{1/2}]^2+\omega\eta/2G_\infty}; \tag{22}$$

$$\frac{X}{(\varrho G_\infty)^{1/2}} = \frac{(\omega\eta/2G_\infty)^{1/2}}{[1+(\omega\eta/2g_\infty)^{1/2}]^2+\omega\eta/2G_\infty}. \tag{23}$$

In the case of simple fluids the measured results satisfy equation (21) for $k = 1$ and $\beta = 0.5$. In the case of complex fluids or their mixtures the formula is modified by the coefficients k and β. Figs. 1-4 give theoretical behaviours of the normalised shear moduli and impedance calculated for $\beta = 0.5$.

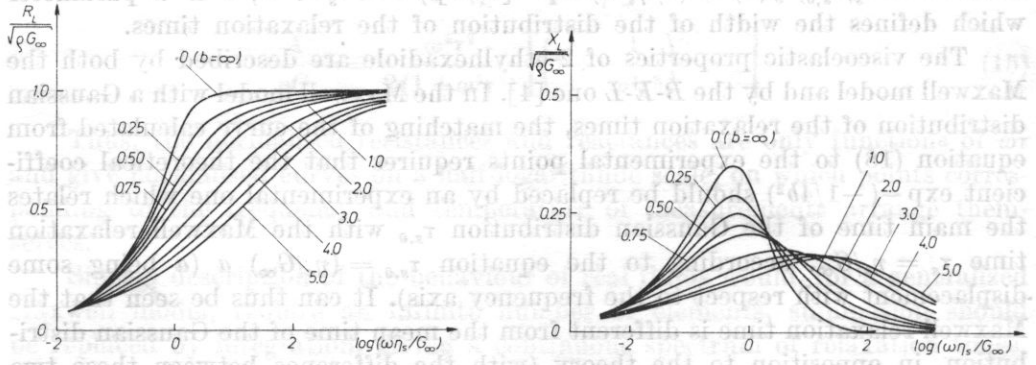

Figs. 1, 2. Theoretical behaviour of the normalised shear impedances $\frac{R}{(\varrho G_\infty)^{1/2}}$ and $\frac{X}{(\varrho G_\infty)^{1/2}}$ as a function of $\log \omega\tau$

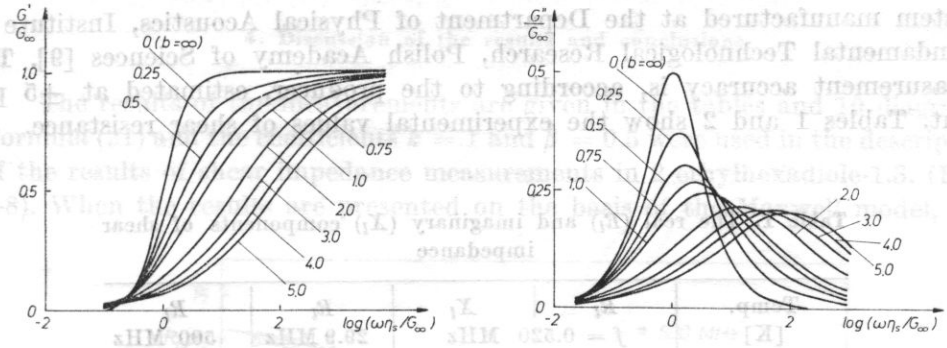

Figs. 3, 4. Theoretical behaviour of the normalised moduli G'/G_∞, G''/G_∞ as a function of $\log \omega\tau$

3. Experimental part

2-ethylhexadiole-1.3. (B.D.H., Ltd.) which was dehydrated by distilation under lowered pressure was used in the investigations. The water content in the diole was determined by the Fischer method at 0.12 per cent by weight.

The density was determined pycnometrically over the temperature range 253-303 K, with an accuracy of up to 0.05 K. For lower temperatures the density (ϱ) was extrapolated from the linear equation $\varrho = A + BT$, where A and B are constant quantities and T is temperature. There is the following temperature dependence of density,

$$\varrho = 1.1206 \times 10^3 - 6.1500 \times 10^{-1}\ T\ [\mathrm{kg/m^3}].$$

The static viscosity (η_s) was determined by a Höppler viscosimeter and capillary viscometers over the temperature range 253-303 K. The accuracy of viscosity measurements varied, depending on the measurement method, from 0.5 to 2 per cent. For lower temperatures the values of viscosity were extrapolated by the equation $\log\eta = C + D/T^3$, proposed by MEISTER [7], where C and D are constants. There is the following temperature dependence of viscosity,

$$\log\eta = -4.7946 + 1.0532 \times 10^8\ T^{-3}\ [\mathrm{Nsm^{-2}}].$$

The shear impedance measurements were carried out at a frequency of 0.520 MHz, using UWE-1 and UWE-2 systems manufactured at the Institute of Fundamental Technological Research, Polish Academy of Sciences in Warsaw, over the temperature range 223-303 K. The principles of the measurements were described in many papers [8], whereas the measurement error, as defined by the producer, was ± 5 per cent.

The shear impedance measurements at frequencies of 29.9 and 500 MHz were carried out over the temperature range 218-303 K, using a measurement

system manufactured at the Department of Physical Acoustics, Institute of Fundamental Technological Research, Polish Academy of Sciences [9]. The measurement accuracy is, according to the producer, estimated at ±5 per cent. Tables 1 and 2 show the experimental values of shear resistance.

Table 1. The real (R_l) and imaginary (X_l) components of shear impedance

Temp. [K]	R_l $f = 0.520$ MHz	X_l	R_l 29.9 MHz	R_l 500 MHz
	$[\mathrm{Nsm^{-3}}] \times 10^{-5}$			
228.15			13.9	13.9
233.15			13.4	13.8
238.15	8.54	1.38	12.8	13.5
243.15	6.09	1.38	11.9	13.1
248.15	4.33	1.77	10.5	12.4
253.15	3.06	1.61		11.9
263.15	1.31	0.953		
268.15	0.886	0.690		
273.15	0.629	0.511		
278.15	0.477	0.378		
283.15	0.364	0.289		
288.15	0.288	0.233		
293.15	0.231	0.182		
298.15	0.192	0.163		
303.15	0.144	0.144		

Table 2. The shear moduli G' and G'', the dynamic viscosity η_d and the relaxation time $\tau_s = \tau_s/G_\infty$

Temp. [K]	G' $f = 0.520$ MHz $[\mathrm{Nm^{-2}}] \times 10^{-9}$	G''	η_d $[\mathrm{Nm^{-2}}]$	τ_s [s]
238.15	0.728	0.242	1.01×10^3	5.30×10^{-7}
243.15	0.363	0.172	3.40×10^2	1.82×10^{-7}
248.15	0.162	0.158	1.25×10^2	6.81×10^{-8}
253.15	0.0702	0.102	4.975×10	2.76×10^{-8}
258.15	0.0232	0.0543	2.12×10	1.20×10^{-8}
263.15	0.00834	0.0260	9.65	5.58×10^{-9}
268.15	0.00323	0.0128	4.65	2.74×10^{-9}
273.15	0.00138	0.00672	2.36	1.42×10^{-9}
278.15			1.26	7.75×10^{-10}
283.15			0.699	4.40×10^{-10}

4. Discussion of the results and conclusions

The results of the measurements are given in the tables and 10 diagrams. Formula (21) and the coefficients $k = 1$ and $\beta = 0.5$ were used in the description of the results of shear impedance measurements in 2-ethylhexadiole-1.3. (Figs. 5-8). When the results are presented on the basis of the Maxwell model, this

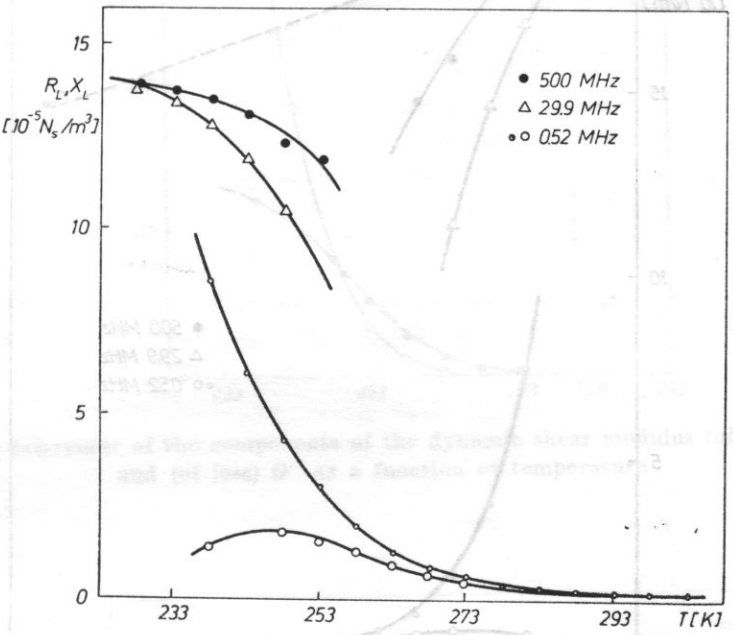

Fig. 5. The results of the measurements of the impedance components R_l and X_l as a function of temperature

corresponds to the parameter of the distribution width $b = 0.35$. A relaxation region was found to exist and was defined as one of viscoelastic relaxation.

The non-Newtonian behaviour of the fluid under these conditions is related to the translational molecular processes and configurational changes.

It can be seen that the range of viscoelastic relaxation of the diole investigated covers 4 decades of frequency (the dependence of the impedance components on frequency in Fig. 8) and that the behaviour of the normalised curve is much different from the behaviour of the relaxation curve in a simple Maxwell model.

The results of the measurements indicate that the behaviour of this diole and other polyhydroxide alcohols investigated by the present authors [10, 11, 12] can be explained within the relaxation theory, under the assumption of a continuous spectrum of the relaxation times with a given distribution. Although the problem of associated fluids still seems to be far from solved, the presence

in alcohols of multimers which form as a result of intermolecular hydrogen bonds has indisputably been confirmed by X-ray, spectroscopic and ultrasonic investigations. The diffraction of X-rays and neutrons indicates the presence,

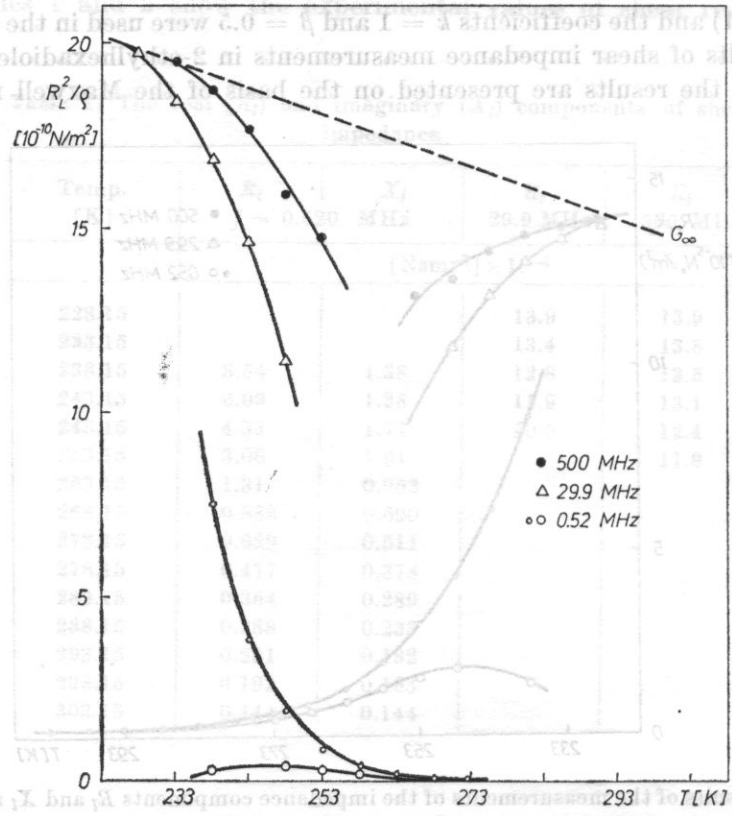

Fig. 6. The behaviour of the high-frequency modulus of shear elasticity as a function of temperature. The dashed line represents the extrapolated limiting shear modulus G_∞

both in a glaceous and a fluid state, of disturbed pieces of the crystalline structure undivided by the limits of discontinuity. Structures of this type should play a particularly important role in a supercooled state, where unlike a glaceous state, structural pieces both undergo translation and disintegrate and reform continually [16].

According to McDuffie and Litovitz [13], the structural rearrangements which occur in fluids as a result of external (electric or mechanical) forces have a cooperative character, since they cover a whole group of molecules (cluster) under the short-range molecular order. They constitute a relaxation process related to the structural relaxation time. The cooperative nature of such rearrangements is reflected in the viscosity of the non-Arrhenius fluid, i.e. a fluid whose viscosity is not proportional to $\exp(-E/RT)$, where E is the activation

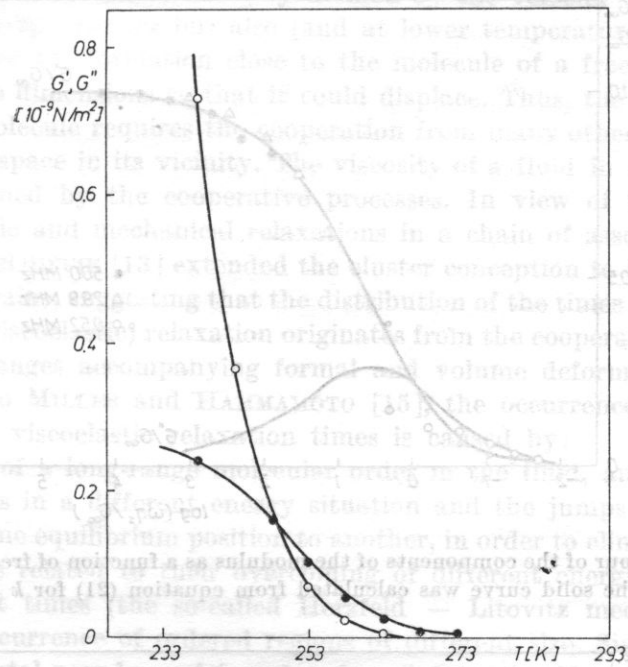

Fig. 7. The behaviour of the components of the dynamic shear modulus (of elasticity) G' and (of loss) G'' as a function of temperature

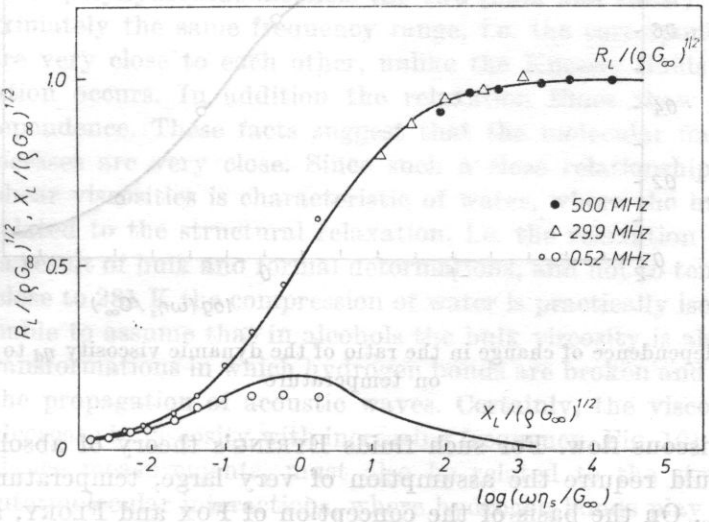

Fig. 8. The behaviour of the components of mechanical shear impedance as a function of frequency, in a normalised system. The solid curve represents the theoretical curve calculated from equation (22) for $k = 1$ and $\beta = 0.5$

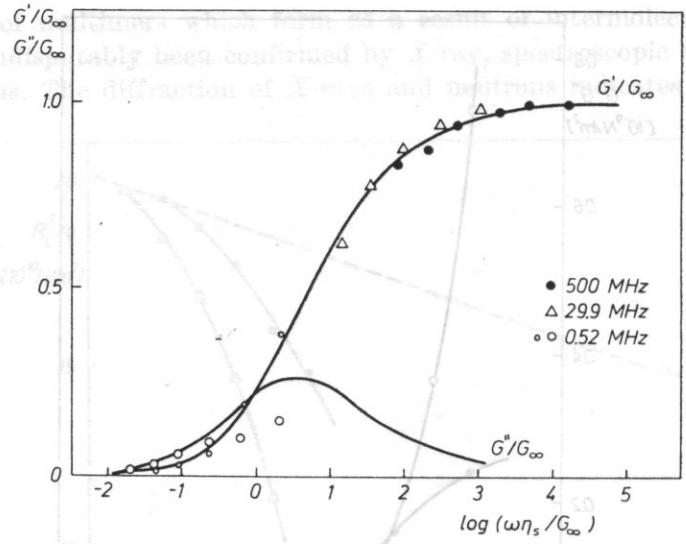

Fig. 9. The behaviour of the components of the modulus as a function of frequency, in a normalised system. The solid curve was calculated from equation (21) for $k = 1$ and $\beta = 0.5$

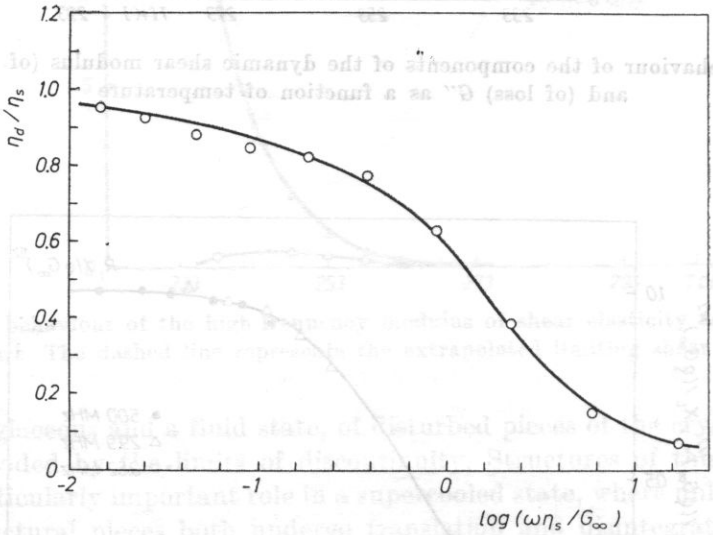

Fig. 10. The dependence of change in the ratio of the dynamic viscosity η_d to the static one on temperature

energy of viscous flow. For such fluids EYRING's theory of absolute reaction velocity would require the assumption of very large, temperature-dependent values of E_a. On the basis of the conception of FOX and FLORY, according to which the translation of molecules of a supercooled fluid is mainly determined by the volume of the free fluid, MACEDO and LITOVITZ [14] assumed that the

mobility of fluid molecules is not only defined by the velocity at which they overcome the energy barrier but also (and at lower temperatures mainly) by the probability of the formation close to the molecule of a free volume with sufficiently large dimensions so that it could displace. Thus, the translation of an individual molecule requires the cooperation from many others which must form an empty space in its vicinity. The viscosity of a fluid in a supercooled state is determined by the cooperative processes. In view of the similarity between dielectric and mechanical relaxations in a chain of associated fluids, LITOVITZ and MCDUFFIE [13] extended the cluster conception to the relaxation of mechanical strains, suggesting that the distribution of the times of mechanical (structural and viscoelastic) relaxation originates from the cooperative character of structural changes accompanying formal and volume deformations [16].

According to MILLES and HAMMAMOTO [15], the occurrence of the wide spectrum of the viscoelastic relaxation times is caused by:

a) the lack of a long-range molecular order in the fluid, and as a result every molecule is in a different energy situation and the jumps of particular molecules from one equilibrium position to another, in order to eliminate mechanical strains, are related to their overcoming of different energy barrier and thus to different times (the so-called Herzfeld – Litovitz mechanism [6]);

b) the co-occurrence of ordered regions of different size. Since the decay time of such crystal pseudo-nuclei, under shear forces, should increase as their spatial range expands, the factors changing the molecular order (e.g. temperature change) should affect the spectrum of the times of viscoelastic relaxation.

The results of the measurements carried out seem to confirm the molecular mechanisms given above.

In the case of polyhydroxide alcohols the two (bulk and shear) viscosities relax in approximately the same frequency range, i.e. the corresponding relaxation times are very close to each other, unlike the Knesser fluids in which thermal relaxation occurs. In addition the relaxation times show a similar temperature dependence. These facts suggest that the molecular mechanisms of the two processes are very close. Since such a close relationship between the bulk and shear viscosities is characteristic of water, where the bulk viscosity must be related to the structural relaxation, i.e. the relaxation of strains which arise as a result of bulk and formal deformations, and not to temperature functions (for close to 281 K the compression of water is practically isothermal), it seems reasonable to assume that in alcohols the bulk viscosity is also related to structural transformations in which hydrogen bonds are broken and reformed again during the propagation of acoustic waves. Certainly, the viscosity relaxation (i.e. an decrease in viscosity with increasing frequency, Fig. 10), observed in shear impedance measurements, must also be related to the structure of the fluid and intermolecular interactions, where hydrogen bonds play the main role. Thus, the phenomena observed in volume and formal deformations of the medium using acoustic waves are closely related to the cybotactic structure

of the fluid, which in the case of associated dioles is an intermediate stage between a weak dispersive structure with thixotropic properties and a condenser structure.

This was confirmed by the present investigations, since the change in the structure of the fluid caused by a temperature change was reflected by a change not only in viscosity, but also in moduli of elasticity and relaxation times.

Acknowledgement. This study was financially supported by the Polish Academy of Sciences (problem MR. I. 24).

References

[1] R. D. ANDREWS, A. V. TOBOLSKY, E. E. HANSON, J. Appl. Phys., **17**, 352, 280-292 (1946).

[2] A. V. TOBOLSKY, A. MERCURIO, J. Polym. Sci., **36**, 467-475 (1959).

[3] J. BARLOW, *Molecular and nonlinear acoustics, ultrasonic investigations of the viscoelastic properties of fluid* (in Polish), Zakład Naukowy im. Ossolińskich, Warsaw–Cracow 1965.

[4] A. J. BARLOW, A. J. ERGINSAV, J. LAMB, *Viscoelastic relaxation of supercooled liquids*, Proc. Roy. Soc., **A 298**, 481-494 (1967).

[5] T. A. LITOVITZ, C. DAVIES, *Physical acoustics*, Academic Press, New York–London 1965.

[6] K. F. HERZFELD, T. A. LITOVITZ, *Absorption and dispersion of ultrasonic waves*, Academic Press, New York–London 1959.

[7] R. MEISTER, C. J. MARHOFFER, R. SCIAMANDA, L. COTTER, T. A. LITOVITZ, J. Appl. Phys., **31**, 854-870 (1960).

[8] R. PŁOWIEC, *Investigations of the rheological properties of oils in the region of viscoelastic relaxation using ultra – and hypersonic shear deformations* (in Polish), Institute of Fundamental Technological Research, 60/1975. Habilitational diss.

[9] R. PŁOWIEC, *Measurement of the viscoelastic shear properties of fluids at frequencies of the order of 1000 MHz* (in Polish), Archiwum Akustyki, **3**, 5, 411-419 (1970).

[10] S. ERNST, M. WACIŃSKI, R. PŁOWIEC, J. GLIŃSKI, Acustica, **47**, 4, 292-303 (1981).

[11] S. ERNST, M. WACIŃSKI, R. PŁOWIEC, Acoustica, **45**, 1, 30-38 (1980).

[12] R. PŁOWIEC, S. ERNST, M. WACIŃSKI (in Polish), XXVIII Open Seminar on Acoustics, Gliwice 1981.

[13] T. A. LITOVITZ, G. E. MC DUFFIE JR., J. Chem. Phys. 39, 729-734 (1 963).

[14] P. MACEDE, T. A. LITOVITZ, J. Chem. Phys. **42**, 245-257 (1965).

[15] D. O. MILLES, D. S. HAMMAMOTO, Nature, **193**, 644-646 (1962).

[16] S. ERNST, *Some physico-chemical aspects of viscoelasticity (in Polish)*, Zeszyty Naukowe Uniwersytetu Śląskiego (in press).

Received on 25 November, 1982.